UNIVERSIDAD DE CANTABRIA

E.T.S. de Ingenieros de Caminos, Canales y Puertos

Departamento de Ciencias y Técnicas del Agua y del Medio Ambiente

---

TESIS DOCTORAL

MID-LONG TERM MORPHODYNAMICS OF THE DRY BEACH AND ITS EQUILIBRIUM PROFILE

Presentada por: **D. Jorge Díez González**

Dirigida por: **Dr. Raúl Medina**

Dr. Adolfo Uriarte

Santander, Diciembre 2016

MID-LONG TERM MORPHODYNAMICS OF THE DRY BEACH AND ITS EQUILIBRIUM PROFILE

Author: Mr. Jorge Díez
Advisor: Dr. Raul Medina
Advisor: Dr. Adolfo Uriarte

Text printed in Santander
First edition, December 2016

A mi abuelo Miguel

Agradecimientos

Si tuviese que dividir en partes la cantidad de mis gratitudes, el 99% irían dirigidas a Andrea. Ella me dio la oportunidad de comenzar en esto, que no es poco. Gracias a su confianza he podido dedicar decenas de meses de mi vida al estudio de las playas, una de mis pasiones, y por ello le estaré siempre agradecido. Dispuesta a ayudar y mostrando interés "desinteresado", ¡Mila esker! Otro 99% iría para Raúl. Le pedí ser el director de esta tesis y aceptó sin dudar, y desde ese momento hasta hoy ha sido un continuo aprendizaje a su lado. Un verdadero gustazo. Mil gracias.

Agradecimientos también a Peter Ruggiero por acogerme en su departamento de la Universidad Estatal de Oregon. Escribimos un artículo y aprendí un montón con él y su grupo, pero lo mejor fue la gran experiencia de vivir y trabajar unos meses en los U.S.A. Me llevo más de una anécdota que seguiré contando de anciano. Agradecimientos también a Vero y a Adolfo por prestarme su ayuda en la primera parte de la tesis, y mención especial para mis compañeros de doctorado en AZTI por crear un ambiente de trabajo tan agradable y por ser tan buena gente. Muchos para nombrarlos a todos: ¡Eskerrik asko! Además quiero dar las gracias a los dos Javis del IH, el físico y el químico. Uno por insistirme un viernes de cada tres para que me colegie como físico, y el otro por tener dos hijos que ya molan más que él. Y a June, que también ha estado cerca los últimos meses y ha escuchado mis quejas al aire. Eskerrik asko.

Kavafis, inspirado en el regreso de Ulises hacia Ítaca, escribió: "*... Pide que tu camino sea largo, lleno de aventuras, de conocimiento, [...]. Que sean muchas las mañanas de verano en que lleno de placer y alegría arribes a bahías nunca vistas; detente en los mercados fenicios y adquiere hermosas mercancías; visita muchas ciudades egipcias y con avidez aprende de sus sabios, [...].Ten siempre a Ítaca en tu mente. Llegar allí es tu meta, mas no apresures el viaje. Mejor que dure largos años, y que en tu vejez arribes a la isla con cuanto hayas ganado en el camino, sin esperar que Ítaca te enriquezca. Ítaca te regaló un hermoso viaje. Sin ella el camino no hubieras emprendido, mas ninguna otra cosa puede darte. Aunque pobre la encuentres, Ítaca no te engañará. Rico en saber y en vida, como has vuelto, comprendes ya qué significan las Ítacas.*" Pues bien, creo que esta tesis ha sido en cierta manera una Ítaca. Desde luego que el fin, sin desmerecerlo, ha

sido lo de menos. Lo aprendido a lo largo de estos cuatro años es el poso que queda y permanece.

Gracias extras al mar y a las montañas por estar ahí y gracias a los amigos con los que las comparto. Los verdaderos tesoros de este mundo no están en un cofre escondido. Por último, el 100% adicional más grande va para Marta y mi familia por hacerme sentir tan bien y por dejármelo todo en bandeja: pareja, padre, madre, hermana y abuelo. Estos son los fundamentales. ¡Gracias!

Jorge

Diciembre 16

Contents

List of Figures

List of Tables

List of Symbols

H_0 - Deep water wave height
H_s - Significant wave height
H_b - Breaking wave height
T_p - Peak period
L_0 - Deep water wave length
Ω - Dimensionless fall velocity
Ω_i - Instantaneous value of Ω
Ω_∞ - Averaged value of Ω
D - Memory of the beach
f - frequency of cluster
ω - Sediment fall velocity
d_{50} - Mean grain size
d - Beach width
$\tan\beta$ - Beach slope
A - Morphological parameter related to the dry beach equilibrium profile
b - Morphological parameter related to the dry beach equilibrium profile
m - Morphological parameter related to the dry beach equilibrium profile
x - Cross-shore lenght/direction
z - Profile elevation
θ - Wave direction
υ_t^* - Threshold of motion shear velocity
ρ_a - Air density
ρ_s - Sediment density
g - Acceleration of gravity ($9.8ms^{-2}$)
w - Moisture content in the sand
q_i - Sand transport rate by wind
F - Fetch distance
ξ_0 - Iribarren Number
B_h - Berm height

κ_r - Wave refraction coefficient

μ - Mean sea level at the shoreline

ϕ - Reduction factor for the dimensionless grain diameter

h - Depth

List of Acronyms

AU - Australia
CP - Clatsop Plains
CRLC - Columbia River Littoral Cell
DBEP - Dry Beach Equilibrium profile
DBP - Dry Beach Profile
DTM - Digital Terrain Model
DOW - Downscaling Ocean Waves
EBP - Equilibrium Beach Profile
EOF - Empirical Orthogonal Functions
EOMHW - Elevation Over Mean High Water Level
GOW - Global Ocean Waves
GL - Grayland Plains
IGN - Spanish Geographical National Institute
IOLE - Elaboración de los Mapas de Peligrosidad y Riesgo de Inundación Costera en España
IPCC - Intergovernmental Panel on Climate Change
KMA - *K-Means* Algorithm
LBT - Longshore Bar and Trough
LB - Long Beach (WA)
LTT - Low Tide Terrace
MHW - Mean High Water Level
MLLW - Mean Lower Low Water Level
MSL - Mean Sea Level
MSV - Mean Square Value
NAVD88 - North American Vertical Datum 1988
NB - North Beach (WA)
NMMA - Alicante Zero Reference Level
NOAA - National Oceanic and Atmospheric Administration
OR - Oregon State
PCA - Principal Components Analysis

LIST OF ACRONYMS

PNW - Pacific North West

RBB - Rythmic Bar and Beach

RMSD - Root Mean Square Deviation

RTR - Relative Tide Range

SBSP - South Beach State Park

TBB - Transverse Bar and Beach

TR - Tide Range

U.S.A - United States of America

WA - Washington State

Resumen en castellano [1]

1 Introducción

1.1 Motivación

El estudio de la playa desde un punto de vista físico ha sido y sigue siendo uno de los principales temas de investigación en oceanografía. Las playas son un elemento esencial en las costas de todo el mundo y gozan de gran importancia fundamentalmente por tres razones.

1. Desde un punto de vista ecológico, la playa se puede definir como la interfase entre tierra y mar que proporciona el hábitat esencial para numerosa vida oceánica y costera. Este ecosistema proporciona la base para los procesos ecológicos más esenciales, para la resiliencia del ecosistema costero y para mantener en equilibrio la relación entre vida silvestre y presencia humana.

2. Desde un punto de vista de protección de la costa, el sistema playa-duna juega un papel fundamental disipando la energía del oleaje y protegiendo la costa de eventos de inundación extremos provocados por aumentos del nivel del mar. El tamaño y anchura de la playa determina la capacidad de amortiguación ante una subida dramática del nivel del mar por oleaje extremo.

3. Desde un punto de vista económico, la playa juega un gran papel en lo que concierne a la actividad derivada del turismo. Las playas son fuente esencial de ingresos para los ayuntamientos, regiones y países que basan gran parte de su economía en el concepto turístico de "sol y playa".

En resumen, además de su importancia ecológica, la playa juega un papel fundamental de protección de la costa en invierno ante eventos extremos de inundación, mientras que en verano la playa seca debe tener la suficiente extensión para albergar con suficiencia la demanda

[1] Este resumen en español es una versión reducida del contenido total de la tesis. Si bien contiene todos los argumentos, resultados y conclusiones fundamentales, se remite al lector a la versión en inglés para una información más detallada.

turística requerida. Por todo lo anterior, un conocimiento exhaustivo de los procesos físicos gobernantes, así como de las interacciones entre fuerzas actuantes y la morfología, resultan esenciales para dar respuesta a los problemas que pueden surgir derivados de cualquiera de los tres puntos anteriores. En esta tesis se pretende profundizar en el conocimiento de esa relación causa (dinámicas) – efecto (cambios en morfología), así como el planteamiento de un perfil de equilibrio de la parte seca del perfil de playa. Esto permitirá calcular y predecir anchuras, cotas y pendientes de equilibrio bajo condiciones medias de oleaje. Así se podrá dar respuesta, por ejemplo, a cómo tiene que realizarse un regenerado o reperfilado sobre la playa seca para optimizar el proceso al máximo, o cómo diseñar una playa para que esté equilibrada, o poder predecir cómo cambiará la forma del perfil cuando se realiza cualquier obra que afecte a la dinámica o al sedimento. A modo de síntesis, las siguientes **preguntas de investigación** surgidas del análisis de las motivaciones para estudiar la playa seca serán respondidas a lo largo del documento:

- *¿Cuáles son los principales agentes que gobiernan la morfología de la playa seca?*
- *¿Cuáles son los índices morfológicos más característicos y representativos del perfil de playa seca?*
- *¿Bajo qué condiciones la playa presenta una tipo característico de perfil de playa seca u otro?*
- *¿Cómo responderá la playa seca a cambios en los factores controladores de la morfología?*
- *¿Cómo modulan los factores gobernantes la forma de equilibrio del perfil de playa seca?*
- *¿Cuáles son las anchuras, pendientes y cotas que definen el perfil de equilibrio bajo las condiciones ambientales medias?*
- *¿Existe una ecuación paramétrica que defina la configuración de equilibrio del perfil? En ese caso, ¿Cuáles son los principales parámetros que definen la ecuación y cómo se relacionan con los factores gobernantes de la morfología?*

1.2 Antecedentes y estado del conocimiento

Esta tesis se centra en el estudio del perfil transversal de la playa seca. Para entender bajo qué condiciones el perfil se puede considerar de equilibrio, que es la meta final de la tesis, es necesario entender y conocer de antemano diferentes aspectos relacionados con la morfología y la dinámica de este segmento del perfil de playa. El enfoque de las ideas sobre cómo abordar el trabajo, la revisión del estado del arte y la presentación de los conceptos previos

fundamentales, nos llevan a organizar el presente capítulo de la siguiente manera: Primero se se revisan las definiciones existentes en la literatura sobre cuáles son los límites dentro de los cuales la playa seca queda definida. Seguidamente se indentifican, a partir de estudios previos, cuáles son las diferentes dinámicas que gobiernan y moldean la forma de este segmento del perfil y cómo es esa respuesta en diferentes escalas espacio-temporales. Finalmente, en base a los estudios previos sobre dinámica y morfología de la playa seca, debemos entender cómo las dinámicas moldean el perfil de equilibrio proporcionando la configuración más estable en relación a las condiciones medias de oleaje y sedimento. Esta sección discute sobre estas cuestiones, ofrece conceptos previos y revisa lo ya conocido en el estado del arte. Se divide, por tanto, en tres sub-secciones.

1.2.1 Límites de la playa seca y primeras aproximaciones a su morfología

La playa seca comprende la zona entre la parte sumergida o intermareal y el borde de la playa, que puede ser el pie de duna, en caso de playas que presentan sistemas dunares, o un acantilado, un paseo marítimo o un muro, en caso de intervención humana. Es una zona afectada por episodios esporádicos de oleaje y viento, y forma una frontera dinámica entre la zona completamente dominada por las olas y la marea y la zona completamente dominada por el viento, que es el sistema dunar (Short 1999). Existen numerosos trabajos en la literatura referentes a la morfología de las partes sumergida e intermareal y sus correspondientes configuraciones de equilibrio (Bernabeu *et al.* 2003, Brunn 1954, Dean 1991), así como trabajos relacionados con el sistema dunar y su configuración (Cariolet & Suanez 2013, deVries *et al.* 2012, Hesp 2012). Sin embargo, a pesar de ser la zona más referida en estudios de inundación y erosión Mull & Ruggiero (2014), se requieren todavía estudios en profundidad sobre la morfología de equilibrio de este segmento de playa.

El Capítulo II de esta tesis [2] se centra en la identificación y estudio de las diferentes morfologías que puede presentar el perfil de playa seca dependiendo de las condiciones ambientales a las que se encuentra sometida. Es decir, pretende investigar sobre cuáles son las principales morfologías que presenta la playa seca en función del oleaje y el sedimento. Esta primera aproximación a la morfología se basa en los conocidos y ampliamente aplicados modelos conceptuales de playa (Short 2006, Wright & Short 1984). Estos modelos predicen morfologías de playa en función de determinados parámetros de oleaje, marea y tamaño de sedimento. El desarrollo de estos modelos ha sufrido una importante transformación y adaptación desde sus orígenes, desarrollados en sus etapas más primigenias bajo ambientes micromareales y con oleajes poco energéticos Chappell & Eliot (1979). Los más recientes y completos tienen en cuenta factores como la marea y la geología de la zona y se desarrollan bajo la influencia de oleajes poco y muy energéticos y englobando playas desde totalmente disipativas a totalmen-

te reflejantes (Scott *et al.* 2011). Sin embargo, estos modelos también presentan limitaciones, no sólo porque cada modelo responde adecuadamente sólo bajo las características regionales sobre las cuales ha sido desarrollado ((Gomez-Pujol *et al.* 2007, Jackson *et al.* 2005, Scott *et al.* 2011), sino también por la parte de la playa que obvian: el segmento emergido correspondiente a la parte seca de la playa. A partir del conocimiento recogido en estos modelos previos, en el Capítulo II de esta tesis [2] se presenta un modelo conceptual del perfil de playa seca en la dirección perpendicular a la línea de costa y que comprende desde el nivel de pleamar media hasta el límite terrestre de la playa.

1.2.2 Fuerzas gobernantes y morfología

Oleaje *vs* viento sobre la playa seca

A pesar de que el viento es el principal agente gobernante sobre el sistema dunar y es el que le proporciona suplemento de arena necesario para crecer, la forma de la playa seca está fundamentalmente controlada por la acción del oleaje, y su forma está directamente relacionada con el estado modal de la playa. Short & Hesp (1982) y Hesp (1988) demostraron que el estado modal de la playa influye directamente en la forma no solo de la parte sumergida e intermareal sino también en la parte emergida y en el tamaño, volumen y altura de la duna. Así, el clima marítimo y el tamaño de sedimento son los principales factores gobernantes sobre la morfología de la playa seca. Posteriores estudios han comparado la acción del viento con la acción del oleaje de manera directa -por ejemplo, Delgado-Fernández *et al.* (2009), Udo & Yamawaki (2006)-, llegando todos a la conclusión de que el oleaje, aunque cubra la playa seca sólo durante unos pocos días al año, es mucho más efectiva que la acción del viento actuando de manera más persistente.

Swash y runup

El transporte de sedimento en la dirección perpendicular a la costa es el principal mecanismo de intercambio entre las partes sumergida y emergida de la playa (Masselink *et al.* 2006). Los procesos de acreción y erosión, y por tanto las variaciones en la forma del perfil, están directamente relacionadas con estos mecanismos. La zona de swash es la parte del perfil de playa que está alternadamente cubierta y expuesta por el uprush y el backwash –variaciones en torno al nivel medio del mar debido al ascenso y descenso del oleaje sobre el frente de playa.- Es una zona muy dinámica que responde a escalas temporales desde segundos en playas poco energéticas o reflejantes, hasta minutos en playas altamente energéticas y disipativas. La energía que no es disipada en la zona de surf es transformada en energía potencial en el frente de playa en forma de elevación del nivel de agua sobre el nivel medio. Es lo que se llama el runup. Este proceso puede generar elevaciones extremas del nivel del

mar (Ruggiero *et al.* 2001) y es un factor clave durante procesos de erosión costera y creación y destrucción de la berma (Holman 1986, Stockdon *et al.* 2006).

La berma

La berma es una formación supramareal formada por el transporte de sedimentos en la zona de swash. La berma es, en cierto sentido, la forma opuesta a las barras intermareales ya que se trata de una forma de acreción y deposición de material sobre el frente de playa, mientras que las barras son consecuencia de la erosión de la misma zona (Bascom 1951). Su formación depende tanto del tipo de sedimento como de los procesos hidrodinámicos como el runup (Orford *et al.* 2002). Así, el transporte de sedimento por el uprush y el overwash sobre la posición de una berma existente son los dos factores fundamentales en su crecimiento y desarrollo (Baldock *et al.* 2005, Weir *et al.* 2006). La presencia de bermas estacionales es clave en este trabajo debido a su importancia en explicar ciertos cambios estacionales en la morfología de la playa seca. Su formación y destrucción depende del desequilibrio entre el transporte del sedimento durante el uprush y el backrush, y también está condicionado por la presencia o no de barras intermareales, que actúan como fuente de sedimento desde la zona intermareal o sumergida hacia la playa seca y el sistema dunar (Anthony *et al.* 2006, Masselink *et al.* 2006). Durante condiciones poco energéticas o de verano, la berma se crea generalmente en el frente de playa entre el nivel medio del mar y justo por encima del nivel medio de runup (Katoh & Yanagishima 1992). Si el nivel total medio del mar aumenta, la berma migra hacia tierra, y cuando el runup aumenta hasta sobrepasar la cota de la cresta, la berma gana elevación. Sin embargo, cuando el runup alcanza el pie de duna, el frente de playa se puede erosionar y la berma puede quedar destruida. Mientras que la erosión de la berma puede ocurrir en una escala de días o incluso horas, el proceso de recuperación y acreción puede durar semanas o incluso meses (Cohn & Ruggiero 2015). Entre las numerosas formulaciones propuestas en la literatura para predecir la altura de la berma, Takeda & Sunamura (1986) sugirieron una en función del oleaje (B_h es la altura de la berma, T es el periodo y H_b es la altura de ola en rotura):

$$B_h = 0{,}125(gT^2)^{3/8}(H_b)^{5/8} \tag{1}$$

1.2.3 El perfil de equilibrio de la playa seca

El desarrollo de una formulación paramétrica que se ajuste al perfil de playa permite la predicción de las cotas, pendientes y anchuras que la playa presenta bajo las condiciones medias de oleaje y sedimento. Una de estas formas paramétricas es la conocida como formulación de equilibrio. Las playas que se encuentran sometidas a diferentes condiciones de oleaje y

sedimento presentarán configuraciones de equilibrio diferentes y en consonancia con su entorno y sus factores gobernantes. Para dar cuenta de estos puntos, esta sección se divide en dos sub-secciones. Primero se sientan las bases para el estudio de las variaciones espacio-temporales en el perfil y seguido se analiza el comportamiento del perfil en el largo plazo bajo las condiciones medias de oleaje y sedimento de la playa.

Variaciones espacio-temporales en el perfil de playa seca

El estudio de variaciones temporales se puede llevar a cabo bajo diferentes escalas temporales: desde movimientos instantáneos como el transporte de sedimentos en la zona de swash o la erosión del pie de duna por una tormenta, hasta cambios que se extienden a lo largo de varios años como las variaciones en la posición de la línea de costa. El estudio de las fluctuaciones en el medio plazo, por ejemplo, dan respuesta a las variaciones estacionales en la creación-destrucción de la berma. En nuestro caso particular, los cambios morfológicos en el perfil de playa seca ocurren desde el corto plazo hasta el largo plazo. Un conocimiento exhaustivo de todas las escalas permite relacionarlas entre ellas para poder entender el comportamiento general (Ruggiero *et al.* 2005). Así, sabemos que los procesos erosivos, generados por eventos extremos de oleaje y que mueven la arena desde el frente de playa hacia la parte sumergida ocurren en un periodo de tiempo que puede ir desde los pocos días hasta las horas, mientras que el proceso opuesto, es decir, el trasporte de arena desde la parte sumergida a la emergida y que provoca que la playa seca crezca, puede llevar desde semanas hasta varios meses y ocurre bajo condiciones medias de oleaje. Por tanto, conocer estos mecanismos en las diferentes escalas es esencial para poder predecir formas de equilibrio en el largo y medio plazo.

Aproximaciones a la forma de equilibrio del perfil de playa seca

El perfil de equilibrio es, teóricamente, la curva bajo la cual el transporte de sedimento es cero en cualquier dirección. Sin embargo, el perfil de equilibrio puede ser obtenido mediante el desarrollo de expresiones paramétricas que buscan la similitud con casos conocidos de perfiles que están en equilibrio (Dean 1977). En la literatura existen numerosos trabajos relacionados con el perfil de equilibrio de la playa (Bernabeu *et al.* 2003, Dean 1991, Holman *et al.* 2014), pero todos se centran en las partes sumergidas e intermareal, y ninguno extiende su dominio a la parte emergida de la playa. Uno de los objetivos de esta tesis es desarrollar y proponer una formulación de equilibrio que comprenda desde el nivel de pleamar hasta el límite de la playa hacia tierra, ya sea el pie de duna o el muro de un paseo marítimo y así completar el perfil de playa completo.

Veremos como el tamaño de sedimento y el oleaje (englobado todo en el parámetro adimensional de caída de grano y en el runup, concretamente) son los factores que determinan la configuración de equilibrio de la playa seca. Así, a partir del conocimiento del clima marítimo en frente de la playa, la morfología de la playa puede quedar definida a partir del cálculo

de las pendientes, curvaturas, cotas y anchuras más estables. Dependiendo del rango del parámetro adimensional de caída de grano, la playa seca presentará – o no- bermas, y estará definida por ciertos rangos en los índices morfométricos más característicos.

1.3 Objetivos

A partir del análisis del estado del arte en relación a la física de la playa seca, ha quedado claro que:

- Los modelos conceptuales de playa son una herramienta adecuada para describir adecuadamente morfologías de playa.
- No hay suficiente conocimiento sobre cuáles son los principales agentes físicos que controlan la morfología de la parte emergida de la playa. Además de la identificación, se deben entender y cuantificar sus efectos.
- Las partes sumergidas e intermareal están bien documentadas en la literatura en términos de configuración de su perfil de equilibrio. Existe por tanto una necesidad de caracterizar del mismo modo la configuración de equilibrio de la zona emergida.
- El perfil de equilibrio de la playa seca ayuda a describir y predecir morfologías *i)* entendiendo de qué manera la playa seca recupera la forma de equilibrio tras los meses de invierno caracterizados por oleajes energéticos; *ii)* proporcionando una cota y anchura de equilibrio; *iii)* estimando el tiempo necesario que la playa seca necesita para cambiar de configuración de equilibrio de verano a configuración de equilibrio de invierno.

Basado en esto, el objetivo general de la tesis es profundizar en el conocimiento del comportamiento del perfil de playa seca bajo unas escalas espacio-temporales bien definidas (medio plazo, o estacional, y largo plazo), así como caracterizar la configuración de equilibrio a partir de los procesos gobernantes. Este objetivo principal se consigue a partir de la consecución de una serie de objetivos específicos.

- **Objetivo 1**. Identificar los principales agentes involucrados en la configuración de la forma de la playa seca y construir un marco de trabajo adecuado que describa las principales formas y configuraciones más comunes que puede presentar el perfil de playa seca con relación a su entorno.
- **Objetivo 2**. Investigar cómo la playa seca responde a variaciones en ciertos factores clave como son el oleaje y el tamaño de sedimento y estudiar las variaciones del perfil

bajo un determinado clima marítimo en dos escalas diferentes: medio (o estacional) y largo plazo.

- **Objetivo 3**. Entender cómo las condiciones medias de oleaje y sedimento modulan la configuración del perfil en el largo plazo y construir un modelo paramétrico de equilibrio que permita predecir los índices morfométricos más comunes (anchura, pendiente, curvatura y cota) en el largo plazo.

1.4 Organización de la tesis

Esta tesis se estructura en un capítulo introductorio [Chapter 1] donde se discute la motivación que genera el desarrollo de esta tesis y se aportan los conocimientos previos sobre el tema principal el estado del arte. Además se explican los conceptos previos básicos para entender el contenido del documento y se introducen los objetivos general y específicos. Los tres capítulos siguientes llevan el peso de la tesis y están confeccionados a partir de tres artículos científicos publicados en revistas de impacto [Chapter 2, 3 and 4]. El capítulo final [Chapter 5] se centra en resaltar las conclusiones y aportaciones del trabajo y sugiere posibles líneas futuras de investigación en relación al tema tratado en esta tesis. Los tres capítulos fundamentales se resumen así:

En el Capítulo II [2] se construye un marco de trabajo mediante el desarrollo de un modelo conceptual de perfil de playa seca. Este modelo caracteriza al perfil de playa seca en cuatro grupos diferentes y caracterizados según su morfología. Además, cada grupo está asociado a un rango de valores del estado modal de la playa. Así, las playas disipativas están asociadas con un tipo bien definido de perfil, así como las intermedias, las reflejantes y las ultradisipativas. Para este estudio se ha empleado satisfactoriamente una técnica de clasificación automática conocida -*K-Means*, Fayyad *et al.* (1996)- aplicada a la clasificación de perfiles debido al gran número de playas seleccionadas para el estudio.

En el Capítulo III [3] se investigan las variaciones espacio-temporales del perfil a lo largo de una extensión de costa altamente energética y disipativa. Además, esta extensión de costa (La celda litoral del Río Columbia, Oregon y Washington, EEUU) está sometida a una marcada estacionalidad en el clima marítimo, lo que obliga a investigar las variaciones estacionales en el perfil: los ciclos de erosión-acreción y las configuraciones más estables en el medio y largo plazo. Para ello se emplearon las técnicas matemáticas *K-Means* y el Análisis de Componentes Principales, también llamada Funciones Empíricas Ortogonales -EOF, Clarke & Eliot (1975)-.

El Capítulo IV [4] propone una formulación paramétrica para el perfil de equilibrio de la playa seca desarrollada (a partir de una base de datos de playas españolas localizadas a lo

largo del litoral peninsular) y testada (con una amplia base de datos de la Playa de Narrabeen, costa Este de Australia) bajo diferentes condiciones de oleaje y sedimento.

2 Caracterización del perfil de playa seca: una aproximación a su morfología [1]

A partir del análisis de 91 playas repartidas a lo largo del litoral peninsular español (Fig. 2.5) se ha llevado a cabo una caracterización del perfil de playa seca en relación a su morfología. Los perfiles comprenden desde el nivel medio de pleamar hasta el borde de la playa, que bien puede ser el paseo marítimo que la contiene o el pie de duna. Dentro de la base de datos utilizada, detallada en Tomás *et al.* (2015), se pueden encontrar playas de diversos tipos, desde totalmente disipativas hasta totalmente reflejantes, pasando por todos los estados intermedios. Este amplio rango aporta al estudio una gran riqueza en términos de variabilidad y permite la caracterización del perfil bajo diferentes condiciones de oleaje y sedimento. Como se resaltó en la introducción, la playa seca se puede caracterizar en términos del estado modal, que viene definido por el valor del parámetro adimensional de caída de grano (Dean 1977):

$$\Omega = \frac{H_b}{w_s T} \tag{2}$$

Donde H_b es la altura de ola en rotura, w_s es la velocidad de caída del grano y T es el periodo. Así, dependiendo del estado modal de la playa, el perfil seco presentará una configuración determinada y directamente relacionada con el valor de Ω.

Para manejar tal cantidad de perfiles se ha empleado un algoritmo de clasificación automática denominado *K-Means*. El algoritmo selecciona las formas más comunes presentes en toda la muestra y organiza grupos caracterizados por un centroide, que representa la configuración más común. Los perfiles de la muestra que más se asemejan entre sí bajo unos criterios matemáticos determinados se agrupan en el conjunto definido por el centroide. Por otro lado, el usuario escoge el número deseado de grupos en que quiere dividir la base de perfiles. En nuestro caso, para que el resultado tenga coherencia física (no hay que olvidar que la clasificación automática es un algoritmo puramente matemático) se ha dividido la muestra en cuatro grupos, asociados con cada uno de los estados modales más comunes: disipativo (dividido a su vez en dos: invierno-verano), intermedio y reflejante. Para la configuración de playas disipativas, el algoritmo las ha dividido en dos debido a que generalmente en

[1] Este sub-apartado resume de manera concisa la metodología y los resultados del Capítulo II del documento en inglés, que a su vez es una adaptación del artículo "Díez, J., Cánovas, V., Uriarte, Ad., Medina, R., 2016. *Characterization of the dry beach profile. A morphological approach.* Journal of Coastal Research (*in press*)". Para una revisión completa del trabajo, se remite al lector al capítulo original de la tesis [Chapter II] redactado en inglés. Las conclusiones y aportaciones del capítulo se resumen en el Apartado 5.1.

este grupo se engloban las playas de la base de datos que se localizan en el Norte de la Península sometidas a una notable estacionalidad en el clima marítimo, pudiendo presentar configuraciones de equilibrio distintas dependiendo de la época del año. Así, los clusters (o grupos) están asociados con: disipativa en configuración de invierno (playa plana y con pendiente positiva, sin formas), disipativa en configuración de verano (playa con una berma marcada y un perfil estacional), intermedia (frente de playa ligeramente pronunciado, berma marcada y pendientes suaves desde la berma hasta el pie de duna) y reflejantes (frente de playa muy pronunciado, berma estable y pendiente casi nula hasta el muro o pie de duna). Además, se ha incluido en la clasificación de perfiles las playas que presentan un estado modal ultradisipativo, generalmente presente en playas solo influenciadas por la marea y sin oleaje (playas en el interior de estuarios, por ejemplo). El resultado de la clasificación es un modelo conceptual de playa seca en el que los cuatro grupos caracterizan el perfil más estable que la playa seca va a mostrar en función de su estado modal (Fig. 2.8, Table 2.3).

3 Variabilidad espacio-temporal del perfil de playa seca a lo largo de una celda litoral altamente disipativa (playas del Pacífico Noroccidental de Estados Unidos) [1]

En este capítulo se lleva a cabo un análisis exhaustivo del comportamiento del perfil de playa seca a lo largo del tiempo en dos escalas temporales bien definidas: las variaciones estacionales y el comportamiento del perfil en el largo plazo. Para el comportamiento en el largo plazo se emplean datos de la celda litoral del Río Columbia (Fig. 3.1), que se extiende a lo largo de la costa de los estados norteamericanos de Oregon y Washington. Esta extensión de costa lleva siendo monitorizada en términos de topografía, batimetría y oleaje de manera detallada desde el año 1997, lo que proporciona una base de datos óptima para la realización de estudio (Ruggiero *et al.* 2005). El clima marítimo es altamente energético y con una marcada estacionalidad, con alturas de ola media en torno a $3m$ en invierno y $1.5m$ en verano (Fig. 3.2). Las playas, por lo general, presentan tamaños de arena finos, en torno a los $0.2mm$ de media, y están soportadas por importantes sistemas dunares. Por otro lado, para el comportamiento del perfil dentro de un año y para observar como el cambio en el oleaje estacional modula el perfil, se emplean datos de la playa de South Beach, en la localidad de Newport, en el estado de Oregon (Fig. 3.3). Esta playa está también siendo monitorizada con

[1] Este sub-apartado resume de manera concisa la metodología y los resultados del Capítulo III del documento en inglés, que a su vez es una adaptación del artículo "Díez, J., Cohn, N., Kaminsky, G., Medina, R., Ruggiero, P., 2017. *Spatial and temporal variability of dissipative dry beach profiles in the Pacific Northwest, U.S.A.*. Marine Geology (*in press*)". Para una revisión completa del trabajo, se remite al lector al capítulo original de la tesis [Chapter III] redactado en inglés. Las conclusiones y aportaciones del capítulo se resumen en el Apartado 5.1

detalle, y ofrece topografías y perfiles medidos con detalle mensualmente durante más de un año.

Se han empleado dos técnicas matemáticas para el estudio de estos perfiles. La técnica de *K-Means* para el estudio de las formas más comunes que presenta el perfil de playa seca a lo largo del tiempo, y la técnica del Análisis de Componentes Principales para conocer en qué parte de la sección transversal de la playa seca y en qué momento se producen los cambios más significativos. Los resultados de este capítulo se han dividido en dos subsecciones. Primero se analiza la variabilidad del perfil de playa seca dentro de un año sobre la playa de South Beach, para lo que se dispone de un perfil monitorizado durante 16 meses con un perfilado por mes. También se dispone del oleaje asociado, lo que permite establecer una relación entre la dinámica y los cambios morfológicos en el perfil. El análisis en el largo plazo se lleva a cabo siguiendo la misma metodología, pero con una cobertura temporal de 17 años, cuatro perfilados por año (invierno, primavera, verano y otoño) y un total de 25 diferentes transectos repartidos a lo largo de la celda litoral. El análisis de las formas más comunes a partir de los resultados del *K-Means* ofrece dos formas características que responden a la estacionalidad en el clima marítimo. Como morfología general de toda la celda, las playas presentan una configuración que está presente aproximadamente un 70 % del año y que responde a las condiciones energéticas de invierno, estando formada por una recta positiva y sin formas. El tiempo restante, el perfil se acomoda a las condiciones menos energéticas de verano construyendo una berma en el frente de playa y generando un perfil estable desde la cresta de la berma hasta el pie de duna (Fig. 3.10). Como complemento esencial al estudio, el Análisis de Componentes Principales permite entender las variaciones a lo largo del año del perfil. Se ha observado que durante el verano hay una constante ganancia de altura en el segmento de runup hasta que la berma alcanza una altura de unos $3.2m$ sobre el nivel de referencia (NAVD88) en los meses finales del verano. Como consecuencia, la playa seca se ensancha durante los meses de verano alrededor de 15-20m de media. Se forma un frente de playa más pronunciado hasta la cresta de la berma, y desde esa cota hasta el pie de duna, el perfil adopta una pendiente suave y sin formas. Se puede comprobar como este comportamiento se reproduce a lo largo del tiempo cada año, observando el todavía no muy bien entendido mecanismo de intercambio de sedimento entre las partes sumergidas y emergidas del frente de playa (Fig. 3.11,Fig. 3.12).

4 Un modelo paramétrico para el perfil de playa seca [1]

En este capítulo se propone una formulación paramétrica que describe la forma de equilibrio del perfil de playa seca. El modelo consiste en una ecuación con tres parámetros y constituida por dos términos:

$$f(x) = A(1 - e^{-bx}) + mx \tag{3}$$

Un exponencial que define fundamentalmente la zona de runup y la morfología de la berma, y un término lineal que define la pendiente desde la cresta de la berma hasta el límite de la playa. Los tres parámetros morfológicos dan forma a la ecuación y están relacionados con el clima marítimo (H_s *y* T_p) y con las características del sedimento (d_{50}) de manera consistente con los conocimientos previos acerca de la morfodinámica de la playa seca. Así se propone el parámetro hidrodinámico que fundamentalmente modula el runup $[HL]^{1/2}$ (Stockdon *et al.* 2006) y el parámetro adimensional de caída de grano Ω como las variables fundamentales que controlan la morfología de la playa seca (Fig. 4.2).

El modelo se ha construido a partir de perfiles de playas españolas repartidas a lo largo de todo el litoral peninsular. De este modo la ecuación puede responder a diversos tipos de morfologías, que van desde playas totalmente disipativas y energéticas hasta playas totalmente reflejantes y poco energéticas. Las variaciones de los tres parámetros de la ecuación permiten adaptarse a las dos morfologías más extremas descritas en el Capítulo II y pasando por todas las intermedias. Es decir, la ecuación propuesta se puede ajustar a perfiles sin formas características, constituidos por una pendiente recta y con pendiente positiva desde el nivel de pleamar hasta el pie de duna, y también puede ajustarse a perfiles reflejantes, con un frente de playa muy pronunciado, una berma alta y escarpada y una zona casi horizontal o con una ligera pendiente positiva desde la berma hasta el final de la playa (Fig. 4.3).

La capacidad de predicción del modelo se ha comprobado mediante su aplicación sobre una amplia base de datos independiente correspondiente a la playa de Narrabeen, en la costa Este de Australia (Turner *et al.* 2016). Una extenso programa de monitoreo que se lleva a cabo desde hace más de cuarenta años ofrece perfiles de playa seca sometidos a diferentes condiciones de oleaje, dependiendo del transecto escogido y la época del año. De esta manera, el modelo es testado bajo diferentes condiciones medias de oleaje. Los resultados de la validación ofrecen ajustes satisfactorios cuando el modelo se aplica tanto a perfiles en torno

[1] Este sub-apartado resume de manera concisa la metodología y los resultados del Capítulo IV del documento en inglés, que a su vez es una adaptación del artículo "Díez, J., Cánovas, V., Uriarte, Ad., Medina, R., 2017. *A parametric model for dry beach equilibrium profiles.* Coastal Engineering (*in press*)". Para una revisión completa del trabajo, se remite al lector al capítulo original de la tesis [Chapter IV] redactado en inglés. Las conclusiones y aportaciones del capítulo se resumen en el Apartado 5.1

a estados modales disipativos, como también a perfiles que se mueven en el rango de estados modales reflejantes, con coeficientes de correlación entre el perfil real medido y el calculado con el modelo de aproximadamente 0.95 (Fig. 4.9,Fig. 4.10).

5 Conclusiones y futuras líneas de investigación

5.1 Resumen de los capítulos y contribuciones

El objetivo fundamental de esta tesis ha sido ampliar el conocimiento sobre los mecanismos que describen la física de la playa seca, es decir, la relación entre su morfología y las dinámicas que actúan sobre ella y los procesos que modulan y configuran su estado más estable o de equilibrio. Este trabajo ha fructificado en tres artículos publicados en revistas científicas de impacto y de referencia en el mundo de la oceanografía costera. Los tres capítulos fundamentales de la tesis se basan en estos trabajos, y la suma de los objetivos que persigue cada uno forma el conjunto del documento y da respuesta al objetivo fundamental.

Resumen y contribuciones de **"Caracterización del perfil de playa seca: una aproximación morfológica":**

- La base de datos proporcionada por el IOLE (Tomás *et al.* 2015) ofrece un amplio espectro de playas en términos de estado modal, desde disipativas hasta reflejantes. Así se ha podido llevar a cabo la caracterización del perfil de playa seca bajo diferentes condiciones de oleaje y sedimento, englobando la mayoría de los tipos de perfil de playa seca.

- La zonificación del perfil propuesta en este capítulo es clave para entender los cambios de curvatura, pendientes y cotas que hay a lo largo del perfil de playa seca. Así se ha definido el segmento de runup, que comprende desde el nivel de pleamar hasta la berma; el perfil estacional, que se forma bajo cambios estacionales en el clima marítimo y comprende el espacio entre bermas estacionales; y el segmento inter-anual, que es la parte más estable del perfil y comprende desde la berma más estable hasta el pie de duna (o muro, en caso de intervención humana).

- Se ha demostrado que la herramienta matemática *K-Means* resulta eficiente y útil para clasificar diferentes morfologías del perfil de playa seca. El algoritmo construyó cuatro grupos diferentes, cada uno de ellos caracterizados por un perfil tipo. Este perfil tipo representa la configuración media más estable, y en torno a ella se agrupan el resto de perfiles de la base de datos que, bajo criterios puramente matemáticos, más se asimilan a él.

- Se ha asociado cada uno de los morfotipos encontrados a partir de la clasificación automática con cada uno de los cuatro estados modales caracterizados y descritos por numerosos autores: disipativo, intermedio, reflejante y ultradispativo. Se obtuvo, por tanto, un modelo conceptual de playa seca en cual el perfil de playa seca queda definido por su estado modal. Se obtuvieron los grupos: Tipo 1, Tipo 2, Tipo 3 y Tipo 4, cada uno de ellos caracterizado bajo unos rangos determinados de cotas, pendientes y anchuras.

- Esta clasificación construye la base esencial para los trabajos posteriores a cerca de las variaciones temporales del perfil y con la configuración de equilibrio que se desarrollan en los capítulos siguientes, así como para cualquier trabajo referente a la playa seca llevado a cabo al margen de esta tesis.

Resumen y contribuciones de **"Variabilidad espacio-temporal del perfil de playa seca a lo largo de una celda litoral altamente disipativa (playas del Pacífico Noroccidental de Estados Unidos)":**

- El extenso programa de monitorización a lo largo de la celda litoral del Río Columbia, ofrece una amplia base de datos de perfiles de playa seca (entre otras medidas topográficas y batimétricas) que se extiende desde 1997 hasta 2016 (todavía en marcha). Salvo excepciones, las playas a lo largo de esta extensión de costa son altamente disipativas y están sometidas a una marcada estacionalidad en el clima marítimo. Así, se parte de la hipótesis de que estas playas presentan un perfil de playa seca Tipo 1 y sujeto a estacionalidad, de acuerdo con la clasificación propuesta en el capítulo anterior. Se asoció el estado modal con su morfología y se observó una clara relación entre las variaciones de este parámetro y las variaciones de la morfología de los perfiles tanto en espacio como en tiempo.

- Se aplicaron dos métodos matemáticos conocidos para entender el mecanismo de intercambio entre las partes emergidas y sumergidas del perfil de playa y para identificar los principales cambios en el perfil en las escalas inter e intra anuales. *K-Means* distingue y caracteriza las dos principales configuraciones que estas playas presentan a lo largo del año; como complemento, el Análisis de Componentes Principales explica la variabilidad de los datos recogidos en espacio y tiempo. Es decir, identifica en qué parte del perfil ocurren los principales cambios y cuándo ocurren en el tiempo.

- A partir de los resultados que ofrecen estas técnicas y basados en estudios previos en la misma zona de estudio, sabemos que las playas disipativas del Noroeste Americano presentan dos configuraciones principales de playa seca, ambas dentro de los perfiles

Tipo 1. Una configuración que se adapta a las condiciones altamente energéticas de invierno, con una pendiente suave positiva y sin formas desde el nivel de pleamar hasta el pie de duna, y otra forma con berma que se adapta mejor a las condiciones de oleaje menos energético de los meses de verano. Se identificaron y se cuantificaron en una escala temporal determinada los principales índices morfológicos que definen el perfil, como son anchuras, cotas y pendientes.

- Este estudio del perfil de playa seca a lo largo de la celda litoral del Río Columbia aporta nuevos datos y conocimiento acerca del comportamiento general de esta celda, ampliamente estudiada en otros estudios bajo diferentes aproximaciones morfodinámicas, pero ninguna hasta ahora referente a la morfología de la playa seca.

Resumen y contribuciones de **"Un modelo paramétrico para el perfil de equilibrio de la playa seca":**

- Se ha propuesto una ecuación paramétrica que es capaz de reproducir los cuatro tipos de perfil de playa seca propuestos en el Capítulo II. Es decir, se ha conseguido reproducir satisfactoriamente cualquier morfología de perfil de la parte seca tanto de playas disipativas como de reflejantes e intermedias.

- La ecuación se ha desarrollado a partir de una base de datos completa que engloba playas sometidas a diferentes condiciones de oleaje y sedimento, caracterizando, por tanto, playas con morfologías muy diferentes. La base de datos la conforman desde playas disipativas con una pendiente suave, positiva y sin formas desde el nivel de pleamar hasta la duna, hasta playas reflejantes, con una berma marcada y un perfil de runup corto y pronunciado. El rango de aplicación del modelo comprende, por tanto, desde valores adimensionales de caída de grano muy pequeños hasta valores en torno a 7.

- La ecuación, propuesta desde una aproximación heurística, está formada por dos términos y tres parámetros: uno exponencial que describe la curvatura y cota de la berma y el perfil de runup, y un término lineal que describe el segmento desde la berma, en caso de que exista, hasta el final de la playa. Los parámetros morfológicos que definen la forma del perfil están modulados por el runup y por el parámetro adimensional de caída de grano. Así, la ecuación, y por tanto el perfil de equilibrio de la playa seca, queda definida conociendo estos valores. Los tres parámetros se adaptan a las variaciones del oleaje y del sedimento, pudiendo por tanto adoptar la forma del perfil a las condiciones ambientales cambiantes.

- Se ha comprobado la validez del modelo frente a una base de datos independiente de una playa Australiana: Narrabeen Beach. Esta playa, que ofrece diversos estados modales dependiendo de la localización del perfil y de la época del año, permite testar el modelo bajo diferentes condiciones. Las aplicaciones del modelo ofrecen buenos resultados, siendo el modelo es capaz de reproducir satisfactoriamente configuraciones que responden a estados modales tanto próximos a disipativos como próximos a reflejantes. La curvatura del perfil de runup, la cota de la berma y la pendiente del segmento que une la berma con el final de la playa seca quedan bien definidos y representados con el modelo.

- El modelo propuesto proporciona una herramienta muy útil para estudios de regeneración y diseño de playas y para calcular y predecir la configuración más estable que una playa equilibrada presentará bajo las condiciones medias de oleaje y sedimento.

5.2 Futuras líneas de investigación

Las metodologías, resultados y conclusiones de este trabajo ofrecen margen de mejora y abren las puertas a trabajos posteriores relacionados. En los siguientes seis puntos se proponen algunas claves:

- Respecto a la comparación del efecto del viento y del oleaje en relación a la capacidad de influir en la configuración de la playa seca, no se han llevado a cabo experimentos o medidas de campo en el presente trabajo. Existen estudios en la literatura comparando el efecto de ambas fuerzas sobre los granos de arena, pero ninguno cuantificando la afección real que el viento puede llegar a tener –o no- sobre la configuración del perfil de equilibrio. Sería pues interesante monitorizar algunas playas en las cuales el efecto del viento puede ser notable (playas situadas en el estrecho de Gibraltar, por ejemplo) para cuantificar este factor potencial.

- Respecto a los mecanismos de intercambio entre las partes sumergidas y emergidas todavía existen varias incertidumbres. La presencia –o no- de barras, condicionadas a su vez por mecanismos de transporte longitudinal, determina la presencia – o no- de bermas en el frente de playa. Debido a esto, una playa sometida a las mismas condiciones de oleaje a lo largo de toda su extensión puede presentar bermas en determinadas zonas y en otras no. Así, un estudio topográfico y batimétrico detallado con la suficiente cobertura temporal sería interesante para estudiar la influencia de las barras en el crecimiento de la berma.

- En relación con el punto anterior, existe una delgada línea entre el crecimiento de

la berma y su repentina destrucción debido al aumento del runup (consecuencia del aumento del oleaje). Este hecho puede condicionar drásticamente la presencia de un tipo de perfil u otro en la misma playa. Un estudio basado en procesos podría llevarse a cabo para investigar este mecanismo tan complejo, conocido en la literatura como "la paradoja de la altura de la berma".

- El modelo paramétrico propuesto tiene una serie de limitaciones. Las playas intermedias y reflejantes están bien testadas y el modelo funciona aceptablemente, pero playas altamente disipativas con estados modales mayores de 7 quedan fuera de nuestro rango de aplicación. Playas de estas características, como las estudiadas en el Capítulo III, deberían ser estudiadas en términos de configuración de equilibrio del perfil de playa seca bajo una aproximación similar a la llevada a cabo en el Capítulo IV de esta tesis.

- Sería también interesante desarrollar una configuración paramétrica de equilibrio que salve los puntos de discontinuidad en el perfil completo de playa y permita predecir, a partir de las mismas condiciones de oleaje y sedimento, un perfil de equilibrio que comprenda desde la profundidad de cierre hasta el pie de duna, incluyendo así en una misma expresión las zonas sumergidas, intermareales y emergidas. Además, términos de segundo orden podrían ser incluidos para representar adecuadamente formas secundarias como pueden ser las barras sumergidas, la cresta de la berma o la concavidad del final del perfil próximo al pie de duna.

- Un gran complemento a este estudio sería la proposición de un modelo de evolución o desequilibrio en el corto o medio plazo. Es decir, un modelo de evolución que incluya las formulaciones pertinentes de transporte de sedimentos y que sea capaz de predecir el tiempo que necesita la playa seca para acomodarse de nuevo a las condiciones medias de equilibrio cuando se encuentra fuera de ellas, bien porque esté erosionada o bien porque presente excesiva acumulación de sedimento. Existen numerosos trabajos en la literatura que proponen una curva energética de equilibrio, pero ninguno relacionado con el segmento del perfil de playa seca.

1

Introduction

1.1 Motivation for the thesis

The study of the beach from a physical point of view has been a research topic for many years and so it will be in the future. Beaches are the main worldwide coastline features and have a huge importance for three main reasons:

i From the **ecological point of view**, the beach can be defined as an interphase between land and sea that provides habitat and nesting grounds for essential ocean and coastal wildlife. This environment provides the basis for ecological processes, ecosystem resilience, and thus the sustainability of ecosystem-service delivery on which human livelihoods depend (Díaz *et al.* 2006, Duarte 2004). The negative impacts that man causes to a beach can derive in a loss of biodiversity, and maintaining this biological factor is a key element in the whole coastal ecosystem. It is also crucial to maintain a good ecological value in beaches to preserve their resilience. According to Berry *et al.* (2014), resilient sandy beach ecosystems adapt to sea level rise while preserving their structure, function and feedback. As an example, the beach front flora plays a major role in stabilizing the foredunes and preventing beach erosion and inland movement of dunes. They trap sand particles and rainwater and enrich the surface layer of the dunes, allowing other plant species to become established (Defeo *et al.* 2009).

ii From the **shoreline protection point of view**, the beach-dune system plays also a necessary role by dissipating the energy from attacking waves, protecting the shore from extreme events and acting as a barrier against flooding. The cross-shore section of the beach, therefore, determines the buffering ability. The sea level change and associated extreme water levels will mainly lead to beach erosion and shoreline retreat, amongst

other related range of impacts like temporary flooding, temporary submergence of low lying areas, wetland change and loss and salinity intrusion into aquifers (Nicholls *et al.* 2007). Long term erosion of beaches is already a widespread phenomenon at the regional and global scale (Bird 1985). As an example of the consequences of sand loss in beaches, Fig. 1.1 shows the dramatic sea level change and the land loss cost for the different scenarios proposed by the IPCC (*Intergovernmental Panel on Climate Change*). There is also a raising appreciation amongst the public opinion concerning the sea level change and frequency and intensity of extreme events and its consequences. News as shown in Fig. 1.2 are highly recurrent and of high interest for public opinion. To preserve the beach resilience against these erosive events is capital to maintain the acceptable level of assumed risk of flooding and damage along the coast.

iii Last but not least, the third reason why the morphology and dynamics of the dry beach should be well understood is motivated by the **economic issue derived from tourism**. Beaches are natural resources that form the basis for tourism all over the world. The concept "beach and sun" is coined by many countries as a lure for tourists. Sandy beaches are unique natural resources and are critical for the economic and environmental development of certain coastal regions (Yepes & Medina 2005). Furthermore, the demand of these spaces is growing. Talking about economics, it can be illustrating some data about the "beach tourism" in Spain and its repercussion. Spain has around $6.500Km$ of coast from which a 28% are beaches of very diverse typology. The number of visitors in Spain is about 56 million per year, and 80% goes to the coast (Fig. 1.3). The economic balance in this sector represents the 11.4% of the Gross National Product and maintained almost 11.2% of the direct employment. It can be assumed that as much capacity a beach has, more people can accommodate and, therefore, more tourism can host a village or a coastal region. Authors like Valdemoro & Jimenez (2006) say that the satisfaction of the tourist is directly related to the wideness of the beach, estimating that the mean capacity of a beach is around 6 m^2 per person.

Summarizing, besides its ecological value, during winter the protective role of the hinterland may be affected and infrastructures such as promenades can be damaged, therefore the beach has to be wide enough to avoid being completely eroded by storms. On the other hand, in the summer, there may not be sufficient emerged beach to allocate users, thus the available sand volume should allow the generation of a beach wide enough to offer an acceptable space for leisure (Fig. 1.2 - b,c).

It is clear from the above that it is essential to have an adequate understanding of the processes governing the dry beach and the linking between dynamics and morphology. After presenting the main reasons why the dry beach should be investigated in detail, some **re-**

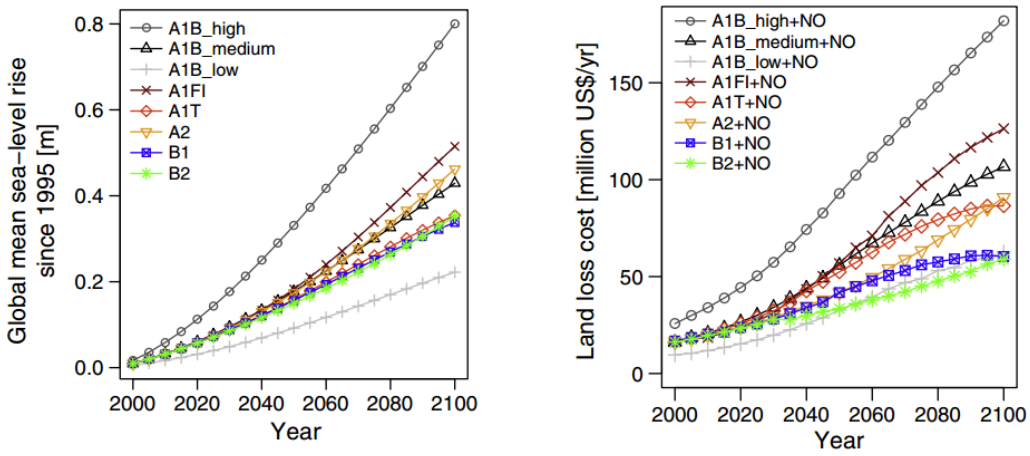

Figure 1.1: Global mean sea level rise and land loss cost for different future scenarios. Obtained from Hinkel *et al.* (2013).

search questions arise. Throughout the development of this thesis we will be able to answer the following questions:

- *Which are the main agents governing the dry beach morphology?*
- *What are the main dry beach profile features and morphological indexes?*
- *Under which conditions the dry beach present one type of equilibrium profile or another?*
- *How the dry beach profile will respond to changes in the driving and controlling factors?*
- *How the controlling factors shape the equilibrium profile?*
- *Which are the widths, slopes and heights that define the equilibrium under the mean surrounding conditions?*
- *Is there a parametric equation that defines the equilibrium profile configuration? In that case, which are the drivers of this equation and how are they related to the main governing factors?*

We want to understand how the dry beach responds to changes in dynamics, how it will retreat after storm events or how it will accommodate to the mean wave conditions. We want also to set the basis for an equilibrium configuration of the beach, which may lead us to calculate widths, heights and slopes of equilibrium. It will be able to know how nourishments should be carried out to be the most efficient or which should be the level or height of the dry beach to reduce the time that the beach is flooded during storm events or to have enough space to allocate users during summer seasons. This thesis will give answer to these questions and it will open gates for new research topics related to the dry part of the beach.

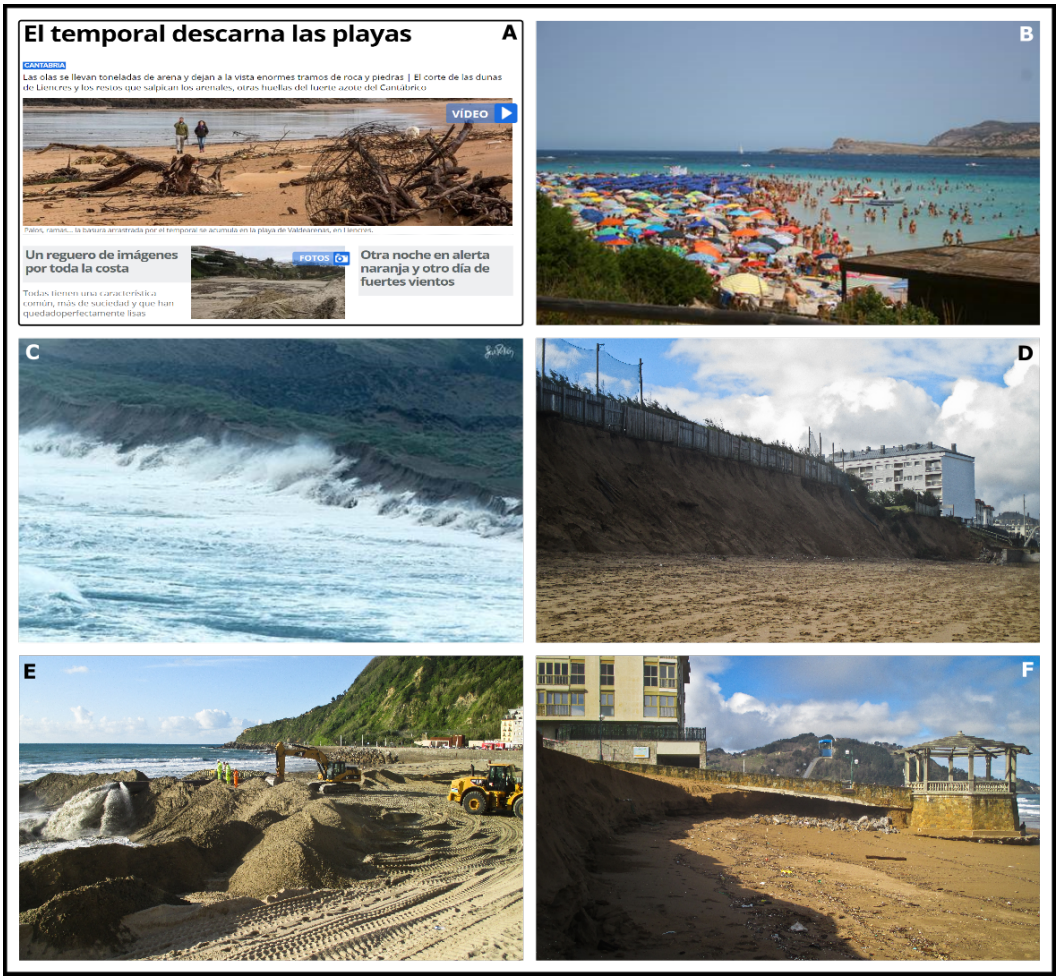

Figure 1.2: *a)* News from 16-feb-2016, Santander, Cantabria (Spain). Translation from Spanish: "*The storm corrode the beaches: The waves wash away the sand [...]; cuts in the dune systems [...]; all beaches have a common feature: they are now perfectly flat [...]; another night under warning [...]*". Source: diariomontanes.com. *b, c)* Examples of the two main roles of the dry beach: Crowded beach in Sardinia (Italy), July 2013; Liencres Beach (Cantabria, Spain) during a strong sea storm in March 2014. *d, f)* Damages and heavy dune erosion in Zarautz Beach (Zarautz, Gipuzkoa, Spain) after several storms during winter 2013-2014. *e)* Zurriola Beach (Donostia, Gipuzkoa, Spain) during nourishment in spring-summer 2014 to widen the dry beach for an intensive tourist summer season.

1.2 Background

This thesis focuses on the study of the dry beach profile. In order to explore the equilibrium configuration, which is the ultimate goal of this work, different approaches must be introduced and investigated beforehand. Firstly, we need to define what the dry beach is and where its boundaries are. Then the commitment is to identify and understand the different dynamics which drive the main changes in the dry beach and how the morphological response is in both spatial and temporal scales. Finally, we must give account about how the driving factors modulate the equilibrium, providing the most stable configuration in relation to the

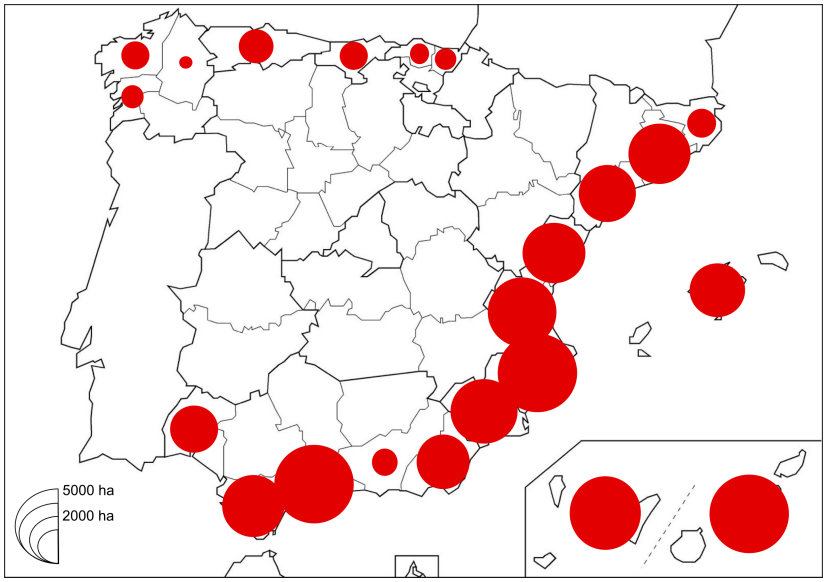

Figure 1.3: Growing of artificial surface along the Spanish Coast between 2000 and 2006. Source: IGN (*Spanish National Geographic Institute*).

environment, *i.e.*, sediments and wave climate. This introductory chapter is therefore split into three sub-chapters. The first sub-chapter deals with the general understanding about what is the dry beach and how it should be investigated in order to give response to the above mentioned research questions. The second deals width the driving factors of the dry beach shape, and the third talks about the first approaches to an equilibrium configurations and how it should be investigated.

1.2.1 The dry beach: Boundaries and how to investigate its morphology

The dry part of the beach, named also subaerial beach, comprises the zone between the intertidal-submerged zone and the landward edge (Fig. 1.4). It is a zone that is episodically impacted by both swash and aeolian sand transport, forming a dynamic boundary between wave and tide dominated zone and the wind dominated dune system (Short 1999). The dry beach is normally backed by a fixed boundary like a cliff, a seawall or a promenade, and it can also be delimited by a non-fixed boundary like a dune system. According to Swart (1976), the upper limit of the subaerial beach is chosen at the highest level from which sediment can be eroded indirectly by wave action. Numerous works can be found in the literature dealing with the morphology of the submerged and intertidal zones and their equilibrium profile (Bernabeu *et al.* 2003, Brunn 1954, Dean 1991, Larson & Kraus 1995), as well as with the morphology of the dune system (Cariolet & Suanez 2013, deVries *et al.* 2012, Hesp 2002; 2012, Nordstrom *et al.* 1992, Otvos 2000, van-der Burgh *et al.* 2011). Conversely, besides it is the primary focus of erosion research (Mull & Ruggiero 2014), morphological studies of

the dry segment require further insight.

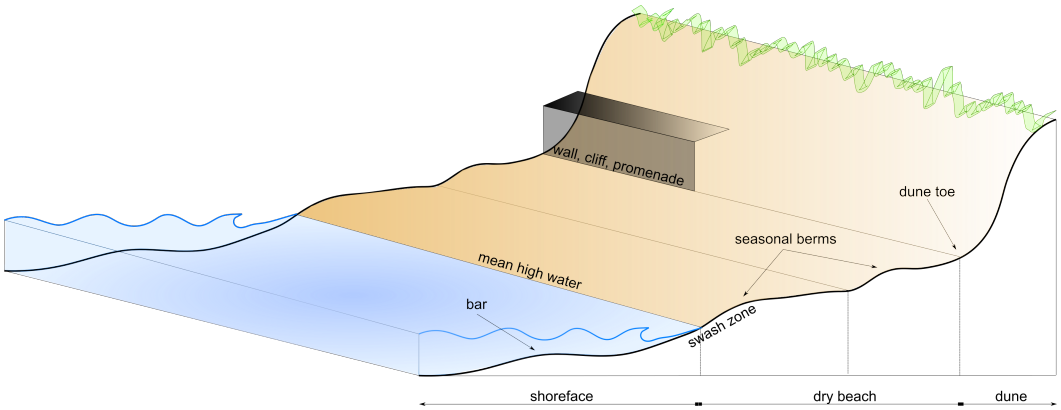

Figure 1.4: Diagram of the coastal planform indicating the different parts of the beach system.

We based the first approach to the study on previous works about "conceptual beach models". The first on proposing these methodologies to investigate beach morphologies were Chappell & Eliot (1979) and Wright & Short (1984). Nowadays, the use of conceptual beach models is largely extended and accepted. They predict beach morphologies as a function of wave, tide and sediment parameters, and provide a specific framework in which beach features and dynamics can be studied precisely. Moreover, these models offer a better understanding of the whole beach system, and are therefore useful for scientists, policy makers and beach users. The specific framework provided by a conceptual model can help to understand and avoid the two main problems affecting beaches, as described in the last section: damage by wave action during winter and lack of space during summer.

The first conceptual beach models proposed by the authors mentioned above related wave climate and sediment characteristics with morphology, but their studies were developed in micro tidal environments, under relatively low energetic conditions and limited to a specific coastal environment. Wright & Short (1984) (Fig. 1.5 - left panel) refined these previous works, while Wright *et al.* (1985) improved the existing classification including energetic environments and tidal influence. Then, Masselink & Short (1993) included rigorously the effect of tides by adding the Relative Tide Range ($RTR = TR/H_b$) as a main hydrodynamic control variable to their model (Fig. 1.5 - right panel). They classified the various morphotypes attending to the relation between RTR and the dimensionless fall velocity Ω (Dalrymple & Thompson 1976, Dean 1977).

$$\Omega = \frac{H_b}{w_s T} \tag{1.1}$$

where H_b is the wave breaker height (m), w_s is the sediment fall velocity (m/s) and T is the wave period (s). In later studies, Short (2006) added the geological constraint as an important

driven factor in governing beach morphology. Recent works like Scott *et al.* (2011), extended the previous beach models by adding beaches ranging from fully dissipative to fully reflective, and from flat to multi-barred in meso-macro tidal environments (Fig. 1.6). Furthermore, they pointed out the importance of geological control and wave power as fundamental variables.

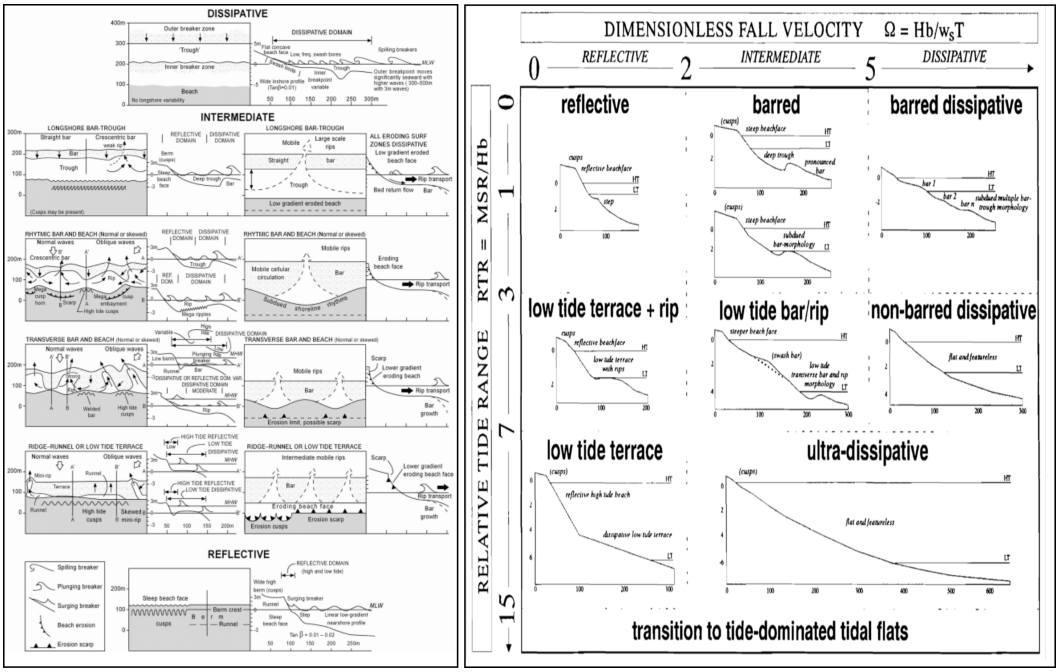

Figure 1.5: Conceptual beach models. Left panel: Beach modal states adapted by Short (1999) from the original work of Wright & Short (1984). Right panel: Beach classification including Relative Tide Range (Masselink & Short 1993).

Nonetheless, all these works have certain limitations. They dealt essentially with the part of the beach which is fully controlled by waves and tides, providing morphologies of the submerged and intertidal zone. Furthermore, Gomez-Pujol *et al.* (2007) found that only 1/3 of the observed states matched the predicted models and demonstrated that intermediate states are not rigorously represented by the controlling variables proposed by Wright & Short (1984). Scott *et al.* (2011) added some insight into applicability of the models and agreed with Jackson *et al.* (2005) arguing that there is no universal beach model and their predictions must be taken carefully and always under a proper understanding of the morphodynamics of the specific study site. Taking all of this into account and based on these previous studies, in *Chapter II* [2] is presented a conceptual beach model which serves as a detailed approach to the morphology of the dry part of the beach in the cross-shore direction and set the basis for further research on dry beach morphology.

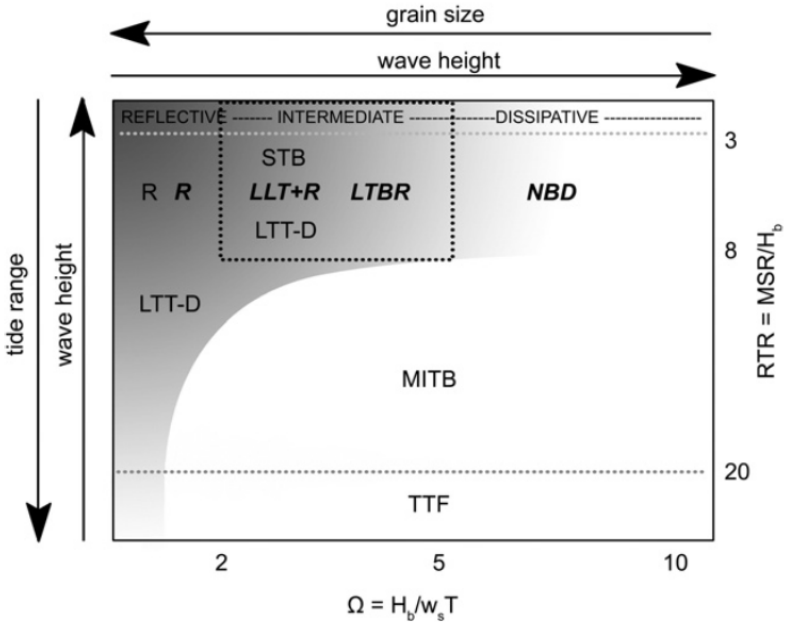

Figure 1.6: Conceptual beach model including beaches from fully dissipative to fully reflective and from flat to multi-barred in meso-macro tidal environments. Scott *et al.* (2011), from sampled beaches throughout England and Wales.

1.2.2 Driving parameters and morphology

This sub-section introduces the main factors controlling the dry beach and talks about how the morphology may be shaped due to these forcings. Firstly, we discuss about the role of wind in modifying the dry beach shape and we give some information about sand transport by wind. Next we introduce some key concepts concerning the runup and the sediment transport by waves in the swash zone, and finally we talk about the berm, which arises as the main morphological feature that characterizes the dry beach profile.

1.2.2.1 Wave action *vs* wind action over the dry beach

Despite the fact that cross-shore aeolian sediment transport supplies sediment to the backshore and allows the growth of dune systems, the shape of subaerial beach is mainly modulated by wave action and tides, and its morphology has a direct relation with modal morphodynamic state of the beach. According to Wright & Short (1984), the term "beach type" refers to the prevailing nature of the beach, including the morphology of the surf zone (waves, currents, bars, troughs), and that of the subaerial beach. He found evidences that the morphology of the subaerial beach is directly related with its modal state. Short & Hesp (1982) and Hesp (1988), showed that there is a direct relationship between modal state and type, volume and size of the front dune, which suggests that the morphology of the zone in be-

tween, *i.e.*, the dry beach, is also directly related to the modal state of the beach. Based on that, the wave climate and the grain size appear to be the main driving factors controlling the equilibrium morphology.

High water levels due to storm surges, high spring tides or combination of both, have the capacity to control the equilibrium shape of the subaerial beach, causing large wave-induced flooding and consequently erosion and accumulation in the backshore. The dominant portion of extreme total water levels that normally flood the dry beach is given by wave-induced events, that is, runup – which is the combination of swash + setup (Holman 1986).- According to previous studies, hydrodynamic forces dominate over wind drag forces in controlling the subaerial beach equilibrium morphology (Delgado-Fernández & Davidson-Arnott 2011), and despite noticeable rates of aeolian sand transport, the significant changes in the dry beach are controlled by the magnitude and frequency of high-water levels (Ruz & Meur-Ferec 2004). Udo & Yamawaki (2006) suggest that over the dry beach, the wave action prevails as a main actor to shape the bed, rather than the wind, even in beaches that are completely flooded by waves only a few days in a year. To affirm these statements, several authors have considered both wave and wind actions over the dry beach, concluding that the wind transport capacity highly depends on sediment availability -*i.e.,* in intertidal bars to supply sand to foredunes (Aagard *et al.* 2004)-, effective fetch and moisture contents (Bauer *et al.* 2008). In any case, to know how the wind acts over the sand, there is here resumed some information about wind transport over the dry beach. Despite it is a secondary force and is dwarfed by wave flooding, it is relevant to give some information about this kind of sand transport. Actually, wind can lead to some rare forms or anomalous accumulations of sand (Fig. 1.7).

1.2.2.2 **Aeolian sand transport**

Sand transport by wind across the beach is a complex mechanism that involves different factors that are very variable in space and time. This sediment transport is controlled by temporal factors such as mean wind speed, wind gusts and surface wetting and drying, and by spatial factors such as surface moisture, grain size, fetch length and surface morphology. Besides, the movement of sand is quite intermittent due to the own nature of the wind regime. When the threshold of motion is reached, the grains begin to move, but is rare to reach a steady state of equilibrium. If the mean wind velocity is over the threshold of motion, the mass flux over the bed is continuous but normally does not get a steady state in terms of mass flux (Davidson-Arnott 1988).

Threshold of motion

The air exerts two types of forces on grains when blowing on a sandy bed: drag and lift

Figure 1.7: *Left panels*: Effects of persistent aeolian longshore sand transport in Barbate Beach (Atlantic South Coast of Spain, Cádiz, Apr' 14). Strong geographical winds due to geological constraints (*Ventury* effect near Strait of Gibraltar) hit this stretch of coast in the longshore direction, causing heavy accumulation of sand at one lateral edge of the beach. *Right panels*: Rare aeolian forms over the dry zone in Agate Beach (Newport, OR, Oct '15) due to the absence of flooding during summer months and the presence of persistent winds.

forces. When the combination of these forces is greater than the forces that maintain the grains united and the forces of gravity, the critical shear stress is reached and the grains begin to move (Fig. 1.8), Bagnold (1941) set the principles of the aeolian sand motion by proposing the critical shear velocity, called the threshold of motion shear velocity v_t^*:

$$v_t^* = A\sqrt{\frac{\rho_s - \rho_a}{\rho_a} gd} \tag{1.2}$$

Where A is a coefficient that depends on the characteristics of the sediment, ρ_a and ρ_s are the densities of the air and sediment, g is the gravity and d is the grain diameter.

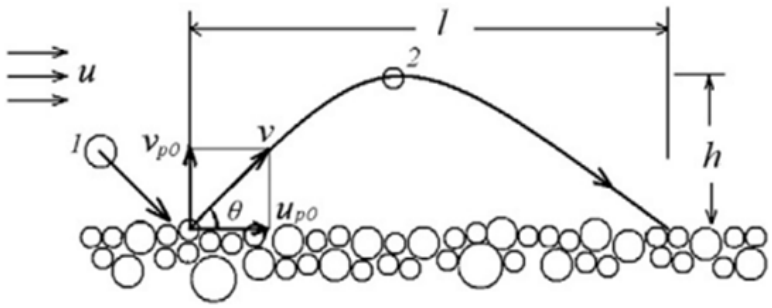

Figure 1.8: A schematic diagram of the impact-ejection process in sand transport with the two forces involved. Modified after Allen (1980).

Effect of moisture content

The presence of humidity is the moisture present in the intra-grain pore spaces. Thus, substantial moisture content in the surface sediments reduces transport potential significantly by enhancing the critical shear velocity. Tides and waves influence moisture conditions on the foreshore, whereas atmospheric humidity and precipitation induce moisture in the dry and back-beach environment. According to Sherman *et al.* (1998), the transport rates are about 25% less with a high humidity content in the surface for velocities around 1 m/s. Sherman *et al.* (1998) reports that the maximum possible gravimetric moisture content of beach sediments is about w =25% (Fig. 1.9).

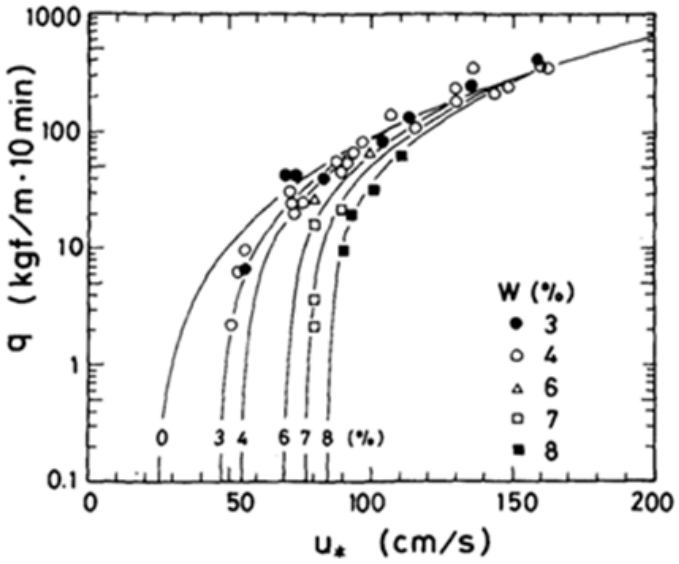

Figure 1.9: Sand transport rate under high shear velocity on a wet sand surface. Source: Sherman *et al.* (1998).

However, Sherman *et al.* (1998) showed that the models with moisture correction inadequately represent the influences of moisture content, especially at larger moisture contents ($w > 7\%$). Hotta *et al.* (1984) make a review of several previous works concerning this particular topic and carried out an extensive field campaign to investigate the effects of moisture. The main conclusions are that the generation of blown sand on a wet sand surface will be strongly affected by the evaporation rate. Also, the sand transport rate on a wet sand surface is comparable to that on a dry sand surface when the water content of the surface is small. However, the transport rate decreases suddenly when the water content reaches a certain value. And last, concerning the wind speed, the sand transport rate on a wet sand surface is low when wind speed is low. However, the transport rate becomes comparable to that on a dry sand surface when the wind speed is high even if the sand layer has water content of a few percent. To know more details about moisture effects on aeolian sand transport on beaches, readers are referred to Bauer *et al.* (2008), Davidson-Arnott & Bauer (2009) and

Wiggs *et al.* (2004).

Effect of rough elements

Sometimes, elements such as vegetation, gravel or shells placed on the sandy surface can alter the threshold of motion shear velocity. They can absorb a portion of the shear stress, protecting the erodible surface below. If the horizontal spacing between the elements is high, the wind field may be altered in a way that can facilitate the lift-off of the grains. On the other hand, if the coverage is high, the elements act as a protection and the shear velocity has to be higher in order to initiate the transport.

Effect of slopes

The firs approach to understand the effect of a non-horizontal bed on the sediment transport by wind was given by Bagnold (1941). The slope increases the amount of transported sediment when wind blows downhill and decreases when wind blows uphill. He added an extra term into the transport rate equation on a smooth horizontal surface. Under the existence of a slope with an angle with the horizontal α and the internal friction angle of the sand θ, the transport rate on an inclined surface q_i is given as follows:

$$q_i = q/(\cos\theta(\tan\alpha + \tan\theta)) \tag{1.3}$$

Fetch length

The fetch effect (Davidson-Arnott & Bauer 2009) is the distance required to achieve full transport conditions. The fetch of wind over beach sand is defined as the length of beach from the water's edge to the dune foot, measured along the direction of the wind. It was calculated using:

$$f = \frac{\omega_c}{\cos\alpha} \tag{1.4}$$

Where f is the fetch length, ω_c is the calculated width of subaerial beach and α is the angle between the wind direction and a line normal to the coast (Fig. 1.10).

Tidal excursions and storm surges can exert strong influences on the 'effective' geometry of beaches as it relates to the aeolian transport of sediment, especially in macro or meso-tidal environments with flat, dissipative beaches (Nordstrom *et al.* 1992). It is important also to notice that the angle of wind approach and fetch distance may be more important than having a very strong wind (Delgado-Fernández & Davidson-Arnott 2011). Dissipative beaches, with a wider foreshore and low gradient, provide less resistance to wind flow, and are more conducive to aeolian sand transport than the steeper reflective beaches (Short &

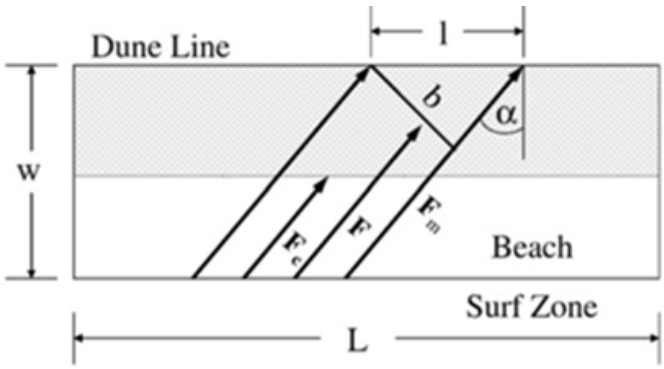

Figure 1.10: Scheme of the relation between wind angle α, beach width ω and fetch distance F. Shaded area indicate the zone of maximum equilibrium transport. F_c is the critical fetch distance, which indicates the minimum distance to achieve the maximum transport conditions, and F_m is the maximum available fetch. Modified from Bauer *et al.* (2008).

Hesp 1982). In addition, dissipative beaches generally comprise finer sand which requires a lower threshold velocity to entrain sediment (Hesp 1999). In contrast, reflective beaches are generally composed of coarse grained material requiring higher threshold velocity to overcome the gravitational force and static friction. The steeper profile and the more irregular nature of the reflective beach also results in a zone of reduced wind speeds at the rear of the foreshore, which is less conducive to aeolian transport (Fig. 1.11, Fig. 1.12).

1.2.2.3 **Runup and swash zone sediment transport**

Concerning the topic of this work, the attention is focused here because the cross-shore sediment transport in this zone is the principal exchange mechanism between the subaerial and submerged part of the beach (Masselink & Puleo 2006). The shape and process of accretion and erosion of the beach face are directly linked to this exchange sediment transport, and, consequently, the longer term stability and evolution of the coastal zone. The swash zone, which is the part of the beach that is alternately covered and exposed by uprush and backwash, or, according with Hughes & Turner (1999), the time varying region extending from the point of bore collapse on the beach face to the maximum uprush limit, controls the sediment transport across the beachface and the foreshore. This part is a very dynamic zone, with a temporal timescale of the processes from seconds, in relative low energy, shelter and reflective beaches, to minutes, in high exposed, dissipative and energetic beaches. The turbulence, strong currents and high rates of sediment transport characterizes this zone (Puleo *et al.* 2011). Taking it as a whole, the velocity skewness during the swash cycle is offshore, because the duration of the backwash is larger than in the uprush (Masselink & Puleo 2006). As a consequence, it could be assumed that the net sediment transport is offshore. Basing on this, the beach should be eroding constantly. However, the bed

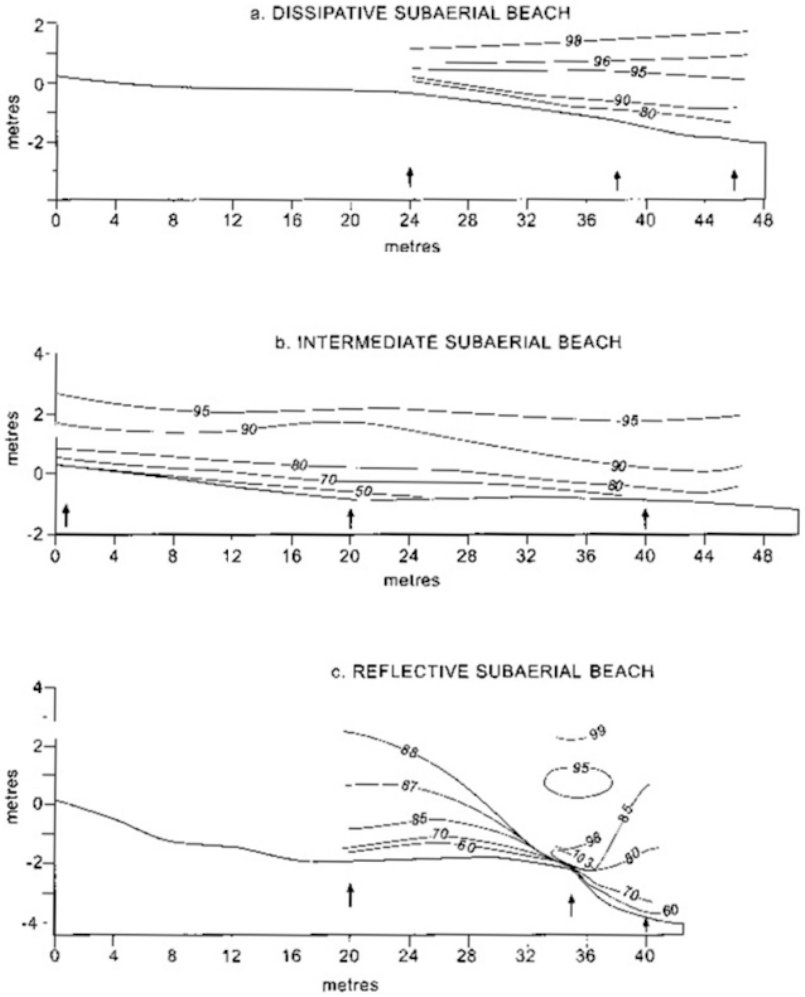

Figure 1.11: Wind speed iso-lines over a dissipative, intermediate and reflective beach (Hesp 2002).

Figure 1.12: Fetch distance for aeolian mobilization may be different between coarse grained-low energetic-reflective beaches (*Left picture*: Gandía Beach, Valencia, Mediterranean Coast of Spain) and fine grained-high exposed-dissipative beaches (*Right picture*: Liencres Beach, Cantabria, North Coast of Spain).

shear stress is bigger in the uprush due to in/exfiltration effects, bore turbulence and flow acceleration (Butt & Russell 2000, Karambas 2003, Nielsen & Hanslow 1992), favoring the development of the beach face (Holland *et al.* 1995). A schematized example of the response

to wave field conditions and morphology response on the beachface is resumed in Fig. 1.13.

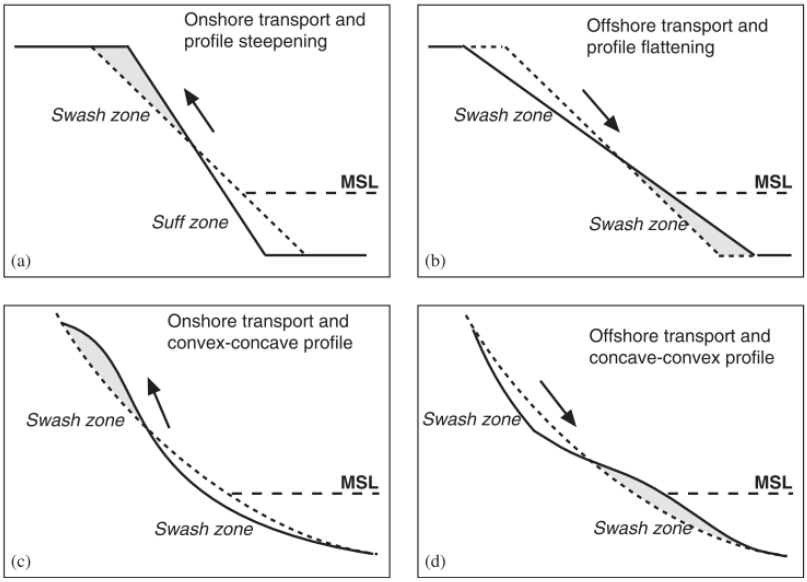

Figure 1.13: Idealized *(a, b)* and realistic *(c, d)* beachface response to changing wave conditions. Masselink & Puleo (2006).

Regarding the runup, the energy that is not dissipated in the surf zone is transformed in potential energy in the foreshore of the beach in form of runup (Holland *et al.* 1995). Runup can be defined as the set of discrete maximum water level elevation, measured on the foreshore, with respect to still water level. Runup results from two dynamically different processes: (1) maximum setup, the time-averaged water-level elevation at the shoreline, and (2) swash, the time-varying, vertical fluctuations about the temporal mean (Stockdon *et al.* 2006). It is a process that can generate extreme water levels (Bellomo *et al.* 1999, Ruggiero *et al.* 2001), and is a key factor during coastal erosion processes (Larson *et al.* 2004). Among the several formulations for calculating runup on beaches (Ahrens & Seelig 2001, Batjes 1974, Holman 1986, Hunt 1959, Mase 1988, Nielsen & Hanslow 1992), Stockdon *et al.* (2006), through the collection of field data in diverse experiments, proposed a direct relation between runup and wave parameters and explain these elevations in terms of H and L:

$$R_2 = 1.1(0.35\beta_f(H_0L_0)^{1/2} + \frac{[H_0L_0(0.563\beta_f^2 + 0.004)]^{1/2}}{2}), 0.3 < \xi_0 < 1.25 \tag{1.5}$$

$$R_2 = 0.043(H_0L_0)^{1/2}, \xi_0 < 0.3 \tag{1.6}$$

Where β_f is the foreshore slope and H_0 and L_0 are the deep water wave height and wave length, respectively. ξ_0 is a surf scale parameter named Iribarren Number (Batjes 1974). It combines foreshore slope and wave steepness and indicates the breaking wave types on beaches

and represents the variations on the amount of wave energy dissipation and reflection (values less than 0.4 indicates spilling breaking type, typical from dissipative beaches). When the beach receive high energy from waves, the beach slope accommodates to a flatter state in order to dissipate more energy, so when ξ gets smaller means that the breaking type is "more spilling", indicating a need to dissipate more energy.

$$\xi_0 = \frac{\beta}{(H_0 L_0)^{1/2}} \tag{1.7}$$

1.2.2.4 **The berm**

The berm is a key dry beach profile (DBP) feature, and in this sub-chapter we deal with it and give some light about the previous studies concerning its morphodynamics. The berm is a supratidal form built by swash. It acts as a sediment source to the dune system through aeolian transport and to the foreshore and surf zone during periods of erosion. Berms are, in a sense, the opposite of bars since they are the depositional sand form and bars are the erosional sand form (Bascom 1951). Their formation depends on both hydrodynamic (runup) processes and geomorphological constraints, which include sediment supply, preexisting topography and mean sea level (Orford *et al.* 2002). Uprush sediment transport and overwash at the position of the existing berm crest is therefore the key to determining berm growth (Baldock *et al.* 2005). The presence of seasonal berms is to this work a primary focus of study due to its importance for explaining certain changes in dry beach morphology (Orford *et al.* 2002). Berms are common beachface features on sandy coastlines and are constantly evolving in response to gradients in cross-shore sediment transport – *i.e.*, imbalance between uprush and backrush sediment transport-, and they are also conditioned by intertidal and subaqueous sandbars, which provide the sand supply from the intertidal zone to the beach face and they are sometimes modulated by longshore gradients (Anthony *et al.* 2006, Masselink *et al.* 2006, Senechal *et al.* 2009): the intertidal - nearshore morphology fronting the dry beach can play a big role in terms of whether a berm is present or can be destroyed. The longshore variability responsible of the presence or not of intertidal - subaqueous bars may determine the presence or not of berms even when the entire beach is subjected to the same wave climate at the nearshore. Focusing only in cross-shore variations, during mild summer conditions, berms are usually formed at the foreshore between mean sea level and just above the mean runup level (Katoh & Yanagishima 1992, Suzuki *et al.* 2013, Thomas & Baba 2001). Under increasing total water level conditions, the berm may migrate landward when the runup exceeds the berm crest height, with the berm gaining elevation in this process. However, the berm growing exhibits a threshold conditions whereby if the wave conditions are sufficient or when the runup reaches the dune toe (Fig. 1.14), the beach face can be eroded and sometimes

even destroyed (Weir *et al.* 2006). At this point in the seasonal cycle, the foreshore dissipates more of the incident wave energy and, correspondingly, morphologic changes on the upper beach decrease in response to reduced total water levels and less wave action above mean high water line (vanGent *et al.* 2008). While erosion of the berm can occur over a single storm event, berm development is a much slower process – often taking weeks to months (Cohn & Ruggiero 2015). Fig. 1.14 shows the two extreme cases in case of berm formation and erosion. On one side, fine grained and energetic beaches rarely displays berms due to the high water levels often reaching the dune toe. On the other side, gravel beaches often display a very stable segment between berm crest and landward edge because it is a zone rarely water covered.

Figure 1.14: *Upper picture*: Landmarks of extreme runup almost reaching the dune toe in a fine grained, high exposed, planar and featureless beach. Netarts Bay, OR, Nov '15. *Lower picture*: High berm and steep foreshore on a gravel beach under energetic wave climate. Cobble Beach, Yaquina Head, OR, Oct '15.

There has been a significant development since Bagnold (1941) first carried out laboratory experiments on the formation of berms. He showed that the height of the berm above still water level is proportional to the wave height in the form:

$$B_h = \alpha H' \tag{1.8}$$

The coefficient α notes the dependence with the sediment characteristics, and H' is the difference between the crest level of offshore waves and the level of the lowest exposed beach line. Some years later, Bascom (1951) introduced the effect of wave refraction:

$$B_h = 1.3\kappa_r H_0 \tag{1.9}$$

With κ_r the refraction coefficient and H_0 the deep water wave height. Then, Rector (1954) added to the formulation the deep water wavelength L_0:

$$B_h = 0.18(H_0 L_0)^{1/2} \tag{1.10}$$

With the support of experimental data, Sunamura (1975) also found the expression:

$$B_h = 0.09 H_0^{3/10} L_0^{7/10} \tag{1.11}$$

Takeda & Sunamura (1982) found another relation, based on field data:

$$B_h = 0.125(gT^2)^{3/8}(H_b)^{5/8} \tag{1.12}$$

Where T is the wave period and H_b is the breaker height. They assumed that the berm height was independent of grain size in the range 0.22-1.3 mm. They found good agreements with the field measurements in the Hazaki Oceanographical Research Facility in Japan. Few years later, Larson (1988) added the beach slope β to the relation:

$$B_h = 1.47 H_0 (\frac{\tan\beta}{H_0 L_0})^{0.79} \tag{1.13}$$

Katoh & Yanagishima (1992) determined that the infragravity waves and the level rising of water table play an important role in the berm formation and erosion in a storm and, therefore, it should be very important to take into account the infragravity waves as the external force. Obtained and tested with field data, the found that the critical level of sand accumulation D_L can be predicted with the following equation:

$$D_L = \mu_0 + 0.96 H_{L0} + 0.31 \tag{1.14}$$

Where μ is the mean sea level at the shoreline and H_{L0} is the height of infragravity waves at the shoreline. The third term represents the effect of the wind waves runup.

In these last formulations is not clear the influence of the sediment grain size. This variable determines the permeability and the roughness of the bottom, and, therefore, the height of the berm. Okazaki & Sunamura (1994) carried out a small scale laboratory study with monochromatic wave conditions to give some light about this, and they found two expressions for collapsing and surging berms (Fig. 1.15):

$$\frac{B_h}{(gT^2)^{5/8} H_b^{1/8} D^{1/4} \phi} = 0.117 \tag{1.15}$$

$$\frac{B_h}{(gT^2)^{5/8} H_b^{1/8} D^{1/4} \phi} = 0.067 \tag{1.16}$$

D is the grain diameter, H_b is the height of breaking waves, and ϕ is a reduction factor which depends on the dimensionless grain diameter.

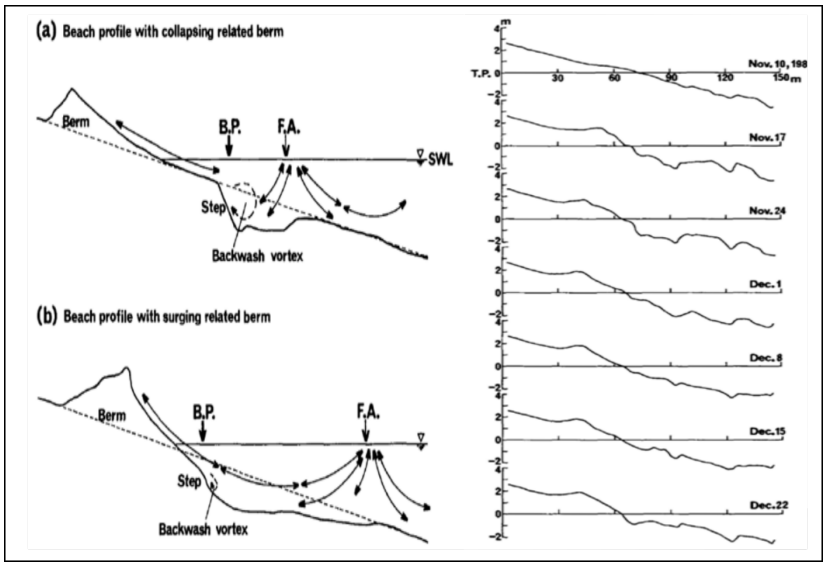

Figure 1.15: left panel: B.P denotes breaker point and F.A denotes the first antinode of standing waves. Right panel: Example of berm development after the attack of storm waves at Ajiga-ura Beach. (Okazaki & Sunamura 1994).

However, the effect of tidal ranges has been no attended in detail in the work of Okazaki & Sunamura (1994). Tidal fluctuations through the spring-neap cycle also influence berm development, mostly when overtopping is taking place (Bascom 1951). The work of Weir *et al.* (2006) gives a detailed explanation about this mechanism and the so called '*berm-height paradox*'. By increasing the wave height, the runup enhances and, consequently, the berm crest grows, but the largest waves erode the beach face and result in a reduction in berm

height. The work of Weir *et al.* (2006) deals with this issue and it is based on the spring-neap tidal cycle. During neap tides, there is no overtopping over the existing berm, and a "neap berm" is formed in a lower place in the beach face. At spring tides, the sediment of the neap berm is moved upwards and is placed on the top and over the higher "spring berm" by swash overtopping as the main process. They found two types of berm development: rapid vertical growth and some horizontal progradation, and formation of a lower neap berm on the face of the principal berm. In this work are explained these behaviors with a conceptual model based on sediment transport shape functions, describing the berm development in four different evolutionary stages (Fig. 1.16). These mechanisms together with the sediment deposition linked to swash infiltration control berm position on the beach (Austin & Masselink 2006).

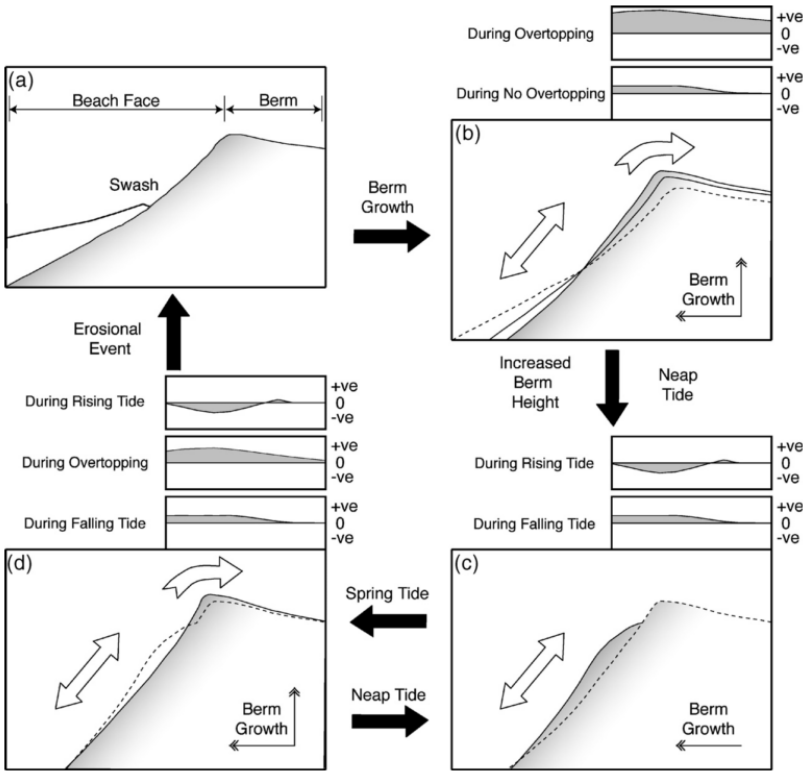

Figure 1.16: Conceptual model for berm growing following a lagoon breakout event on steep intermediate type beaches with an energetic wave climate. Weir *et al.* (2006).

.

1.2.3 Equilibrium dry beach profile

The developing of parametric forms for the cross-shore sections of the beach may lead us to give account of the main features, widths and heights that define the beach shape under the mean wave and grain size conditions. One of these parametric forms is the widely used

equilibrium beach profile (EBP). In order to develop a parametric form for the equilibrium of the dry beach, we must first understand how the changes in wave field induce changes in DBP morphology: beaches under different wave climate and sediment characteristics display different morphologies, and beaches affected by seasonality in wave climate also offer different seasonal configurations. This sub-chapter is also sub-divided into two. Firstly we talk about the temporal and spatial variations on the DBP, which may help us to set the basis for the understanding of the seasonal and inter-annual changes that the seasonality in wave climate may cause to the DBP. Secondly, we discuss about how the long term equilibrium profile is reached in response to the mean wave climate and the sediment forming the beach.

1.2.3.1 Temporal and spatial variations on the dry beach profile

The study of temporal variations, which provide essential information to coastal planning programs, can be analyzed at various scales, ranging from almost instantaneous movements such as wave driven sand transport in the swash zone, to decadal coastal evolution associated with oscillations in shoreline position along a sandy littoral cell. The long term variations explain the final stage of a beach, which can be stable, prograding or retreating. The medium-term responses, often associated with summer-winter variations, can give an idea about the location, height and width of the berm, and it helps to plan, for example, the space for beach services accommodation during summer season. Short term variations explain beach sudden retreat after a storm or flooding heights, necessary to know the location or height of infrastructures as buildings, promenades or seawalls. Coastal evolution is explained over these three temporal scale approaches. Three examples corresponding to these three temporal cycles are displayed in Fig. 1.17: storm induced scarping, seasonal cycle of erosion and recovery, and long term trends in sediment transport.

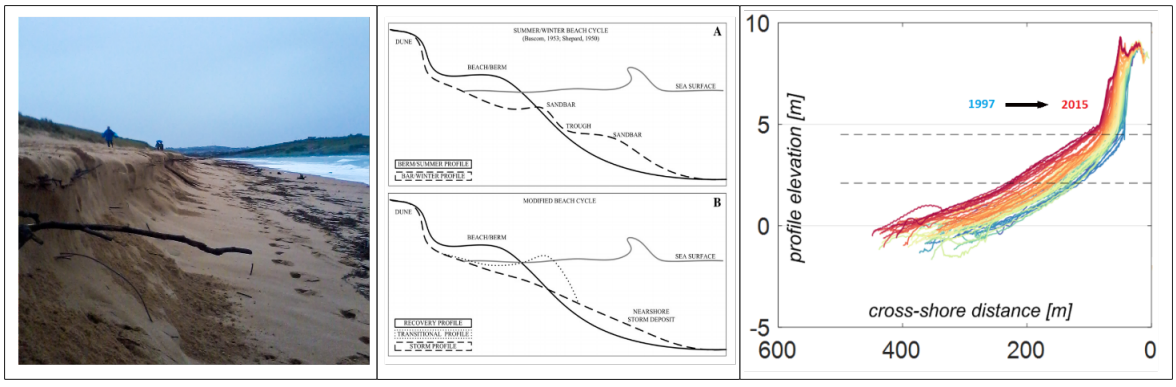

Figure 1.17: Examples of the three different temporal scales in beach processes. *Left panel*, short term: Storm scarp in Liencres Beach (Cantabria, Spain, March 2014); *Middle panel*, medium term: Seasonal changes on a beach, from Komar (1998); *Right panel*, long term: Coastline progradation from 1997 (blue) to 2015 (red) of about 150m in Clatsop Plains, OR, USA, due to long term changes in longshore sediment transport (adapted from Ruggiero *et al.* (2005).

Based on that, the time and space scales of DBP changes can be classified in different scales, according to the interaction between morphology and flow (Birkemeier 1984). In our particular case, *i.e.*, morphological changes in the DBP, occur over timescales of days or even hours - dune toe scarping or dune erosion (Suanez *et al.* 2012)-, but also over several years due to changes in cross-shore and longshore sediment annual transport rates (Aagard *et al.* 2004). Long term variations are thus closely related to short-term variations, and therefore, to predict future changes at large scale, knowing short and medium term variations is important (Morton & Speed 1998, Ruggiero *et al.* 2005). The cross-shore sediment transport can be onshore or offshore, allowing the beach to grow or to retreat, respectively. These two processes are entirely asymmetric in their origin and also in their corresponding temporal scale. Offshore sediment transport is associated to storm conditions and it occurs normally in a time scale of hours, whereas onshore sediment transport is driven by mean wave conditions and the time span is much larger, ranging from weeks to months (Fig. 1.18).

Understanding changes in the morphometrics that define the DBP, such as width, slope, berm characteristics and changes in the equilibrium shape, is essential for making predictions of coastal retreat or advance and to assess coastal hazards and associated risks. In the *Chapter III* we will study DBP changes over the medium and long term (*i.e.*, intra and inter-annual variations), both in spatial and temporal approaches.

1.2.3.2 Approaches to the equilibrium dry beach profile

The equilibrium beach profile, theoretically, is the curve under which the sediment transport is equal to zero in any direction. Nonetheless, the EBPs can be estimated as simple parametric forms obtained from looking for the similarity to well know real equilibrium cases (Dean 1977). Numerous works deal with EBPs: Bernabeu *et al.* (2003), Fig. 1.19; Dean (1991), Holman *et al.* (2014), Larson & Kraus (1995), Romanczyk *et al.* (2005) since Brunn (1954) made the first approach by proposing a power law approach in the form:

$$h = Ax^{2/3} \tag{1.17}$$

Where h is the depth, x is the cross-shore length and A is a sediment dependent parameter (Dean 1991). However, most of these works deal with the submerged and intertidal part of the profile. In this thesis we capture the characteristics for mid-long term average profile related to the emerged part, *i.e.*, the subaerial or dry profile, which comprises from the mean high water level (MHW) to the dune toe or to the wall, in case of human intervention. We refer it hereinafter as DBEP (dry beach equilibrium profile).

Concerning the dry part of the beach, as discussed in the last section, it is proved that sedi-

Figure 1.18: Canallave Beach, Liencres, Cantabria, Spain. The picture on the upper panel, taken on March '14, shows the beach after three consecutive severe sea storms. The dry beach was completely eroded in a few days and the sand was moved far offshore. The picture on the lower panel, taken on June '16, shows the recovery and the gaining of sand on the dry zone. This recovery process under mean wave conditions needs several months or even years, whereas the sea storms can shape the beach in days or even hours.

ment characteristics and wave drag forces –rather than wind drag forces (Bauer & Davidson-Arnott 2002, Davidson-Arnott 1988) - arise as the two main factors that modulate the equilibrium morphology of the dry part of the beach (Delgado-Fernández *et al.* 2009, Hesp 2012, Nordstrom & Jackson 2012, Ruz & Meur-Ferec 2004, Udo & Yamawaki 2006): the dimensionless fall velocity, which encompasses both controlling factors (H_b breaking wave height, T wave period and Ω sediment fall velocity), is a fundamental parameter not only to define the morphology of the sub and intertidal part of the beach, but also to determine the morphology of the emerged part. Furthermore, the sand supply from the shoreface to the dry

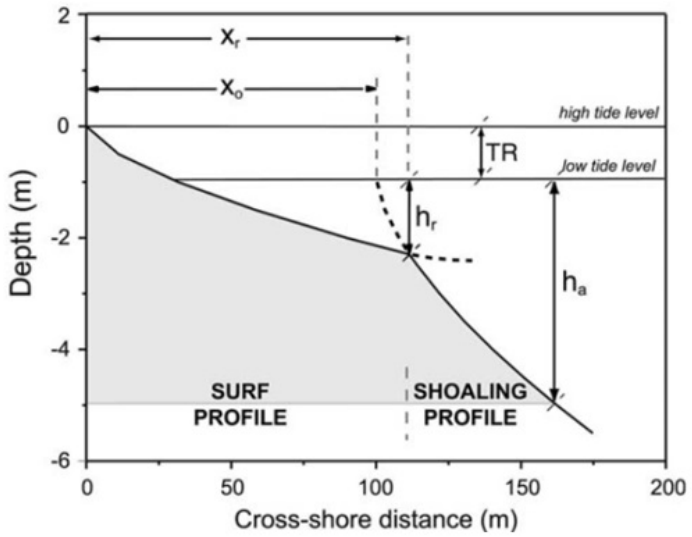

Figure 1.19: Example of a parametric equilibrium beach profile including tidal influences, from Bernabeu *et al.* (2003).

beach is controlled by the welding of the tidal banks that moves the sand onshore, which is also a function of the modal state of the beach (Anthony *et al.* 2006). Based on that, by just knowing the values of the wave climate and sediment characteristics -and consequently the value of Ω at the beachfront- here we will see how the morphology of the dry beach profile can be also determined. Depending on the range of Ω, the DBEP may present a specific configuration, defined by the presence –or not- of berms, and also by certain range of slopes, widths and grades of curvature.

When analyzing the equilibrium, we can establish for certain kind of beaches a static and seasonal model of equilibrium. When both equilibrium –summer-winter- configurations are well known, it can be obtained the relative displacement between profiles, always assuming the sediment conservation along the entire profile and no sediment transport in the long-shore direction -considering, therefore, the orthogonality of the processes-. There can be infinite equilibrium profiles, each of them associated to the different incident waves. The circumscribed curve that encompasses all these profiles is called "envelope" (Jara *et al.* 2015).

On the other hand, we must be aware that the beach morphology does not react immediately to changes in wave field. Several authors captured how the instantaneous measurements of Ω and the observed beach state rarely show good correlations (Anthony 1998, Jiménez *et al.* 2008, Lee *et al.* 1998). They observed low correlations and emphasized it on high energetic beaches with frequent storms and seasonal recovery periods. In addition, Wright *et al.* (1985) suggested that the recent history of the beach morphology and the wave field determine also the current beach state. This time lag between stress and response implies that the beach have "memory" about past forcing. As a consequence, the shape of the subaerial beach is

not modulated by the today-wave height, but for the past wave climate (Jara *et al.* 2015). Here we will see through the following chapters (*II, III and IV*) how this recommendation from Wright *et al.* (1985) is key when calculating hydrodynamic values at the beachfront and their associations to the current state of the beach.

1.3 Goals

Through the analysis of the state of knowledge concerning the dry beach and its relations with the environment, it is clear that:

- Conceptual beach models describe beach morphologies properly.
- There is not enough knowledge about which are the main factors controlling the morphology of the emerged part of the beach and the way they act.
- Submerged and intertidal parts of the beach are well documented in terms of equilibrium configuration: There is a need to characterize the equilibrium profile of the dry beach.
- DBEP can help to predict beach morphologies *i)* through the understanding of the dry beach recovery after winter months; *ii)* by giving a height and a width of equilibrium; *iii)* by estimating the time needed to change the winter to summer equilibrium configuration.

Based on this, the primary (general) objective of this thesis is to focus on improve the knowledge of the dry beach behavior on a clearly defined space and time scales and characterize the equilibrium state in terms of the governing processes.

This main goal is achieved by the consecution of three specific objectives, which ultimately are the topics of each of the main three chapters of this thesis:

- ***Objective 1***: To identify the main involved factors related to the dry beach dynamics and to set a proper framework to study the equilibrium by identifying the most common shapes and features that the DBP presents.
- ***Objective 2***: To investigate how the dry beach profile accommodates as response to changes in controlling factors such as wave climate and sediment characteristics and to study the fluctuations of the DBP under a specific wave climate in both intra and inter annual scales.

- ***Objective 3***: To understand how the mean surrounding conditions -*i.e.*, wave climate and sediment characteristics- modulate the long term equilibrium of the DBP and to develop a parametric equation that allows predicting long term morphologic indexes such as width, slope and height of equilibrium.

1.4 Layout of the thesis

Here, the structure of the thesis is explained. The specific objectives proposed in the last chapter have been published in peer-reviewed journals as research papers, and the following three chapters (*II, III and IV*) are based on these works and address these objectives. Each Chapter consists of and abstract, and introduction, a description of the methodology framework and field sites, the results, their discussion and conclusions.

Chapter 1 presents the motivations that lead to the development and consecution of this thesis and provide the background for a better understanding of the basic structure of the document, constituted by the Chapters *II, III* and *IV*.

Chapter 2 sets the adequate framework to study the dry beach profile by proposing a conceptual model in which the dry beach profile is classified into four Types according to the modal state of the beach. The profile data base used to this porpoise was large enough -91 different beaches along the Spanish Coast and encompassing diverse wave climates- to require the use of automatic classification techniques –*K-Means* Algorithm in this case-.

Chapter 3 investigates the spatial and temporal variations of the dry beach profile along the highly dissipative and energetic coast of the Pacific *NW* U.S.A. Furthermore, this stretch of coast is subjected to a marked seasonality on wave climate, so the two main configurations that this beaches present along a year are identify and studied in both spatial and temporal scales. Two mathematical methods were employed satisfactory to this commitment: *K-Means* Algorithm and Empirical Orthogonal Functions.

Chapter 4 proposes a model that describes the equilibrium dry beach profile under different sediment and wave conditions by means of a parametric equation. The model was developed using a European profile data set that encompasses a wide range of modal states and it is tested and validated against an independent data set from Narrabeen Beach (AU), offering good results.

Chapter 5 reviews the main results of the thesis and proposes interesting points to continue this research that may be developed in the future.

2

Characterization of the dry beach profile: a morphological approach

Abstract [1]

The dry part of the beach is probably the most extensively used part of the beach system. It comprises the zone from high tide level to the landward edge, which can be either a dynamic (dune field) or a fixed boundary (cliff, rocky ledge or promenade). Here is presented a complete description of its morphology based on the analysis of 91 study sites selected along the entire coast of Spain. The analysis comprises four different regions in terms of wave climate, geology and tidal range, covering a wide range of coastal environments. In this study we present a zonation of the dry beach profile attending to the dynamics, the morphometric index and the time scales of variation, in which three different segments are defined: the foreshore segment, from the mean high water level to the berm, if present; the seasonal segment, which represents the zone between seasonal berms; and the inter-annual segment, which comprises the segment between the winter berm (or the most stable berm in case of no seasonality) and the landward edge of the beach. Besides, through cluster profile analysis -applying the *K-Means* Classification Algorithm to the entire data set of profiles-, four types of dry beach profile are proposed, described and related to a particular beach modal state: dissipative, intermediate, reflective and ultradissipative. The observations and results presented here contribute to understanding the morphodynamics of the dry part of

[1] This chapter is based on: Díez et al. (2016): Díez, J., Cánovas, V., Uriarte, Ad., Medina, R., 2016. *Characterization of the dry beach profile. A morphological approach.* Journal of Coastal Research (in press).

the beach and set the basis for subsequent studies concerning the equilibrium dry beach profile.

2.1 Introduction

In the introductory chapter of this thesis we talked about the conceptual beach models, its usefulness and its limitations. We base the approach of this chapter under the basis set out by the authors who propose these models but focusing the efforts on the dry part of the beach. Based on the demonstrated relation between the surf's zone modal state and dry beach morphology, explained in detail in the introductory Chapter, the aim of this Chapter is to present a description of the dry beach profile, *i.e.*, from the mean high water level (MHW) to the landward edge. Here is proposed a classification into profile types, based on observations and analyses of 91 different beaches along the Spanish Coast, encompassing diverse wave climate zones and tidal regimes, and formed within different sedimentological and geological environments.

2.1.1 Dry beach profile zonation

A conceptual zonation, or a division in segments of the dry beach profile, was carried out to ease the interpretation of the clustering results and to set the basis for the morphology based classification of the dry beach profile. This zonation helps to understand in a comprehensive way the different morphologies and shapes along the dry beach profile, and is based on the analysis of morphometric indexes: widths, composite slopes, changes in curvature and heights. Thus, the dry beach profile was divided into three segments or zones attending to their specific morphologies and their own temporal scales of variability. In Fig. 2.1, a schematic illustration of the three segments, *i.e.*: foreshore segment, seasonal segment and inter-annual segment, is presented.

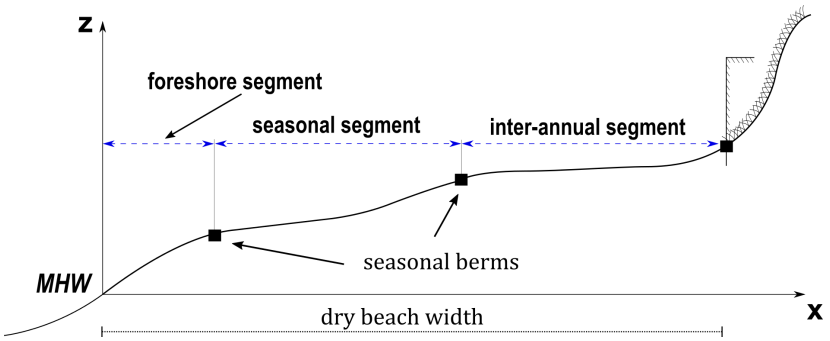

Figure 2.1: General scheme of the proposed zonation of a dry beach profile.

Foreshore segment. This segment covers from the MHW to the berm, if present. The berm is built by wave action and its width varies depending on daily wave height and tidal moon cycles. Comprehensive studies on berm development and erosion which provide tools to calculate berm height precisely can be found in the literature (Bendixen *et al.* 2013, Weir *et al.* 2006). The surf zone beach state, given by sediment size, wave breaking height and peak period, determines the slope, width and temporal variability of this part of the dry beach. In case of highly energetic environments or beaches formed with very fine grain size, the profile may not display berm and the extension of this segment may encompass the entire extension of the dry beach profile.

Seasonal segment. This segment appears in locations under significant seasonal variations in wave climate (mostly on Zone I in this study, Fig. 2.5-a). It covers the zone of the profile between seasonal berms. According to Bascom (1951), berm crest height is a function of the wave height at the time of formation. Seasonality in wave climate induces, therefore, the construction of two main berms. During high energy wave events, beaches display a residual or abandoned berm on the upper backshore, formed as the beach retreated: the winter berm. During lower energetic periods or seasons, they are fronted by an active berm on the lower beach, which is formed during lower wave energy periods. The presence and extension of this segment depends directly on wave climate variability, but also on sediment characteristics, and thus on the state of the beach's surf zone (Katoh & Yanagishima 1992).

Inter-annual segment. It comprises the segment of the profile ranging from the winter berm (or the most stable berm in case of no seasonality) to the landward edge of the beach (wall, foredune or cliff). It is the most stable part of the profile, and differs significantly between reflective and dissipative beaches due to the fact that the modal state controls its size and variability (Hesp 2002). Beaches tending to be reflective are steeper and receive less energy from waves than beaches that tend to be dissipative, which present gentler slopes and receive more energy. Thus, the inter-annual segment of reflective beaches is generally more stable Dissipative beaches of our data base do not display inter-annual segment, while reflective beaches present a wide and stable inter-annual segment. Beaches tending to be dissipative, or beaches subjected to an energetic environment, may not display this segment because storm surges cover the entire beach every year displacing the berm to the edge and even causing dune scarping (Short & Hesp 1982, Suanez *et al.* 2012).

2.2 Methods

In a brief, we input the 91 beach profiles to the *K-Means* Algorithm to obtain a certain number of clusters or groups, each of them characterized by a centroid. Then we calculated the value of Ω for each beach site at the time of survey and associated it with the corresponding cluster. Finally we relate the clusters with the main beach modal states (Fig. 2.2). In this section we first introduce the wave and profile data base and the methods to manage the profiles; then the mathematical basis of the *K-Means* clustering algorithm is described, and finally the regional setting is described.

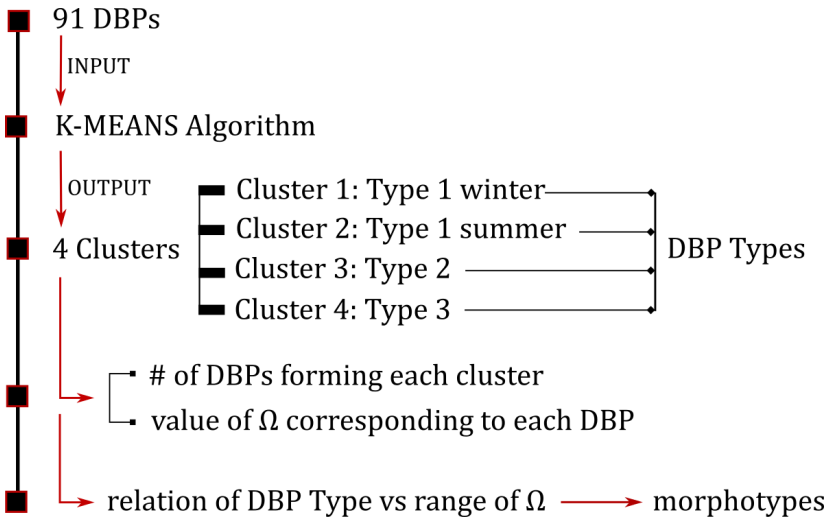

Figure 2.2: Flow chart detailing methodology. DBP: dry beach profile.

2.2.1 Data base and selection of the dry beach profiles

The profile data base used for this study was obtained from an European profile data base collected in IOLE (Tomás *et al.* 2015). They obtained dry beach profiles from Digital Terrain Models developed by the IGN (Spanish Geographical National Institute). The DTMs were obtained from LIDAR surveys that cover the entire Spanish coast, and the dates of the flights comprises from 2009 to 2012. The mesh of the DTMs was built with a resolution of $5x5m$. The profiles, obtained by interpolation of the DTMs, offer vertical and horizontal resolutions of $0.1m$ and $5m$, respectively. The interpolation method along each profile line allows obtaining one profile in the cross-shore direction every $200m$ along the coast, so nearly all the Spanish beaches dispose at least one profile covering the dry zone. Profile data is available from the zero reference level for the Spanish Coast (Alicante Zero Reference Level, named NMMA) to the beach landwards boundary. To validate the LIDAR profiles, detailed topographic data is available from beach surveys of Zone I and coincident with the LIDAR surveying dates. The measurements were obtained using an RTK-DGPS system mounted to

a backpack and referred to a fixed GPS station, and with a cross-shore coverage ranging from wading depth during low tide to the dune or to the promenade toe. The accuracy, according to the geodic reference system EGM2008 REDNAP IGN, is $0.1m$ in the horizontal and $0.02m$ in vertical. The validation offered good results, with a mean correlation coefficient between LIDAR and topographic measurements of 0.95 (Taylor 2001). As an example, Muskiz Beach, Zone I, in Fig. 2.3.

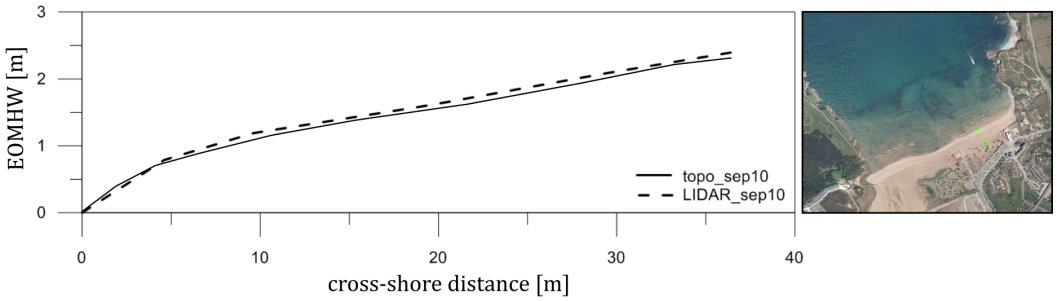

Figure 2.3: Comparison vs topographic and LIDAR survey in Muskiz Beach (Gipuzkoa, Spain, Zone I). Correlation coefficient: 0.95; Root Mean Square Deviation: $0.11m$. The vertical axis represents the elevation over the mean high water level (EOMHW).

Such a large spatial coverage requires a proper selection of the profiles used for the study. We carried out an accurate selection of 91 different beaches, taking into account two key points: *i)* The profile data base must encompass beaches ranging from fully dissipative to fully reflective and covering most of the intermediate beach modal states. *ii)* The selected dry beach profiles must display a configuration that responds accordingly to the mean wave conditions at the beachfront near the date of survey, *i.e.*, -and according to the definition of Pilkey *et al.* (1993)- the dry beach profile must present some sort of average shoreface profile cross section.

For computing wave statistics and the value of Ω at the front of each beach site, we used *DOW* hindcast data base (Downscaling Ocean Waves, Camus *et al.* (2011)). It is a new grid of the 60 years wave hindcast (*GOW*, Global Ocean Waves) developed by Perez *et al.* (2015) with 0.25 grades of resolution nearshore and a temporal resolution of one hour. The hindcast data provide wave statistics coincident to the date of each beach survey. To calculate the wave statistics –and consequently the values of Ω that configure the current beach state at the date of survey- we follow the recommendation of Wright *et al.* (1985): the selection of instantaneous values of the wave parameters in order to associate it with the current form of the profile is not recommended. They introduced the concept "memory of the beach" through the evaluation of the time averaged dimensionless fall velocity values Ω_∞ in Narrabeen Beach (AU), and stated that the immediate value of Ω made a negligible contribution to explaining day-to-day beach state observations, whereas the antecedent conditions show good correla-

tions for predicting current beach states. Through the analyses of diverse parameters for calculating Ω_∞, the dimensionless fall velocity for the equilibrium, they found that the best values that better represent the current state of the beach were those with $D = 30$ days, better than the instant value of Ω, where D is the memory of the beach. The range of Ω values calculated for each site using this criterion is displayed in Fig. 2.5-b. Regarding the selection of the cross-shore line of each beach site, we selected single profiles which were non-affected by lateral boundaries -jetties, river mouths, shadow zones- and which best represent the averaged configuration of the different profiles along a beach stretch characterized by similar exposure conditions.

Once the profiles are selected, some considerations must be pointed out concerning both landward and seaward limits of the dry beach profile. Fixation of a universal point to establish the origin of the dry beach can be controversial. According to Finkl (2004), neither landward nor seaward limits can be established as fixed lines because these limits are always moving following changes in wave, tide and wind conditions. For this study, we considered the mean high water level (MHW) as the starting point or the seaward edge. On the other hand, the landward edge is clear in beaches backed by a promenade or a cliff, but in the case of beaches that end in dune systems or other depositional landforms, the establishment of a fixed point is not simple. A stable dune and the adjacent beach may form a continuum which is difficult to split. According to Swart (1976), the upper limit of the subaerial beach is chosen at the highest level from which sediment can be eroded indirectly by wave action. A more extended explanation can be found in Hesp (1999) and Hesp (2002), who provides a detailed explanation about beach-dune interactions and the formation of foredunes. Stable dunes, which are not eroded or scarped, present a concave curvature that ends seaward into the dry beach. It's a smooth transition and the exact point is unclear. In the present study, for beaches backed by dunes, the profile cut was made for each site individually and this transition point was established where an abrupt change of curvature existed (Mull & Ruggiero 2014); in case of cliff or seawall, the cut was made just at the seawall-cliff toe.

2.2.2 Clustering classification: *K-Means* Algorithm (KMA)

When working with large data sets, data mining methods may be particularly effective in selecting the most representative cases of occurrence. In this particular case, it helped in selecting the most frequent or characteristic types of profile from the data base used. Specifically, data mining consists in producing a particular enumeration of patterns or models from the data for the basic goals of prediction or description (Fayyad *et al.* 1996). They found the *K-Means* Algorithm as effective in selecting common features and equilibrium shapes from large data sets, both temporally and spatially. These techniques extract features from the

data, providing a more compact and manageable representation of some of the important properties contained in them. One of these methods is called clustering, which identifies a set of categories. These mathematic algorithms, applied to discriminate beach profiles, use as an input a raw database of profiles. Within the numerous automatic classification techniques to compare and classify any kind of data (*K-Means* algorithm, *Maximum Dissimilarity* Algorithm, *Self-Organizing Maps...*), the *K-Means* Algorithm was selected. This algorithm (KMA) is a clustering technique that selects specified number of clusters from a multidimensional data space. Each cluster is defined by a prototype which is selected directly from the data and stands for the most representative feature. Given a database of n-dimensional vectors $X = \{x_1, x_2, ..., x_N\}$, where N is the total amount of data and n is the dimension of each data $x_k = \{x_{1k}, x_{2k}, ..., x_{nk}\}$, the KMA is applied to obtain M groups defined by a prototype or centroid $\nu_k = \{\nu_{1k}, \nu_{2k}, ..., \nu_{nk}\}$. These centroids have the same dimension as the original data, where $k = 1, \ldots, M$, and they are moving every each iteration to minimize the overall distance between clusters until a certain degree of convergence is reached. The vector which is nearest to a centroid M is set as the M cluster. A complete description of this classification method and others can be found in Hastie *et al.* (2001), while their application in oceanography and coastal research is explained in Camus *et al.* (2011) and Barcena *et al.* (2015). In the present work, this technique has been applied to classify a set of 91 dry beach profiles. The criterion to select the optimum number of clusters is not universal. Guanche *et al.* (2014) recommended selecting a number of groups which simplifies the interpretation of the results without losing too much variability in the resulting fields. For coherence reasons and to find a physical meaning to the results, the number of clusters -4, in our case- was chosen based on the association with the main types of morphodynamic beach states defined by Short (1999).

2.2.3 Regional setting: Spanish coastline

The Iberian Peninsula has around 6500 Km of coast, 28% of which are beaches of diverse typology. These range from narrow, long, dissipative, and fine-grained beaches, to wide, short, pocket, reflective and coarse grained -and even gravel- beaches (Losada *et al.* 1996, Ministerio de Medio Ambiente 2007). This variety is mainly associated to the different tidal and wave climate environments (Fig. 2.4), but also to the diverse geology and sediments (Fig. 2.5-a). In regard to the specific wave and tidal regimes and geomorphological considerations, and following the recommendations made in Ministerio de Medio Ambiente (2007), the Spanish Coast was divided into four Zones (Fig. 2.5-a). The main value ranges of variations are shown in Table 2.1.Wave data statistics along the text and from Fig. 2.4 were performed by carrying out a statistical analysis of wave data series *DOW* and *GOW*. With wave data

values from *DOW* corresponding to the dates of surveying and with the sediment grain sizes presented in Fig. 2.5-a, dimensionless fall velocity for each beach site were calculated. Values are shown in Fig. 2.5-b.

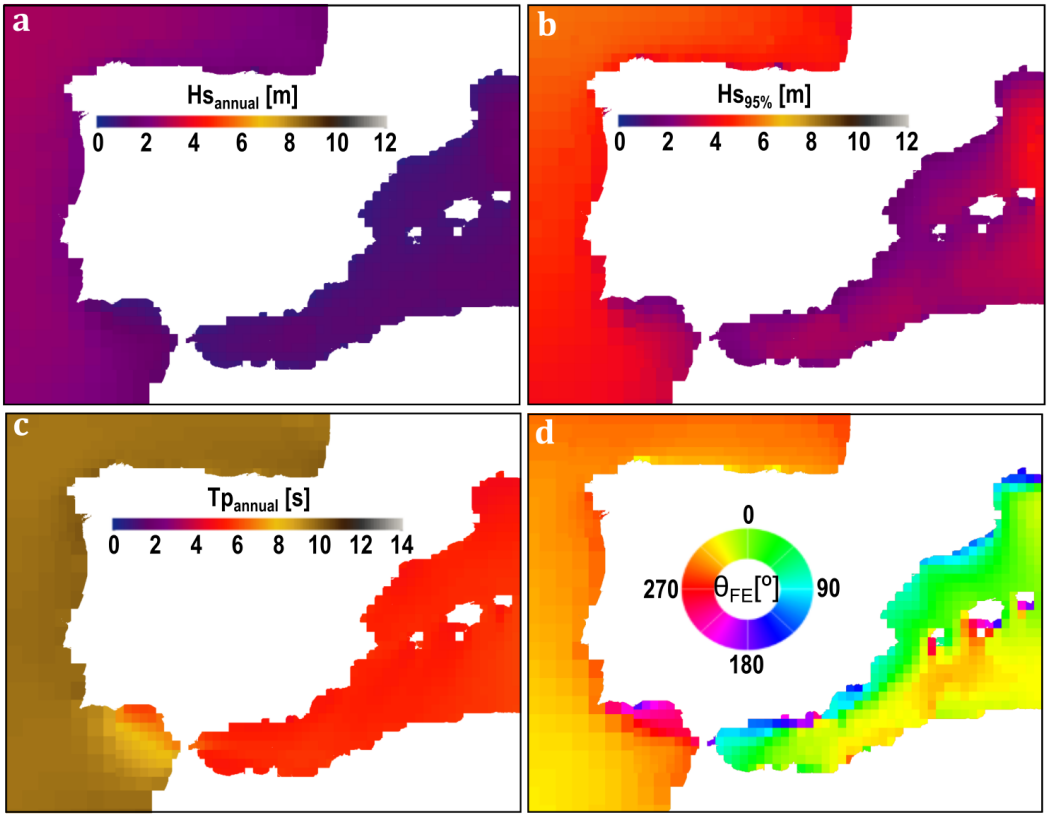

Figure 2.4: *(a)* Annual averaged significant wave height. *(b)* Statistical parameter $H_{s95\%}$, which indicates that only the 5% of the waves during a year exceed this value. It is representative of the annual extreme wave conditions. *(c)* Annual averaged peak period. *(d)* Direction of the mean energy flux. Deep water wave data statistics obtained from *GOW* database and shallow water wave data statistics obtained from *DOW* database.

Zone I: Cantabric Coast. It comprises the North Coast of Spain, from the mouth of the Bidasoa River in Gipuzkoa, to the *NW*-most part of Galicia, and covers around $1000Km$ of coast. It is a mesotidal environment with semidiurnal tides of around $4.5m$ and is generally exposed to persistent *NW* swells generated in high latitudes of the North Atlantic Ocean, but also to summer wind seas from the *NE* (Woolf *et al.* 2002). There is a marked seasonal variability in wave climate. During the winter season, the significant wave height (H_s) is around $2.5m$ with peak periods (T_p) of around $12s$, while in the summer they reach values of around $1.5m$ and $8s$, respectively. Beaches present generally fine sand forming sand spits and coastal dune systems. The coast has also sheltered, narrow and high cliff flanked beaches can be found. Medium-coarse grained pocket beaches backed by promenades are also common around urban emplacements.

Zone II: Atlantic-Galician Coast. It extends from the NW-most part of the Iberian coast to the mouth of the Miño River. The Atlantic-Galician Coast is subjected to meso-tidal fluctuations (4-5m) and under the influence of an energetic wave climate with noticeable seasonal variations. In winter, the H_s is around 3.5m and the T_p around 12s. During summer, H_s and T_p are around 1.5m and 9s, respectively. In open and exposed locations, the same kind of beaches described for the Cantabric Coast can be found. On the other hand, due to the presence of large coastal plain estuaries (Rías Baixas), sheltered and embayed beaches with very fine sand and under the main influence of tidal fluctuations are also present.

Zone III: Atlantic-Andalusian Coast. It extends over 380km from the Guadiana river mouth to the Point of Tarifa. The Strait of Gibraltar marks the division between the Atlantic Ocean and the Mediterranean Sea. The tidal range is quite variable in this area with a decrease from about 3.5m at the Guadiana River to less than 2m at Tarifa. The wave climate is less energetic than in the Northern Coast of Spain due to the comparatively less exposure to huge and persistent NW swells from high latitudes in the Atlantic. In winter, H_s varies between 0.8m and 1.2m, and T_p ranges from 6s to 10s. During the summer period, the same variables are around 0.5m and 5s, respectively. The main feature along this coast is the presence of large coastal dune fields and very large and straight beaches of fine-medium sand.

Zone IV: Mediterranean Coast of the Iberian Peninsula. It is about 1800Km long and comprises from Tarifa, the southernmost part of the Peninsula, to the north side of the Cape Creus in Girona. It is a micro tidal environment, with fluctuations of around 0.3m. The wave climate is much less energetic than in the Atlantic Ocean, while seasonal variations are not so remarkable. H_s and T_p vary from 0.8m - 5.5s to 0.5m - 4.5s between winter and summer, respectively. Generally, two characteristic types of beaches can be found depending on backshore morphology. One type corresponds to small, narrow beaches formed by coarse sand or even gravel, and flanked by rocky points in zones where the coast is steep, wild and dominated by cliffs. The other type is represented by long, straight and coarse-medium grained beaches. The backshore can be formed by foredunes if the environment is natural; however, hundreds of kilometers along this coast are highly anthropogenic, so beaches often lie between breakwaters, coastal barriers, jetties, or harbors and are backed by seawalls or promenades.

Table 2.1: Range of values of the main hydrodynamic and sediment characteristics affecting the study sites. Range of dimensionless fall velocity is also shown. 91 beach sites were analyzed for this study. Locations presented in Fig. 2.5.

	ZoneI		*ZoneII*		*ZoneIII*		*ZoneIV*	
	min	*max*	*min*	*max*	*min*	*max*	*min*	*max*
$H_{sannual}[m]$	1.5	2.5	1.6	3.5	0.6	1.2	0.5	0.8
$H_{s95\%}[m]$	4.8	5.3	5.3	5.5	2.3	3.1	1.1	1.7
$T_{pannual}[s]$	8	12	9	12	5	10	4.3	5.5
$D_{50}[mm]$	0.16	0.4	0.15	0.19	0.2	0.3	0.25	1.5
Ω	3	8.2	6	10.3	3	5.5	0.2	5

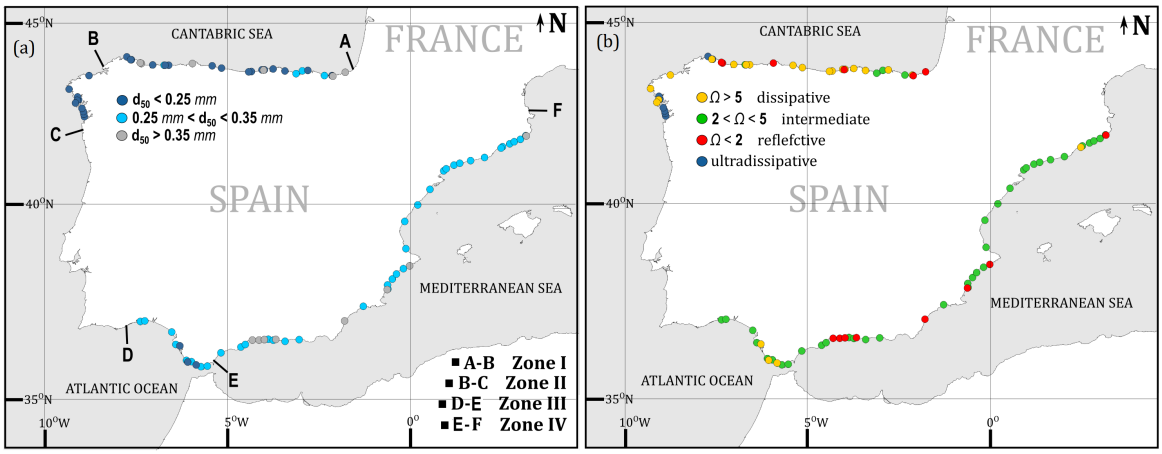

Figure 2.5: *(a)* In one side, this panel shows the zonation of the coast based on the different wave regimes shown in Fig. 2.4. On the other side, the grain size distribution of the study sites is also presented. *(b)* The modal state [Ω] of each studied beach is shown and categorized into four subgroups: dissipative, intermediate, reflective and ultra-dissipative.

2.3 Results

Results presented in this section are based in the *K-Means* output showed on Fig. 2.6. Here is showed the *K-Means* output and its associations with physical processes and variables. This mathematical grouping set the basis to build a reasoned morphological classification about the main different configurations that the dry beach profile present depending on the environment.

Four clusters were selected to represent the entire profile data set following the indications of Guanche *et al.* (2014). Site-specific horizontal and vertical profile dimensions were normalized. Fig. 2.6 shows the proposed *K-Means* classification of the different types of dry beach profile, displaying the frequency f of each cluster. For this cluster classification, beaches that were only tide affected were not included due to their very low occurrence in the data base (Beaches on Zone II located inside estuaries, Fig. 2.5-a). The data base used for this clustering technique was thus only composed of dissipative, the entire spectrum of intermediate

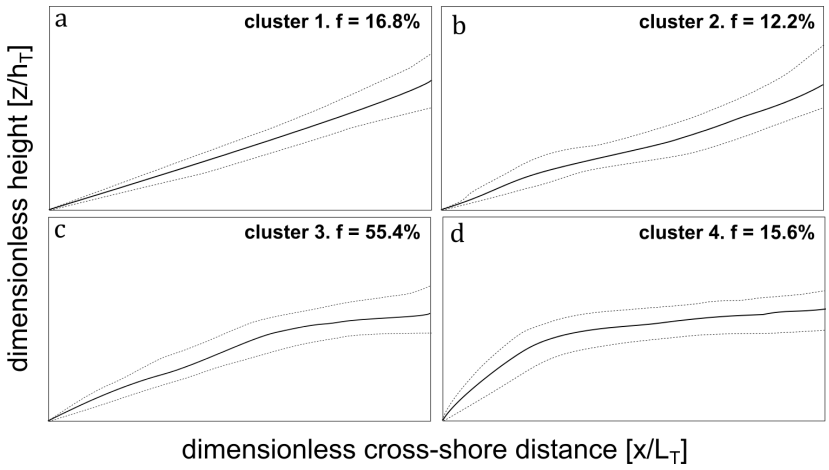

Figure 2.6: Cluster analysis using four centroids (clusters) plotted with 95% confidence bands, where f is the frequency of the cluster in percentage (%).

states and reflective beaches. *K-Means* results, therefore, must be related to these modal states and considering also that most of dissipative beaches of the Zone I may display winter (flat) and summer ("bermy" shaped) configurations, depending on the profiling date. As pointed out by several authors (see Chapter 1), there are evidences that the modal state of the beach is the most appropriate parameter that relate the shape of the subaerial profile with the main driven factors: wave flooding and sediment size. Following these indications, Fig. 2.7 relates the clustering results with modal state by setting up a correspondence between the cluster associated to each profile and its corresponding modal state, calculated following the recommendations of Wright *et al.* (1985) and with the wave data from *DOW* hindcast database (Fig. 2.5-b).

The `Cluster 1`, schematized in Fig. 2.8-a, largely encompass study sites that present dimensionless fall velocity values associated to dissipative modal states (according to Short (2006), dissipative beaches present values of $\Omega > 5$, whereas reflective beaches present values of $\Omega < 2$). In `Cluster 2` fit mostly dissipative beaches which present a slight bermy shape, which mainly occur in beaches from Zone I under moderate summer wave climate. In addition, beaches presenting Ω values between 2 and 5 (intermediate beaches) fit mainly in `Cluster 3` (Fig. 2.8-c). `Cluster 4` encompasses reflective beaches with Ω values mostly less than 2. Some oddities can be recognized in all four clusters, but a clear relation between morphology and modal state is distinctly detected. The oddities are referred to the relation between clustering classification and beach modal state. We must to keep in mind that *K-Means*, as many other clustering-classification algorithms, are just pure mathematical results and have not any physical significance. Interpretations of these results and the associations with physical processes should be taken carefully. Furthermore, the association of a single value of Ω to a determined beach configuration is always controversial. We followed the recommendation of

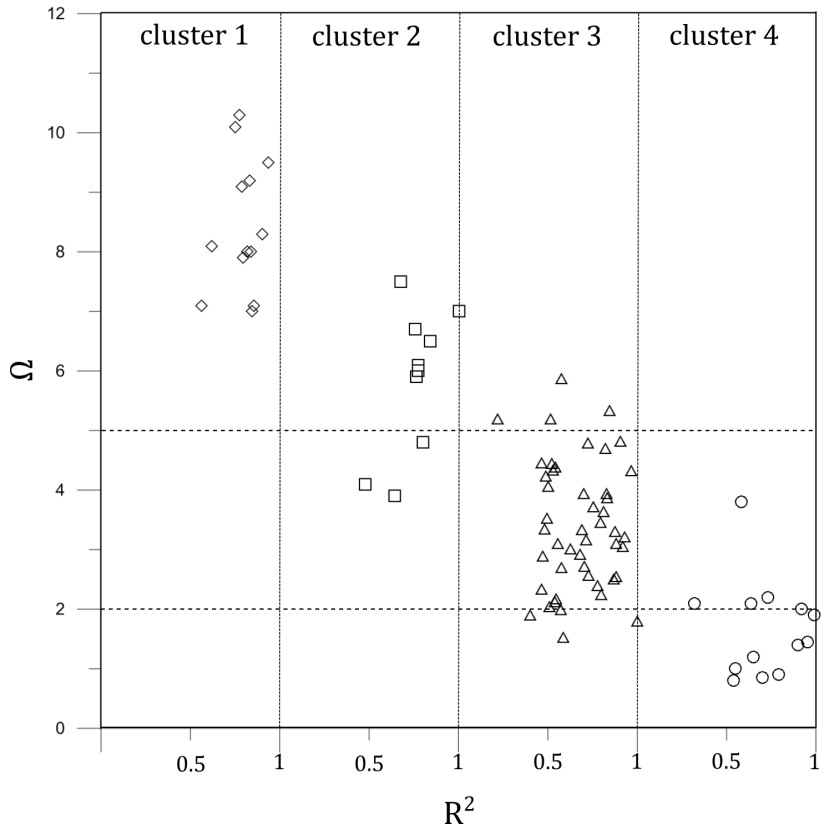

Figure 2.7: In the vertical axis is represented the dimensionless fall velocity value Ω for each study site. The horizontal axis is divided into four groups, one for each cluster. The scale makes reference to the *R*-squared value from the linear fittings between each single normalized profile and the corresponding centroid of its cluster. The closer to 1, the more similarity between the single profile and its cluster. Horizontal grid lines represent the values where transition between reflective, intermediate and dissipative beaches occurs.

Wright *et al.* (1985), but it is important to have also present that the use of different values of wave height and sediment size can deeply influence the final result (Anthony 1998, Jackson *et al.* 2005). However, despite these oddities, a clear relation between number of cluster and Ω is observed.

Following this idea, we propose an all-inclusive and physically-coherent scheme of the four types of dry beach profile obtained by clustering classification plus the configuration that ultradissipative beaches present (not included in the input data base for clustering). In Fig. 2.8, the four main types of dry beach profile are shown.

By relating the number of cluster where each study site fits and comparing with their values of Ω, Fig. 2.9 displays the type of dry beach profile that each study site presents. Through the comparison between Fig. 2.5-b, Fig. 2.7 and Fig. 2.9 we propose a direct relation between modal state of the beach and the type of dry beach profile that present. Reflective beaches present a **Type 3** dry beach profile; intermediate beaches present **Type 2**; dissipative beaches

present **Type 1**, and ultradissipative beaches present **Type 4**.

2.3.1 Description of the four types of dry beach profiles

In this section, a description of the four different profile Types is presented. The characterization is first focused on the occurrence of each type under its specific wave climate and geological environment, and second, the main morphological features and dynamics are described.

- **Type 1.** Through the analysis of the occurrence of this Type within the data base (67% within Zones I and II, Table 2.2), we assume that this Type appears on fine grained, dissipative or intermediate to dissipative, and both wave and tide dominated beaches. These profiles are located on open swell coasts within areas of fine sand and are normally backed by large coastal dune systems. This is the typical configuration of open-sea North Atlantic Spanish beaches. As an example, Somo (Cantabria), Oyambre (Cantabria) and Rodiles (Asturias) fit in this category (Fig. 2.10-a). In our study area, beaches within Type 1 appear mostly in Zone I, which is strongly seasonal in terms of wave climate. During winter, strong meteorological tides and wave storm events raise the water level and cover the entire profile, reaching the dune toe and sometimes inducing dune scarping. During the summer season, a seasonal berm may appear due to lower energetic conditions (Fig. 2.10-a). This Type of profile is characterized by a wide foreshore segment, normally flat and featureless with a gentle positive slope (Table 2.3). During high energy periods, the entire profile of the dry beach is formed by the foreshore segment, and modulated by daily swash zone dynamics. The seasonal segment varies in size depending on seasonality; it is straight and steeper than the foreshore segment. The inter-annual segment may not exist due to high energetic winter dynamics, while the landward edge adopts the dune's curvature under stable conditions. Fig. 2.6-a and Fig. 2.6-b in case of clustering results, and real cases in Fig. 2.10-a, showing both seasonal configurations.

- **Type 2.** The Type 2 profile appears over the range of intermediate beaches described by Short (1999). We associate `Cluster 3` (Fig. 2.6-c) with profile Type 2, described schematically in Fig. 2.8-b. Through the analysis of the results of Fig. 2.6, we assume that these beaches can occur in a mix environment and where the wave climate at the beach front ranges from low to medium energy. The sediment varies around medium grain sizes; these Type of profiles are most common in Zone IV, (Fig. 2.9, Table 2.2), where the grain sizes ranges from $0.25mm$ to $0.35mm$, (Fig. 2.5-a). This Type represents the typical configuration of long, straight, medium grain sized, medium energy,

intermediate to reflective, man-intervened Mediterranean beaches (Fig. 2.9). Examples of this category are Isla Cristina, (Huelva), Mataró (Barcelona) and Gandía (Valencia) (Fig. 2.10-b). Due to the association with intermediate beaches, the grain size is generally coarser than that in/of Type 1 beaches, making the profile steeper and higher. Seasonal changes in wave climate may cause a widening of the effective dry profile during summer seasons. These beaches present a narrow foreshore segment, with a gradient that can range from moderate to high, depending on grain size (ranges of different morphological index in Table 2.3). In the case of beaches affected by moderate seasonal wave climate variations, the profile may display a "remnant berm", formed during high energy wave events, and fronted by an active berm on the lower beach, built during summer wave conditions. The inter-annual segment is medium-wide depending on sediment size and availability, and presents a slightly positive slope (Table 2.3).

- **Type 3.** The Type 3 profile appears on coarse grained, reflective, medium-low energy and mixed environments (Table 2.3). These beaches cannot support a dune system due to the coarse grain size of the sediment (Hesp 2002). All beaches presented in this study displaying this type of profile are backed by waterfronts or promenades. Beaches with this configuration are found mostly on embedded and sheltered locations (mainly around urban emplacements), forming closed sediment cells flanked by rocky ledges, breakwaters or headlands, and the seasonality in wave climate is either damped or inexistent due to their location. Examples of this type include Blanes (Girona), Orio (Guipuzkoa) or Usgo (Cantabria) (Fig. 2.10-c). The wave climate at the beachfront is in most cases in this study low energetic and does not have large seasonal variations, whether for the low deep water energetic conditions (Zone IV beaches with coarse grain size) or for the sheltered location of the beach (sheltered and coarse grained beaches of Zone I). The low energetic environment and the presence of a high and stable berm reduce the potential of flooding. The three examples in Fig. 2.10-c present a high and stable berm, and so do the `Cluster 4`, related here with Type 3 profile. These beaches present a narrow, steeply sloping foreshore segment ending in a high, pronounced and stable berm (Fig. 2.8-c). All beaches categorized by this type of profile are associated with `Cluster 4`. The centroid of this cluster presented in Fig. 2.6-d represents the most common or the mean configuration. The high berm can be clearly identified. Low seasonal variations in wave climate inhibit the formation of large seasonal segments but they may appear. The inter-annual segment is stable and wide in the analyzed beaches, normally with a smooth positive featureless or even horizontal slope, running from the berm to the wall (Table 2.3).

- **Type 4.** This profile appears in tide dominated beaches located mostly inside estuaries or embayed locations where the effect of waves is negligible. All beaches that fit

in this category are in Zone II (Table 2.2). They are normally composed of fine or very fine sand ($d_{50} < 0.2mm$), which leads to a typical configuration of ultradissipative beaches. Beaches located inside the Rias Baixas (Pontevedra, Zone II) are good examples (Fig. 2.10-d). These beaches are mostly tide affected and do not present seasonal changes due to the lack of variations in wave climate at the beach-front. The small importance of swash leads to a very stable, featureless and straight profile with a smooth and positive slope (Fig. 2.10-d). This type of profile may present a very narrow foreshore segment, if there is any exposure to small waves, but generally the profile is formed entirely by the inter-annual segment.

Table 2.2: Percentage of occurrence of Type of dry beach profile depending on the Zone of study and occurrence of the study sites in terms of their Ω within each Type of profile.

	$ZoneI$	$ZoneII$	$ZoneIII$	$ZoneIV$	$\Omega > 5$	$2 < \Omega < 5$	$\Omega < 2$	$\Omega \sim 0$
$Type1$	57%	33%	27%	2%	87%	13%	–	–
$Type2$	17%	–	73%	80%	8.7%	80.5%	10.8	–
$Type3$	22%	–	–	18%	–	30%	70%	–
$Type4$	4%	67%	–	–	–	–	–	100%

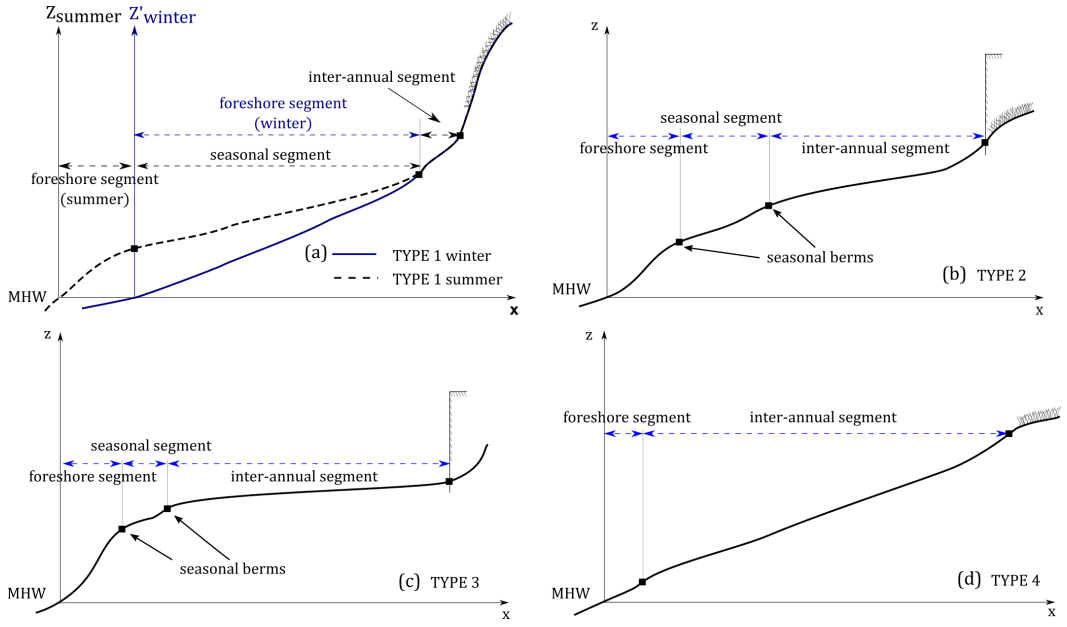

Figure 2.8: Morphotypes of dry beach equilibrium profiles. Each sub-figure (*a, b, c* and *d*) corresponds to the four different Types of profile, including Type 1 in two configurations.

2.4 Discussion

As the results of the last section suggests, the morphology of the dry beach is directly related to the wave regime and the specific sediment characteristics. As shown in Fig. 2.9,

Table 2.3: Overview of dry beach equilibrium profile morphology. $tan(\beta)$ is the mean slope of each segment of all the profiles that fit in each cluster. % dtotal represent the mean percentage of extension of each segment *vs* the total extension of the entire profile through the analysis of the entire database. Slope: Sub-horizontal: $tan(\beta)$ <0.008; Gentle: tan(β) 0.01-0.03; Intermediate: tan(β) 0.03-0.07; Steep: tan(β) 0.07-0.1. Slope ranges adapted from Masselink *et al.* (2006). Symbol −− indicates that the size of the segment is negligible compared to others.

	foreshore		*seasonal*		*interannual*	
	$\tan\beta_{mean}$	$\%d_{total}$	$\tan\beta_{mean}$	$\%d_{total}$	$\tan\beta_{mean}$	$\%d_{total}$
$Cluster1$ $[Type1wi]14sites$	0.02 *gentle*	∽ 100%	−−	−−	−−	−−
$Cluster2$ $[Type1su]16sites$	0.03 *gentle*	∽ 55%	0.017[*gentle*]	∽ 45%	−−	−−
$Cluster3$ $[Type2]46sites$	0.04 *intermediate*	∽ 30%	0.019[*gentle*]	∽ 5%	0.01[*gentle*]	∽ 65%
$Cluster4$ $[Type3]13sites$	0.06 *intermediate*	∽ 30%	−−	−−	0.008[*subhor*]	∽ 70%
$[Type4]$ $8sites$	0.08 *steep*	∽ 5%	−−	−−	0.08[*steep*]	∽ 95%

each coastal environment presents a dominant type of profile. It follows that dominance or presence of a type of profile depends directly on wave climate and the geological environment present. This fact can lead to corroborate the indication from Hesp (1988) that the modal state is a key parameter controlling the morphology of the subaerial beach.

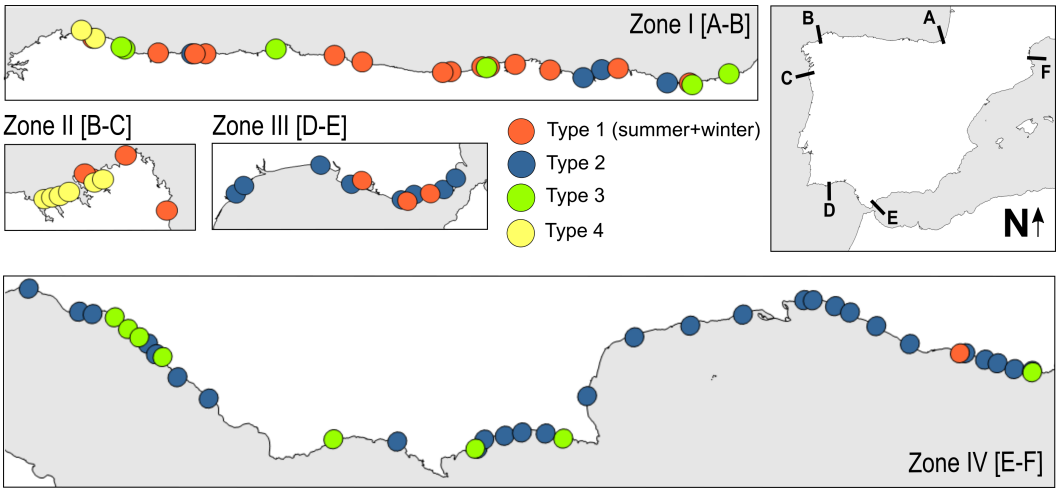

Figure 2.9: Distribution of the Spanish beaches analyzed in this study and categorized by their dry beach profile type.

2.4.1 Profile characterization

The analysis and identification of the main processes occurring on a beach leads to an understanding of the general features of beaches (Davidson-Arnott 1988). Thus, the proposed

zonation is derived from previous knowledge (Ministerio de Medio Ambiente 2007) and experience about the various dynamics acting upon the dry beach and the response of the beach's morphology to these actions. The equilibrium configuration for each segment is reached at different stages. Foreshore segment variations around the equilibrium configuration depend on daily wave height, whereas variations in the seasonal segment can be prolonged over several weeks or even months, depending on seasonality. The segment we refer to as "inter-annual" responds to changes that vary at temporal scales of over a year or more, when storm surges that cover the entire subaerial zone take place.

Table 2.3 summarizes the main morphological features of each segment of the profile. Supported by the aforementioned fact that morphology of the subaerial beach is modulated by wave climate and sediment characteristics (Hesp 1988), here we prove it and associate each morphotype with a beach modal state. Type 1 profiles are adopted by dissipative beaches or by beaches at intermediate states near the dissipative one (*LBT*, longshore bar-trough going to dissipative). Type 2 encompasses the range of intermediate states (re)defined by Wright & Short (1984), from *RBB* (rhythmic bar and beach) to *TBB* (transverse bar and beach). The Type 3 profile is associated to *LTT* states (low tide terrace) going to strictly reflective. However, although extreme beach states (dissipative and reflective) are easy to identify and associate with Type 1 and Type 3 profiles, respectively, Type 2 profiles embrace a more extensive range where variability is higher. Therefore, the scheme for Type 2 in Fig. 2.8-b stands for a representative state that can vary depending on specific intermediate modal states. Actually, if one is to be more precise, the four type classification presented here can be improved by splitting these Type 2 profiles into two or more subtypes. Finally, Type 4 profiles appear on tide dominated locations with an almost negligible wave influence. Tidal fluctuations modulate the size of the entire profile, making this type of profiles more stable than the others.

2.4.2 Profile distribution along the Spanish coastline

Clustering input data base encompasses all ranges of grain sizes and wave climates, and thus all the main beach modal states, and the results showed in Fig. 2.7 reflect that; *K-Means* classification clearly distinguishes four Types of dry beach profile, which can be associated to the four main beach modal states. Coasts under common wave climates generally show a characteristic type of beach defined by its modal state (Fig. 2.9). Short (2006) stated this fact for the Australian beach system, showing the predominance of one type of beach over the others depending on coastal zone location. Based on the earlier description of the Spanish coastal zonation and through the analysis of Fig. 2.9, clear type-of-profile distribution patterns can be observed on the dry beach, in our case of study.

2.4.3 The wind role on dry beach morphology

The idea that subaerial beach morphology is mainly dominated by wave and tidal forces leads to thinking about the role of wind action, especially on the inter-annual segment, which is the one that remains dry most of the time. The modal state of a beach has implications for sediment exchange between the beach and the dunes due to its capacity to modify aeolian processes. The three main morphological features that affect the wind regime on a beach are: beach slope, size and distribution of the sand, and width of the beach (Bauer *et al.* 2008, Davidson-Arnott 1988, Sherman & Bauer 1993). Furthermore, Hesp (1999) also demonstrates how the wind field acting upon the subaerial beach is different between a characteristic reflective profile with a large berm and a dissipative and featureless profile. However, several authors (Short & Hesp 1982) assert that wave action is much more effective than wind in governing equilibrium morphology by the development and erosion of the dry beach and dune. One important fact that supports the prevalence of wave over wind action was set out by Delgado-Fernández *et al.* (2009), who showed that the windiest season (winter) is the least effective season for transport due to the moisture content of the sand or the reduced fetch, and despite extreme winds during intense storms, such events often lead to wave scarping rather than effective aeolian sediment transport. Wave inundation represents the main event that prevents significant aeolian sediment movement across the beach, and exerts strong influences on the 'effective' geometry of beaches by limiting effective fetch (Davidson-Arnott & Bauer 2009). According to this study results, it is suggested that the effect of drag wind forces should be taken into account on the last segment of the profile, particularly in beaches where the inter-annual segment is wide. However, these types of beaches are mostly coarse grained, like Orio or Blanes (Fig. 2.10-c), which represents a major constraint to set an equilibrium configuration formed by aeolian mobilization of the sediment. Nevertheless, even though wind action is negligible in most cases, further and more exhaustive studies should be carried out to discern the real influence of wind in shaping the equilibrium of the dry beach profile.

2.4.4 Cluster analysis: advantages and limitations

Cluster analysis highlights the basic shapes and curvatures that identify each type of profile. As stated in the methodology section, the selection of an optimal number of clusters was made in such a way that it would be consistent with the current knowledge about beach types and still providing satisfactory results. Contents of the data base were selected to be representative and similar to the occurrence of the different types of profile along the Spanish coast. Nevertheless, this assumption may be refuted in future studies by mapping all beaches along the entire coast of Spain and adding their dry beach profiles to the data base used for

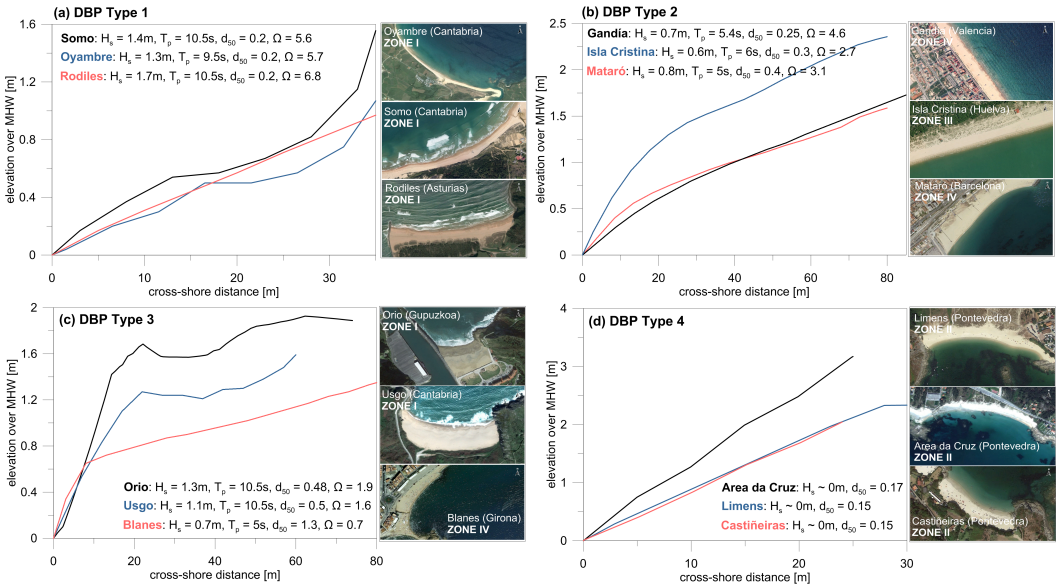

Figure 2.10: Examples of the four morphotypes described. *(a)* Type 1 in summer (Somo, Oyambre) and winter (Rodiles) configurations; *(b)* Type 2; *(c)* Type 3; *(d)* Type 4.

clustering. An exhaustive knowledge of the morphology of the dry part of all the beaches in Spain –and, in addition, to any other worldwide stretch of coast- would be a good contribution to integrated coastal zone management to optimize any kind of beach intervention. Future studies may also include more types of dry beach profile and so encompass the intermediate beach modal states previously defined by Short (1999): *LBT, RBB, TBB* and *LTT*. Focusing on the present study, the *K-Means* algorithm arise here as a good tool to automate profile classification of large profile datasets. However, the method has also its limitations. The output itself does not have physical meaning, so the interpretation of the results has to be made according to previous knowledge on the matter. Furthermore, applying it to profile morphologies can be challenging since the data set must be homogenous enough. Otherwise, the method may not distinguish correctly the different morphologies and it can split one type into other subtypes, obviating a clear Type with very small representation in the data set.

2.5 Conclusions

A comprehensive description of the morphology of dry beach equilibrium profiles through the analysis of 91 beaches along the Spanish Coast has been presented. This study, based on a morphological approach, leads to the development of a zonation of the dry beach profile, arguing that three different temporal scales of variation can occur over the entire profile. From the MHW level to the berm lies the foreshore segment, where daily wave action and sediment size determine the width and the slope. If the beach is exposed to seasonal variations in wave climate, during the summer period a seasonal segment appears, delimited by

summer and winter berms, while from the winter berm to the landward edge of the profile, a segment with inter-annual variations rises. This zonation supports the initial idea of establishing a correspondence between the equilibrium morphology of dry beach profiles and its modal state. Our analyses prove this association to be valid, showing that dissipative, swell dominated beaches with fine sand tend to develop a dry beach **Type 1** profile, which is characterized by a wide, flat and featureless foreshore segment, whereas reflective, coarse grained-low energetic beaches tend to show a **Type 3** profile, characterized by a steep foreshore segment and a marked berm followed by an almost horizontal segment up to the dune toe or wall. Intermediate beaches present **Type 2**, which is an intermediate morphological state between Types 1 and 3, and ultradissipative beaches, **Type 4**, characterized by a flat and featureless upward slope from the mean high water level to the landward edge. The results presented here may open up gates to other related studies focused on giving more insight into the relationship between specific modal states and the morphology of the equilibrium dry beach profile. Detailed experiments and exhaustive field measurements may be carried out to support this classification, but the work presented here represents a good framework and a solid starting point for future research in pursuing the definition of the equilibrium dry beach profile, which is still a remarkable gap in current beach morphology understanding. Studies concerning the dry beach profile are required, for example, to accurately predict dry beach erosion events and to optimize beach fill designs.

3

Spatial and temporal variability of dissipative dry beach profiles in the Pacific Northwest, U.S.A.

Abstract [1]

U.S. Pacific Northwest dissipative beaches are subject to a marked seasonality in wave climate, which leads to periodical oscillations in the dry beach profile morphology. The back and forth seasonal sediment exchange between emerged and submerged parts of the beach system induces two main dry beach profile equilibrium configurations. During approximately the 70% of the year, the dry beach adapts its configuration to a flat and straight positive slope from the Mean High Water Level to the dune toe elevation. The remaining 30% of the time, corresponding normally to summer, the profile progressively adopts a berm-like profile. We quantify these changes by studying inter- and intra-annual variations of the dry beach profile shape. For intra-annual variations we used a monthly profiling campaign from South Beach State Park, OR, collected between Jul '14 and Oct '15; for inter-annual variations we used 17 years -1997 to 2015- of quarterly beach monitoring along 31 transects spread along the four sub-cells that constitute the Columbia River Littoral Cell. We identify several morphological phenomena by the application of two data mining routines: *K-Means* clustering technique (KMA) and Empirical Orthogonal Functions (EOF). Through the clustering

[1] This chapter is based on Díez et al. (2017a): Díez, J., Cohn, N., Kaminsky, G., Medina, R., Ruggiero, P., 2016. *Spatial and temporal variability of dissipative dry beach profiles in the Pacific Northwest, U.S.A.* Marine Geology (in press).

we obtain the main configurations that the dry beach profile experiences over time, while the EOF analysis explains the variability of the collected data in space and time. In this way it is possible to examine berm formation and destruction as well as the shifting of the profile between summer/winter configurations –among other changes induced by cross-shore sediment exchange such as beachface and dune toe erosion and recovery.

3.1 Introduction

Extensive topographic, bathymetric and wave data available for beaches in the US Pacific Northwest (PNW, Oregon and Washington) allow for a detailed characterization of both spatial and temporal variations of the DBP. Concerning the beach morphology, previous work in the region has mainly focused on large scale shoreline change (Ruggiero *et al.* 2010), beach erosion (Ruggiero *et al.* 2001) and the description of sandbar generation, degeneration and variability, and other submerged and intertidal features (Cohn & Ruggiero 2015, Leonardo & Ruggiero 2015). In this Chapter we assess the spatial and temporal variations in DBP shape along the Columbia River Littoral Cell and South Beach State Park, OR, and present a detailed description of temporal changes on the DBP, both at intra-annual and inter-annual scales.

The primary objective of this Chapter is to link spatial differences in hydrodynamic forcing and grain size to the shape of the DBP and to understand the changes along the profile induced by hydrodynamics. Díez *et al.* (2016) demonstrate empirically that beach modal state and DBP morphology are directly related. They applied data mining techniques to discriminate the most common morphologies present in a large European DBP data base formed with beaches ranging from fully dissipative to fully reflective, observing that dissipative beaches affected by seasonality present a characteristic type of profile, named Type 1; intermediate beaches present Type 2, and reflective beaches present Type 3 (Fig. 2.8). Here we hypothesize that, with few exceptions in cases of coarse grained or sheltered locations, PNW beaches present Type 1 DBP configuration due to their highly dissipative beach modal state and also due to their marked seasonality (Ruggiero *et al.* 2005). During the winter season, above average meteorological tides and storm events raise the water level may result in a coastal profile which is entirely inundated, reaching the dune toe and sometimes inducing dune scarping. The winter Type 1 profile is characterized by a wide foreshore segment, normally flat and featureless with a gentle positive slope. The entire DBP is composed during this season by the foreshore segment and is modulated by daily swash zone dynamics. During summer, a seasonal berm may appear due to lower energy conditions, and the segment between the berm and the dune varies in size and slope depending on seasonal wave climate variations. The DBP segment between the higher and most stable winter berm and

the landward limit may not exist due to high runup and strong meteorological tides that cause elevation of water levels up to the dune toe height. Here we investigate the frequency of the two Type 1 sub-configurations (flat *vs.* bermed profiles) and their variations with two PNW beach profile data sets and two different mathematical techniques that have historically proved useful for investigating profile morphologies (Aubrey 1979, Fayyad *et al.* 1996). We first applied the *K-Means* Algorithm to the Columbia River Littoral Cell (CRLC hereinafter) profile data set. The temporal coverage for these data extends from 1997 to 2015, with four samples per year (details explained below). This technique applied over the entire data set allows us to discriminate the main configurations that the DBP presents during the 17 year measurement campaign, and it is also feasible to investigate the most common configuration that the beach presents in each season (summer, autumn, winter and spring). To investigate seasonal morphological changes we incorporate data from South Beach State Park, OR (Cohn & Ruggiero 2015). An Analysis of Principal Components (PC), or also called Empirical Orthogonal Functions (EOF), is applied to the data, and through the analysis of the different spatial and temporal components we identify and explain the main types of variation in the cross-shore direction. In order to see how the seasonal variations are replicated in time over a yearly cycle, EOF analysis is also applied to a representative profile from the CRLC data (Fig. 3.4). We report on an intensive analysis of the DBP behavior in space and time to help characterize PNW dissipative beaches. We assess the behavior over time of the DBP, obtaining the two main configurations that these beaches present during a year and we observe how these configurations are seasonally distributed. We also evaluate the specific variations on the DBP over a year, assessing the erosion-accretion processes and the creation and destruction of the main DBP feature, the berm.

3.2 Study areas

3.2.1 Columbia River Littoral Cell

The CRLC extends approximately $165km$ between Tillamook Head (OR) and Point Grenville (WA) (Fig. 3.1). It can be divided into four different sub-regions due to the presence of four barrier plain sub-cells delimited by estuary entrances (Kaminsky *et al.* 2010, Ruggiero *et al.* 2005; 2016). These sub-cells, fed with sediments from Columbia River, are North Beach, Grayland Plains, Long Beach and Clatsop Plains (Fig. 3.1). The CRLC is characterized by low accreted barrier beaches (Peterson *et al.* 2010) that are wide, smooth sloped and fine grained, and mostly dune backed. In the northern half of the of the North Beach sub-cell, coastal bluffs back the beaches. CRLC beaches receive high energy from waves in a marked seasonal pattern (Garcia-Medina *et al.* 2014), resulting in a wide surf zone with

multiple sandbars (Leonardo & Ruggiero 2015). The highly dissipative environment generates a nearshore zone dominated by infragravity energy (Ruggiero *et al.* 2004). The wave climate is highly energetic, with significant wave height around 3m in winter (mostly from WSW direction) and 1.5m in summer (mostly from WNW direction), with peak periods around $13s$ and $8s$, respectively (Fig. 3.2). During winter, storms can generate wave heights up to $14m$ (Allan & Komar 2007). The tide regime along the littoral cell is semidiurnal with a tide range between $2m$ to $4m$.

3.2.2 South Beach State Park, Newport, OR.

South Beach State Park (SBSP, hereinafter) is located immediately south of the Yaquina Bay South Jetty in Newport, OR, on the Central Oregon Coast (Fig. 3.3 - b). The jetty, constructed beginning in 1896 to ease navigation through the channel (Komar *et al.* 1976), resulted in significant growth of the beach and dune system by stopping northward longshore sediment (Cohn & Ruggiero 2015). The jetty also creates a shadow zone for high energetic NNW swells preventing significant sediment transport to the south. The beach is formed with fine grained sand ($d_{50} \backsim 0.2mm$) and receives high energy from waves under approximately the same pattern than in CRLC, detailed above, which makes the beach profile flat and dissipative. The backshore is wide and dune erosion is rare due to the large sediment supply (Ruggiero *et al.* 2013). Fig. 3.3-a shows the monthly averaged wave height and period for the study period obtained from DOW statistical analysis (Perez *et al.* 2015).

3.3 Methods

This section captures the overall methodology, outlined in detail in the flow chart of Fig. 3.4. The data collection is also described for CRLC and SBSP through the explanation of the different techniques and methods to carry out the topographic measurements, as well as the wave and tidal data. The assimilation and processing of the topographic data by applying the two mathematical methods KMA and EOF is also further described.

3.3.1 Data collection

3.3.1.1 CRLC topographic data

Data from the four CRLC sub-cells come from a nested, regional beach monitoring program that was initiated in summer 1997 (Ruggiero *et al.* 2005). With sufficient spatial and temporal resolution, the main goal of this ongoing monitoring program is to understand local sediment

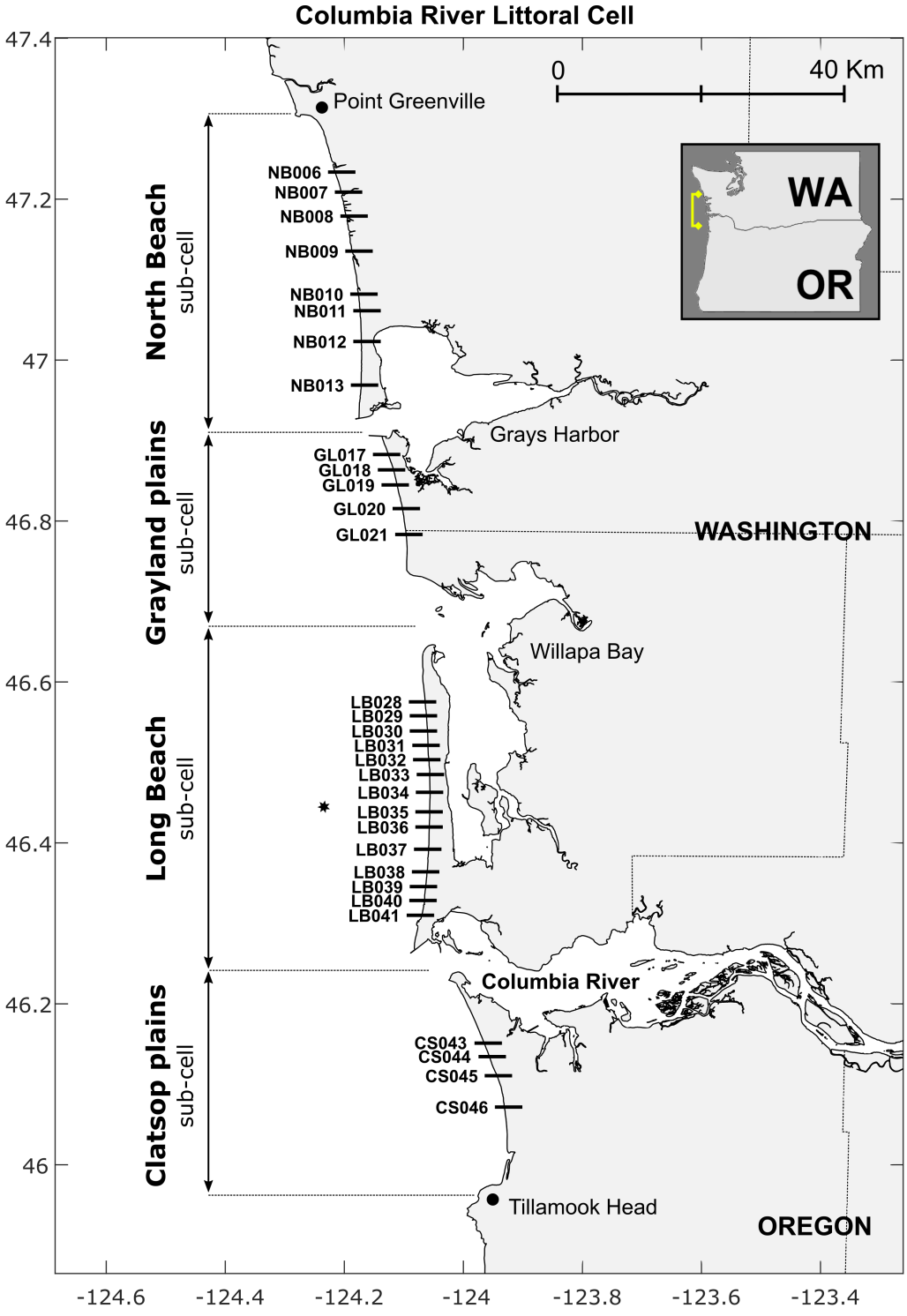

Figure 3.1: Map of the Columbia River Littoral Cell (CRLC) with the location and ID of the profiles that were investigated. Adapted from Ruggiero *et al.* (2005). Sub-cell lengths: North Beach: $43Km$; Grayland: $18Km$; Long Beach: $42Km$; Clatsop: $29Km$. Sampling dates: Aug'97-Feb'15, four profiles per year: winter, spring, summer and autumn. Star: *GOW* hindcast node (Perez *et al.* 2015, Reguero *et al.* 2012).

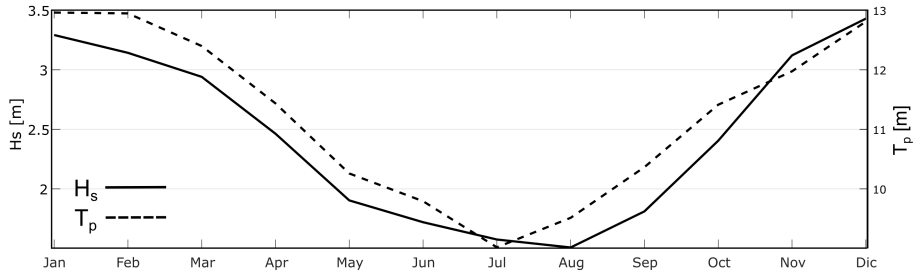

Figure 3.2: Monthly mean significant wave height and peak period obtained from *GOW* hindcast point (Fig. 3.1 for location).

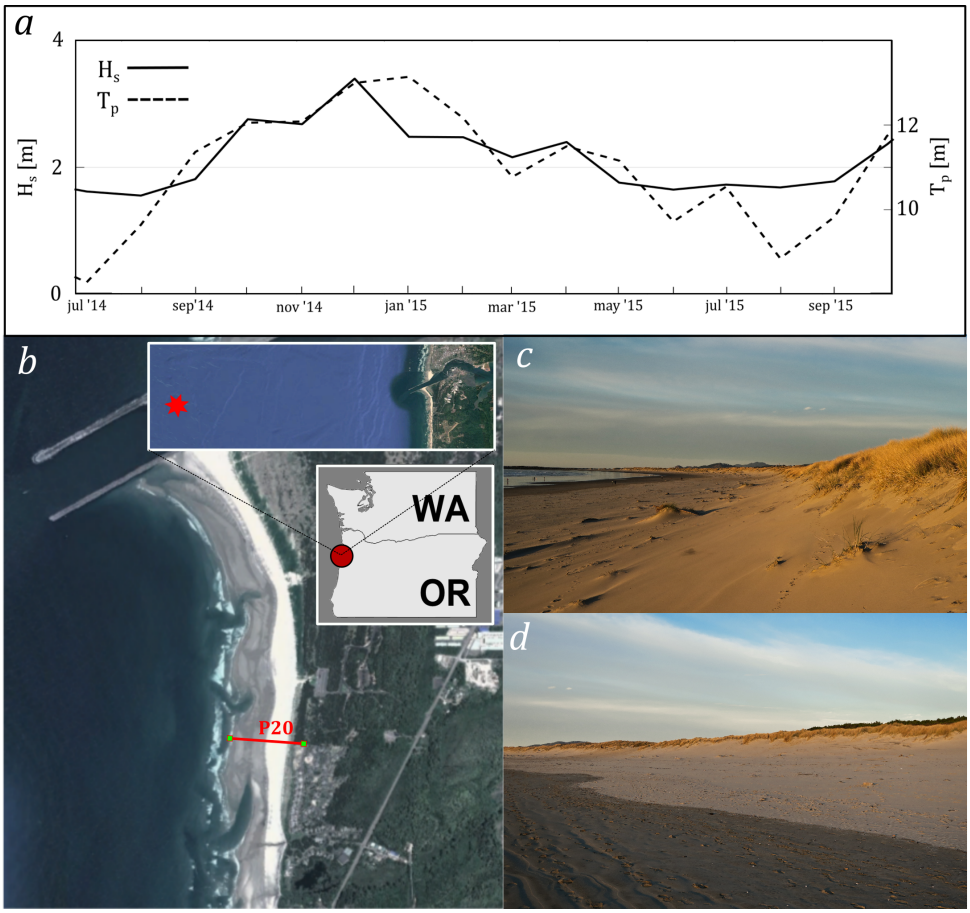

Figure 3.3: South Beach State Park, Newport, OR. *(a)* Monthly averaged significant wave height for the studied period at hindcast *GOW* point (red star in *b*; 44.5°N -124°W). Wave data description in 3.1.3. *(b)* Location of SBSP and P20. *(c)* and *(d)* Study site pictures around P20 transect (Nov'15).

transport processes and relate them with large-scale coastal dynamics. The main data sets that are collected periodically have information about grain size, beach slope and dune and sandbar height and position. Topographic beach profiles were conducted quarterly at 47 different locations (Fig. 3.1) using RTK DGPS systems. Measurements were taken by walking with a GPS mounted backpack from the landward side of the primary foredune ridge

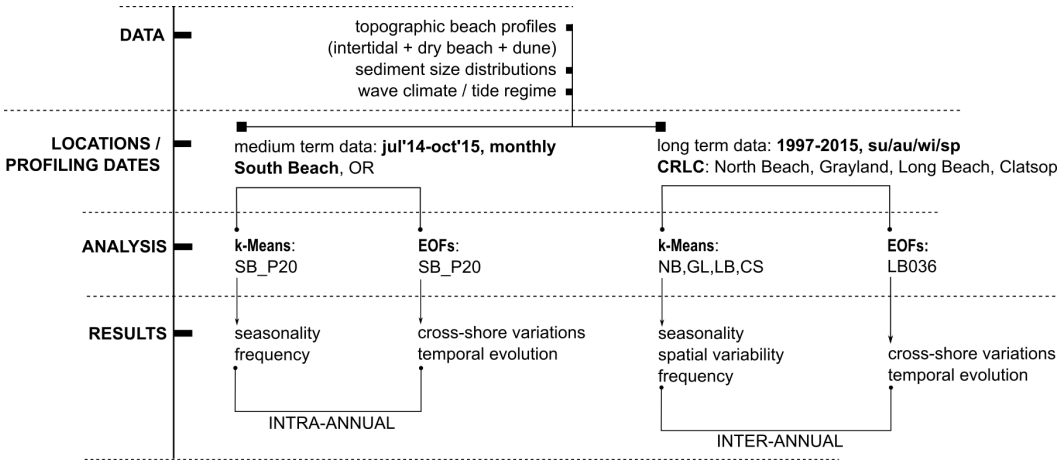

Figure 3.4: Flow chart detailing the methodology followed to characterize both intra and inter-annual variations in DBP through the application of KMA clustering and EOF.

to wading depth during a spring low tide. The accuracy is around $\pm 3cm$ in the horizontal and $\pm 5cm$ in the vertical. Sediment samples were collected at each site by hand typically at the mid beach location during the summer campaigns. A complete description of the techniques and the sampling schemes of the monitoring program for the CRLC can be found in Ruggiero *et al.* (2005). All levels are referred to NAVD88 in which the zero reference level is very close to MLLW. The shoreline is defined as the Mean High Water (MHW) contour, taken to be the $2.1m$ in the region (Ruggiero *et al.* 2013). These values are applied also to SBSP data.

3.3.1.2 SBSP topographic data

Monthly beach profiles were collected at South Beach State Park between summer 2014 and autumn 2015 (Cohn & Ruggiero 2015). 22 cross-shore transects, from mean lower low water ($MLLW$) to the dune, were surveyed over a $2.2km$ stretch of coast. The DBPs were measured with a RTK GPS mounted on a backpack, and the sampling frequency was bi-weekly or more frequently throughout the summer.

3.3.1.3 Wave and tidal data

Wave data for both study sites were obtained from *DOW* hindcast data base (Reguero *et al.* 2012). It is a new grid of the 60 year *GOW* wave hindcast developed by Perez *et al.* (2015) with 0.25^{o} resolution nearshore and a temporal resolution of one hour. The locations of the hindcast nodes are displayed for CRLC and SBSP in Fig. 3.1 and Fig. 3.3, respectively. Fig. 3.2 shows the monthly averaged wave data for the temporal coverage of CRLC profiling data (*i.e.*, from 1997 to 2015) and Fig. 3.3-a shows the monthly averaged wave data for the

studied period in SBSP (*i.e.*, from Jul '14 to Oct '15). The tidal regime was characterized with tide predictions for *NOAA* operated tide gauge stations located in the study area.

3.3.2 Data processing

We applied two different data mining methods to study changes in beach morphology. First we study the morphological DBP variations within a year using monthly data from South Beach P20 to be non-affected by jetty diffraction (Cohn & Ruggiero 2015). We chose data from 16 months of monitoring for a more clear interpretation of a yearly cycle. Since the summer '14 configuration did not display berm at this single transect (Fig. 3.5-a), we extended the temporal coverage for more than a year to capture a clear summer-bermy configuration during summer '15. The *K-Means* Algorithm KMA, Hastie *et al.* (2001) is first applied to discriminate summer from winter configurations and then EOF analysis is performed to quantify the main morphological changes in space and time. Nonetheless, 16 months of monitoring are not enough to clearly see the yearly cycle on DBP erosion-accretion. For this reason we also apply EOF analysis to a single profile of CRLC due to the longer monitoring time span (17 years) at that site –taking LB036 as representative after analyzing the behavior of the different monitored profiles along the CRLC in Ruggiero *et al.* (2005). We then investigate how the variations on the DBP along the CRLC take place. The KMA method classifies each profile in the desired number of clusters to identify the most common configurations of the DBP for the 17 years of surveying. We obtain the dominant modes that describe the variance within the data set without complicating interpretation of the results (Guanche *et al.* 2014). Based on the wave climate statistics (Fig. 3.2), which show a clear seasonality and offers two main wave climate regimes along a year, we use two clusters to distinguish the two corresponding configurations. We first apply the technique individually to each of the 31 profiles in Fig. 3.1, indicating then the most common configuration that each transect presents. Then we apply the technique to all profiles within the individual sub-cells, obtaining four results indicating the mean configuration that each sub-cell presents. Finally, to obtain the two mean seasonal configurations representative of the entire CRLC, we combine data from all 31 transects into a single matrix of the four sub-cells for the entire time period. A flow chart overview of the methodology is shown in Fig. 3.4.

3.3.2.1 *K-Means* Algorithm

Fayyad *et al.* (1996) found the *K-Means* Algorithm as effective in selecting common features and equilibrium shapes from large data sets, both temporally and spatially. The algorithm divides high-dimensional data into a number of clusters, each defined by a profile type and

formed by the data for which the prototype is the nearest (Hastie *et al.* 2001). Given a database of n-dimensional vectors $X = \{x_1, x_2, ..., x_N\}$, where N is the total amount of data and n is the dimension of each data $x_k = x_{1k}, x_{2k}, \ldots, x_{nk}$, the KMA is applied to obtain M groups defined by a prototype or centroid $v_k = v_{1k}, v_{2k}, \ldots, v_{nk}$. In our context, the dimension N is the number profiles forming the matrix to input to the algorithm; n is the number of elements of each vector –profile- along the x-shore direction (the number of data points must be equal) and the centroid ν_k is the standard profile representing the main configuration of each cluster. Each centroid, or profile-type, is associated to a specific set of profiles, grouped in one of each M groups or clusters. These centroids have the same dimension as the original data, where $k = 1, \ldots, M$, and they are moving every each iteration to minimize the overall distance between clusters until a certain degree of convergence is reached. The vector –or profile- which is nearest to a centroid M is set as the M cluster. Once the algorithm is running, on each iteration r, the nearest vector to each centroid is set as the mean of the corresponding set of profiles. *I.e.*, on the $r + 1$ step, each profile vector x_i is assigned to the j^{th} group, where $j = min\{\|x_i - v_j^r\|, j = 1, \ldots, M\}$, defines the Euclidean distance between the vector and the centroid in v_j^r in the r step. The centroid in each step is updated as:

$$v_j^{r+1} = \sum_{x_{i \in C_j}} \frac{x_i}{n_j} \tag{3.1}$$

Where n_j is the number of elements in the j^{th} group and C_j is the subset of the data included in group j. In each iteration the algorithm moves the centroids minimizing the distance within each cluster until certain grade of convergence is reached. Finally, the profile which offers the minimum Euclidean distance to the M centroid is considered the M cluster, which in our case represents the mean *DBP* of the data base. Due to the different heights and lengths of the profiles, the profiles of data set used to input the algorithm are normalized. Next, the user selects the number of clusters M for the classification and run the algorithm. We obtain then M groups of clusters with their corresponding occurrence of probability f. Díez *et al.* (2016) classify homogeneous data sets of beach profiles into a certain number of groups, characterized by their specific morphologies, and conclude that this technique is appropriate for classifying DBP morphologies. Here we apply the same general approach as Díez *et al.* (2016) used for Spanish beaches, but here extend the analysis to cover temporal variability.

3.3.2.2 **Empirical Orthogonal Functions**

EOFs have been widely used in coastal research to study several aspects of beach morphological variability, under medium- and long-term approaches and in both cross-shore and

long-shore (Clarke & Eliot 1975, Larson 1988, Lemke *et al.* 2014, Losada *et al.* 1991, Medina *et al.* 1993, Miller & Dean 2007, Muñoz-Perez & Medina 2010, Wijnberg & Terwindt 1995, Winant *et al.* 1982). This technique, also termed as Principal Component Analysis (PCA), is a statistical method that separates the spatial variability from the temporal variability of a given dataset. It splits the variations of a temporal data set of profiles into spatial patterns of variability, but it also provides a time signature related to each mode of variance. Applied for this case of beach profiles, the method is as follows. The function $f(x,t)$ that represents the profile elevation at a particular time or date can be defined as a linear combination of eigenfunctions in both spatial $X_n(x)$ and temporal $T_n(t)$ forms by:

$$f\left(x_i,t_j\right)=\sum_{l=1}^{N}a_l X_l(x_i)T_l(t_j) \tag{3.2}$$

Where $a_l=(n_x n_t \lambda_l)^{1/2}$, n_t is the number of surveys for each profile, n_x is the number of elements of the vector in the cross-shore direction (X) and λ_l is the eigenvalue associated to each eigenfunction. The weight of each eigenfunction gives a value of the percentage of variability of the data, and it corresponds to the mean squared value of the data (MSV). Assuming that the physical processes that drive the changes in the morphology explain the profile variability (*e.g.*, changes in grain size have no influence on temporal variability in morphology), each eigenfunction can be associated to a particular physical process. By studying the derivatives of the temporal coefficients, the EOF outputs can be related to changes in the wave forcing over a year following the approach of Jackson (1991). Here we implement this technique applied to a particular DBP over a time span of 16 months (SBSP, P20) and 17 years (LB036). We characterize the main changes in the cross-shore morphology and then we associate them with the variations in the environmental forcing.

3.4 Results

We present in this section the results from analyzing SBSP and CRLC DBPs by the application of KMA and EOF. We first introduce the results of applying these techniques to SBSP P20 for analyzing the intra-annual variations. To investigate how the seasonal pattern of erosion-accretion is replicated each year and to elucidate the most common configurations that DBP adopt along CRLC, we apply the same two methods to the entire CRLC. To give context of the variable forcing and morphometrics for the rest of the results section, we introduce here Table 3.1, which synthesizes the main hydrodynamic and sediment characteristics that modulate each studied profile and also the main morphometric indices that characterize their morphology (beach width, d, and mean DBP slope, $\tan\beta$). Frequencies of occurrence

f and fitting parameters R^2 are also given to indicate the variations around the equilibrium configuration. Values of surf scaling parameters such as dimensionless fall velocity Ω (eq. 1.1) and Iribarren Number ξ (eq. 1.7) are also calculated.

Table 3.1: Morphometric parameters and environmental variables at the different locations, displaying three transects per sub-cell in CRLC cases to ease the interpretation of the data. $\tan\beta$ and d are the slope and the width of the dry beach, from the 2.1m elevation (corresponding with MHW) to the dune toe (normally between $4m$ and $5m$ of elevation); R^2 is the mean of all the values from each linear fit between the normalized profiles and the corresponding centroids; f are the frequencies of occurrence. Hydrodynamic parameters for winter and summer are also displayed: Breaking wave height H_b, deep water wave length L_0, peak period T_p, wave steepness (H_b/L_0), Iribarren number ξ and dimensionless fall velocity Ω.

ID	P_{20}	NB 010	NB 011	NB 013	GP 017	GP 018	GP 020	LB 032	LB 036	LB 037	CP 043	CP 044	CP 045
$\tan\beta_m$	0.030	0.015	0.014	0.027	0.060	0.063	0.027	0.027	0.032	0.028	0.035	0.035	0.030
$\tan\beta_{su}$	0.024	0.013	0.013	0.022	0.044	0.048	0.026	0.021	0.031	0.027	0.030	0.026	0.030
$\tan\beta_{wi}$	0.033	0.016	0.016	0.028	0.064	0.065	0.027	0.028	0.033	0.028	0.036	0.038	0.030
$d_{su}[m]$	95	160	120	90	45	35	70	70	55	60	70	70	80
$d_{wi}[m]$	65	140	110	80	30	20	65	55	45	55	60	50	80
R^2_{su}	0.97	0.98	0.98	0.91	0.91	0.98	0.99	0.98	0.97	0.97	0.98	0.98	0.99
R^2_{wi}	0.99	0.99	0.99	0.99	0.99	0.99	0.99	0.99	0.99	0.99	0.99	0.99	0.99
f_{su}	31.2	36.2	31.8	13.0	33.3	31.8	56.5	28.9	27.5	33.3	32.7	16.6	16.3
f_{wi}	68.8	63.7	68.1	86.9	66.6	68.1	43.4	71.0	72.4	66.6	67.2	83.3	83.3
$d_{50}[mm]$	0.21	0.13	0.15	0.24	0.59	0.71	0.17	0.18	0.21	0.21	0.16	0.16	0.17
$H_{bsu}[m]$	1.9	1.9	1.9	1.9	1.9	1.9	1.9	1.9	1.9	1.9	1.8	1.8	1.8
$H_{bwi}[m]$	3.4	3.7	3.7	3.7	3.6	3.6	3.6	3.6	3.7	3.7	3.5	3.5	3.5
$L_{0su}[m]$	110.1	112.7	112.7	112.7	110.1	110.1	110.1	110.1	110.1	110.1	107.5	107.5	107.5
$L_{0wi}[m]$	175.3	182.0	182.0	182.0	175.3	175.3	175.3	172.0	172.0	172.0	172.0	172.0	172.0
$T_{psu}[s]$	8.4	8.5	8.5	8.5	8.4	8.4	8.4	8.4	8.4	8.4	8.3	8.3	8.3
$T_{pwi}[m]$	10.5	10.8	10.8	10.8	10.6	10.6	10.6	10.5	10.5	10.5	10.5	10.5	10.5
$(H_b/L_0)_{su}$	0.176	0.172	0.172	0.172	0.176	0.176	0.176	0.176	0.176	0.176	0.174	0.174	0.174
$(H_b/L_0)_{wi}$	0.020	0.021	0.021	0.021	0.020	0.020	0.020	0.021	0.021	0.021	0.020	0.020	0.020
ξ_{bsu}	0.465	0.205	0.228	0.342	0.459	0.467	0.203	0.210	0.463	0.369	0.264	0.242	0.264
ξ_{bwi}	0.452	0.110	0.110	0.194	0.446	0.453	0.188	0.191	0.225	0.191	0.252	0.266	0.210
Ω_{su}	9.1	15.4	13.2	7.8	2.9	2.4	11.5	10.8	9.1	9.1	12.1	12.1	11.3
Ω_{wi}	15.5	23.6	20.1	12.0	4.3	3.5	17.0	16.5	13.9	13.9	17.8	17.8	16.7

3.4.1 South Beach State Park: intra-annual variations

From all data available, we selected one profiling per month from July '14 to October '15, giving 16 measurements for the same profile over 16 months. P20 has been selected as it is representative of the system and because it is relatively unaffected by the jetty (Fig. 3.3-a). The KMA is first applied to obtain the two most common configurations over the 16 months of monitoring as well as the respective frequency of each configuration, assuming that this beach can be characterized as a DBP Type 1 (Fig. 2.8). Fig. 3.5-a and Fig. 3.5-b show the surveys and the two centroids for the *K-Means* analysis for an easier interpretation of the EOF results. The centroids represent the two main configurations that this beach exhibits over the 16 months, representing the winter configuration for a DBP Type 1 and to the summer configuration with the "bermy" shape on the foreshore segment. From the EOF analysis (Fig. 3.5-c and Fig. 3.5-d) we represent two spatial components, which together comprise around 95% of the cross-shore variance of the data. The two corresponding temporal components evaluate how the cross-shore variations in the profile evolve in time along the 16 months. The evolution of the DBP also gives information about how morphometric indices such as dry beach slope and beach width (both parameters computed from the MHW to the

dune toe) evolve in time. Dry beach slope and dry beach width are linearly related (R^2 = 0.88) based on the South Beach data (Fig. 3.6).

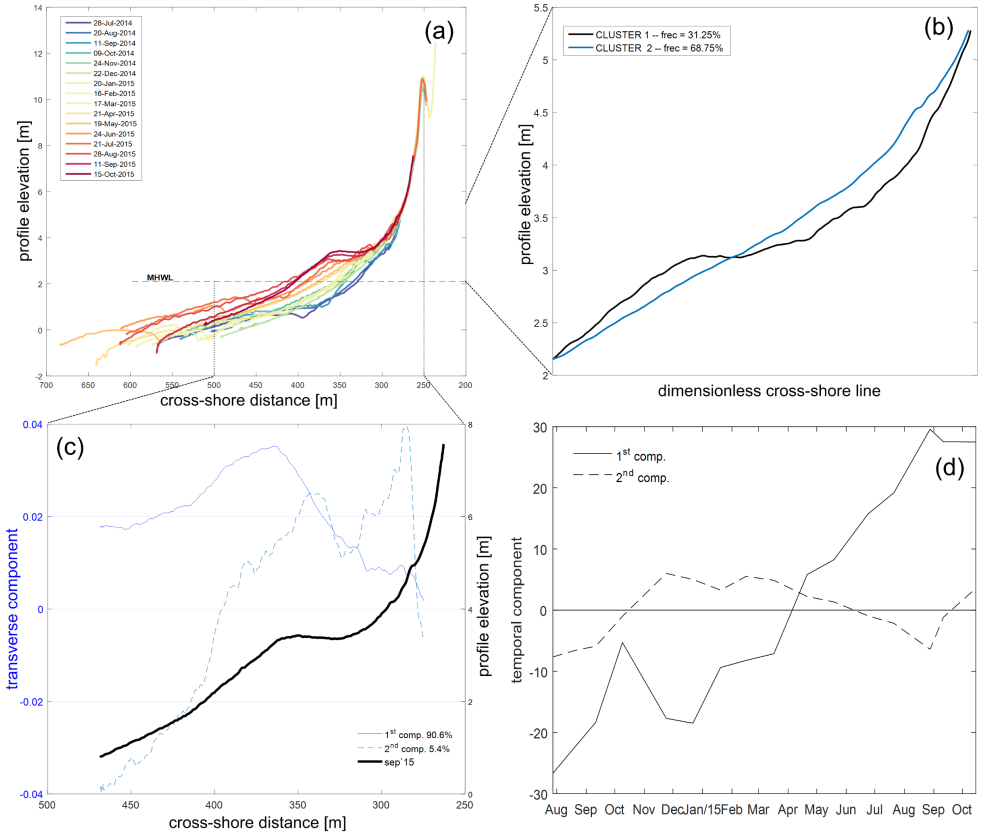

Figure 3.5: *(a)* Raw P20 profiles (MHW at 2.1m and dune toe elevation at 5m); *(b)* results from *K-Means* classification into two centroids; *(c)* First and second spatial components with Sep'15 profile sample as a reference; *(d)* Temporal components from EOF analysis for all temporal coverage.

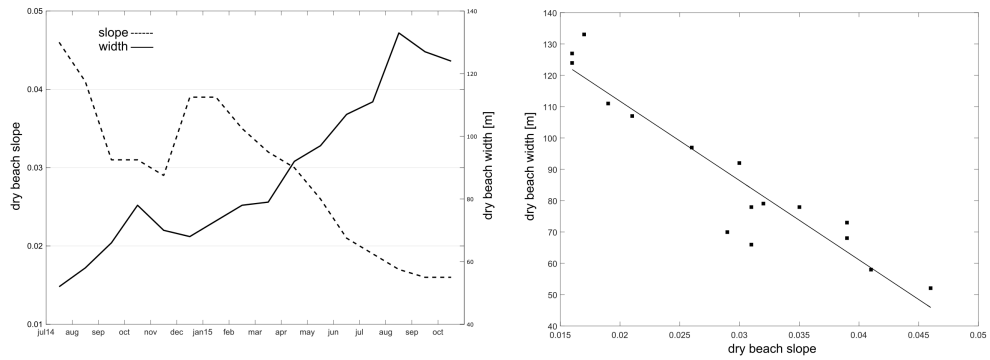

Figure 3.6: Relation between dry beach width and dry beach slope and temporal evolution during the studied time. Equation for the linear regression: width d *vs* slope $\tan\beta$ [$d = 162.3 - 2531.1 \tan\beta$. $R^2 = 0.88$].

3.4.2 CRLC: interannual variations

Beaches along the four CRLC sub-cells receive essentially the same energy from waves (Garcia-Medina *et al.* 2014) and they are generally constituted of fine grain size with a few exceptions (Ruggiero *et al.* 2005). However, despite the common environmental forcing, differences are evident in profile shape throughout the CRLC. The KMA clustering analysis is completed to determine the two predominant seasonal beach configurations for all CRLC profiles from 1997 to 2015 collected quarterly (4 times per year). Fig. 3.7 shows one representative profile of each sub-cell from this analysis: NB010, GP020, LB036 and CP045 taking as representative after analyzing profile longshore variability in Ruggiero *et al.* (2005). The selected profiles were unaffected by lateral boundaries and best represents an averaged form of the profiles at the same beach site and oriented to similar mean exposure situations. Fig. 3.7 shows raw profiles, normalized cross shore profile lines for the two centroids, and frequency of occurrence of each morphologic state for each season. In Fig. 3.8 the clusters are plotted with their 95% confidence bounds to demonstrate the most significant cross-shore variations around the centroids. Small deviations identify relatively stable segments, while large and wide envelopes are associated with segments of the profile with high variability. The centroids represent the most frequent or stable configuration; Fig. 3.7 also shows the R-squared value computed by fitting each individual profile with its corresponding cluster. It is evaluated over time to see how each profile deviates from its centroid. The closer the value is to $R^2 = 1$, the smaller the deviation of each configuration from the centroid (stable profile).

While the representative profiles generally show the characteristic behavior for each sub-cell, there may be significant variability in the morphologic evolution between different profiles. Fig. 3.9 illustrates the aggregate results of all profiles within each sub-cell – in part demonstrating that while individual profiles may not always necessarily show the summer berm behavior (Fig. 3.8) regionally this trend is observed in all CRLC littoral cells (Fig. 3.9). Shown in Fig. 3.9 blue (winter) and black (summer) bars are the R-squared values obtained from the linear fits between the main sub-cell centroid and the corresponding centroid obtained by applying *K-Means* in each transect. It can be seen, for instance, how all Long Beach Peninsula transects are quite similar to the averaged summer and winter configurations. In the case of North Beach, especially for NB013 and NB015 summer configurations, R^2 values relatively far from 1 indicate the larger morphological deviation from the standard configuration. In general, winter configuration (blue) deviate less from the mean sub-cell configuration than the summer configuration (black). Fig. 3.10 shows the result of combing all data from the CRLC into the KMA (31 transects, sampled quarterly for 17 years). The most common seasonal configurations of CRLC DBPs averaged through 17 years of data

are apparent. Lastly, to complete our analysis of CRLC intra-annual variations, an EOF were computed using Long Beach, LB036. The first and second spatial components after computing the eigenfunctions, displayed along with a profile sample from April'05 for easier interpretation of the EOF results, are presented in Fig. 3.11 to understand the cross-shore variations. The application of EOF to this larger temporal coverage allows appreciating how the seasonal pattern of erosion-accretion is replicated through the years. Fig. 3.12 shows the corresponding first and second temporal components, calculated quarterly for the entire study time period for a better interpretation.

3.5 Discussion

This study reports on the seasonal cycle of beach loss and recovery along a high energy dissipative coastline with a marked seasonal pattern in wave climate, documenting the seasonal exchange of sand between the onshore and the offshore. During mild conditions in summer season, onshore sediment transport dominates, resulting in a widening of subaerial beach of around $15m$. Then, the energetic winter wave climate and high mean water level elevations cause a net offshore transport, inducing a retreat in the subaerial beach. During summer, a "bermy" configuration appears in most of beaches along CRLC and the foreshore becomes steeper and narrower than during winter. When the berm is destroyed, the water often can reach the dune toe (and even causing dune erosion) due to enhanced runup, and all the DBP is formed by the foreshore segment, fully dominated by swash processes, as predicted. Thus, the hypothesis set out at the beginning of this study stating that this kind of beaches should present a Type 1 DBP, according to Díez *et al.* (2016), is here demonstrated. We analyze these statements in detail through the following subsections.

3.5.1 Intra-annual variations: SBSP case

The temporal variability of PNW DBPs is clearly modulated by the seasonality in wave climate, which induces seasonality in the exchange of sediment in the cross-shore direction. The KMA clustering analysis applied to the 16 months of SBSP data indicates the two main configurations that this transect presents during that period. Approximately 70% of the measured profiles present a configuration associated to the cluster that represents the winter-flat configuration (Fig. 3.5-b blue line), and approximately 30% of the profiles along the 16 months are similar to the summer-"bermy" configuration (Fig. 3.5-b black line). We must point out that the DBPs do not display exactly the same two configurations arisen from cluster analysis. The transitionary stages are also grouped into these two configurations. That can be appreciated from looking at the confidence bounds in Fig. 3.5. The more

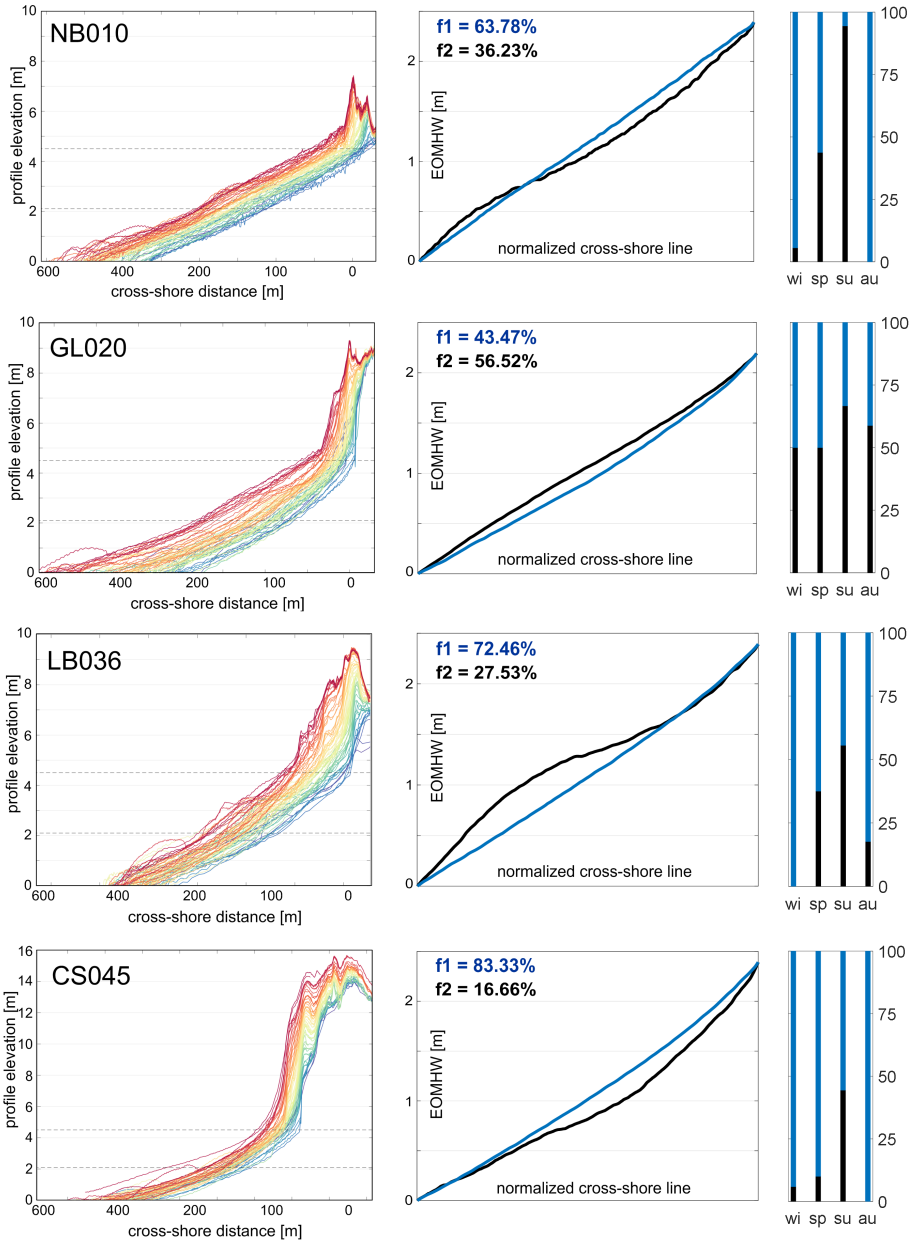

Figure 3.7: *Left panel*: Raw profiles going from 1997 (blue) to 2015 (red). The dry beach is delimited from MHW, 2.1m, to the dune toe, between 4m and 5m elevation; *Middle panel*: Normalized centroids from *K-Means* algorithm output with their corresponding frequencies of occurrence f, averaged over the 17 years of sampling. The vertical scale corresponds to the elevation over mean high water level (EOMHW) Blue line represents the winter configuration and the black line is associated with the summer configuration; *Right panel*: Seasonal averaged occurrence in percentage for each centroid.

variability in the bounds, the more transitionary stages are encompassed in each cluster. The EOF analysis provides insight to how the profile shifts from its flat to its berm-like profile. The first spatial eigenfunction (Fig. 3.5-c), representing 90% of the profile variability, explains the general temporal evolution of the profile. The maximum variability occurs around 3m

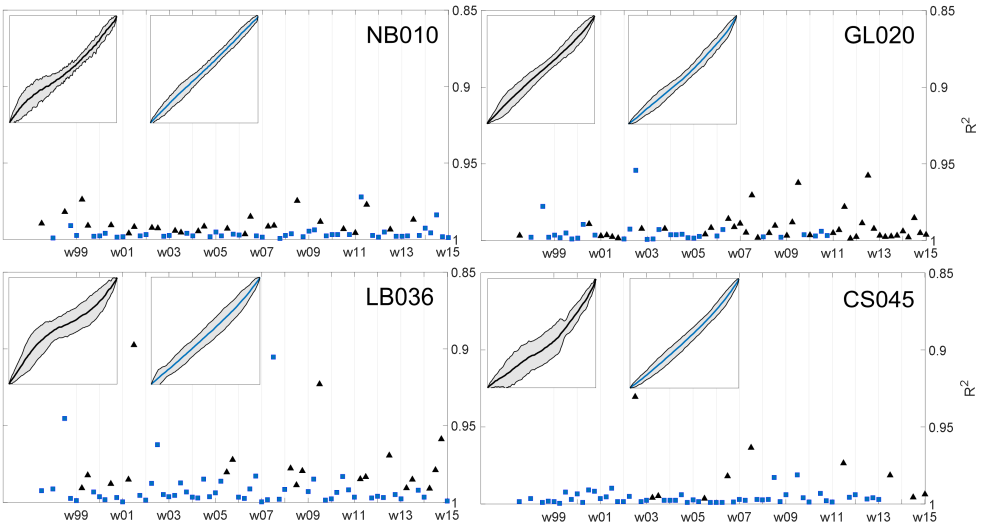

Figure 3.8: Time series of R-squared values from each linear fit between the normalized profiles and the corresponding centroid. Inset figures show the two centroids with 95% confidence bounds demonstrating cross-shore variability in beach profile variance.

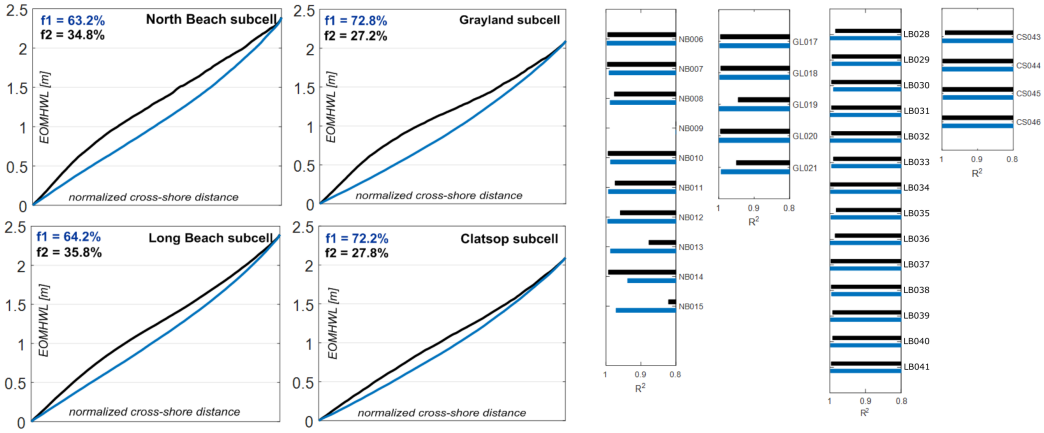

Figure 3.9: *K-Means* results for each sub-cell. The input data for each sub-cell are all the corresponding sub-cell transects (Fig. 3.1) from 1997 to 2015. The right panel indicates the R^2 value derived from fitting each sub-cell centroid (blue is winter and black is summer) with the corresponding centroids of *K-Means* analysis of each transect.

NAVD88, which corresponds to the zone where the berm is built. There is a gain of elevation from the dry beach towards offshore along the 16 months, with a peak around the berm position. By analyzing the second spatial component we observe that a peak rises at the dune toe, representing the dune recovery after an eroded state. The wider peak around $340m$ in cross-shore direction represents the development of the berm crest. The shifting between negative and positive values of this second transverse component around $400m$ in the cross-shore position indicates the sand movement from the intertidal region to the beach

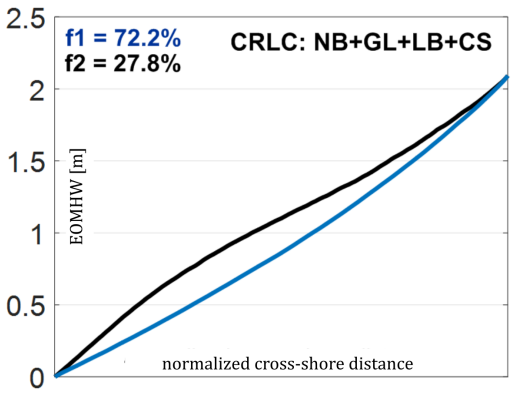

Figure 3.10: Centroids derived from combining all transects in each of the four sub-cells. Blue and black line corresponds to the centroids associated with winter and summer configurations, respectively.

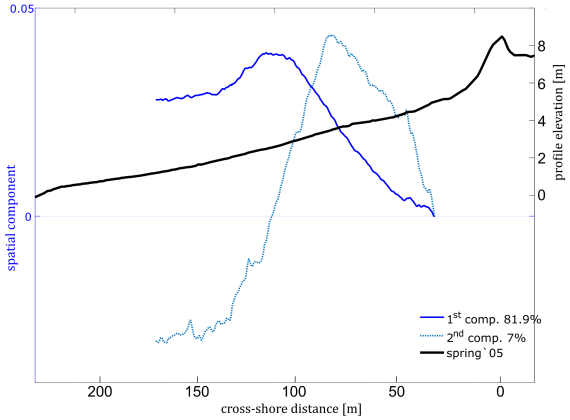

Figure 3.11: First and second spatial eigenfunctions from EOF analysis of LB036 (see the profile evolution during the entire temporal coverage in Fig. 3.7.)

face, indicating its recovery. From this analysis arise two mechanisms, described by both spatial components: the total gaining of elevation along the entire profile (first component), and the beach face recovery and building of the berm, and also the recovery of the dune toe (second component). The temporal components from the EOF analysis help to clarify the relevant processes. The first temporal component shows a positive trend indicating a growing in elevation from Jul'14 to Oct'15 –except for the decaying from October to January, which suggests offshore transport and beach face erosion. The summer profile of 2014 does not display a berm, so the temporal component does not show the winter-summer pattern (erosion-accumulation) in the upper beachface. Although other transects (analyzed in detail in Cohn & Ruggiero (2015)) display berm, P20 may be affected by a rip embayment or break in the intertidal bar at P20 in 2014, leading to no berm at that site. The profile, at least for this year, is always gaining elevation. From Jul'14 to late Sep'14, the lower energy wave conditions (Fig. 3.3-a) allowed the dry beach to grow. The storm conditions from the end

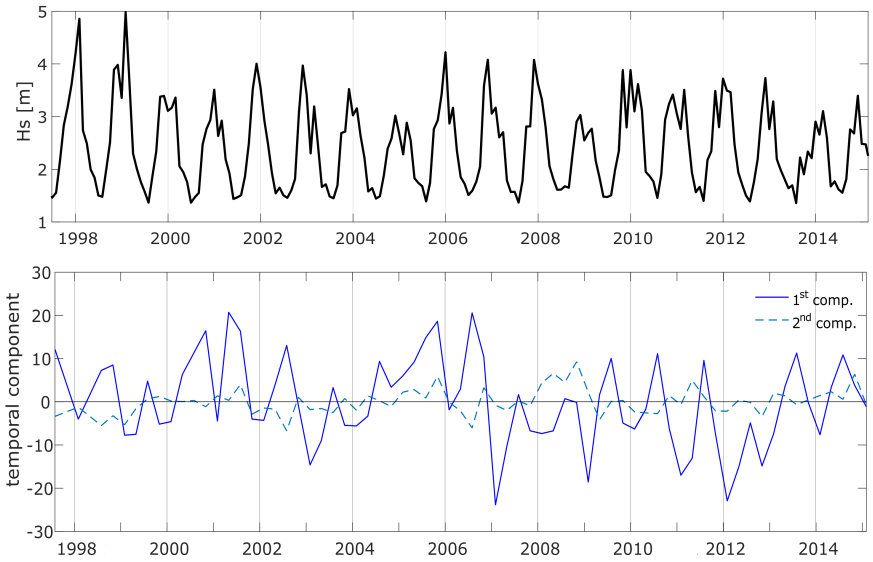

Figure 3.12: *Upper panel*: averaged significant wave height; *Lower panel*: first and second temporal components from EOF analysis on LB036. Wave data from upper panel obtained from *GOW* hindcast data.

of September to late December cause recession, as can be seen in the downward trend of the temporal component until Jan'15. Then, the lower energetic mean wave climate, around $1.5m$, causes a constant dry beach growing around the berm position and over the beach face, causing a gain in elevation. This trend keeps constant until Oct'15.

3.5.2 Inter-annual variations: CRLC case

3.5.2.1 CRLC K-Means results

Fig. 3.7 displays the two main DBP configurations over the 17 years of data for each representative sub-cell location and their seasonally averaged frequency of occurrence (winter, spring, summer and autumn). The two centroids are associated with "winter" and "summer" profiles, referring to the two main configurations that a beach with Type 1 profile may present over a year (Fig. 2.8); with the specific sub-type dictated primarily by the mean monthly wave conditions at the beach site. From the seasonal distribution of clusters (Fig. 3.7, LB, NB, CP), we observe that during the winter season a winter-flat DBP is almost always evident. During summer, the profile accommodates the less energetic wave climate via a berm-like profile (*i.e.*, LB, NB, CP). For Grayland (GP020, Fig. 3.7), winter and summer configurations are fairly similar, due to the incapacity to build a stable berm during summer season. As stated in the introductory chapter, the presence of berms can be conditioned by the intertidal and subaqueous sandbars. The generalized absence of summer berm on GP020 may be affected by this fact, but this is not demonstrated by the current data. Further

insight is required to investigate this complex mechanism. Moreover, through the variations of R^2 in time (Fig. 3.8) we assess how the winter setting deviates less from the most common configuration(or centroid) than the summer season, which has much wider confidence bounds. When the DBP profile presents the summer configuration (black triangles) the deviations from the equilibrium (represented by the centroids) are larger, indicating also that the time needed to adopt the final equilibrium stage is different between winter and summer configurations. DBP adopts its winter configuration in a time scale much smaller than the summer configuration. Beaches responds rapidly to increasing energy conditions, but adjust slowly to decreasing energy conditions, as found in several previous studies (Jackson *et al.* 2002, Stive *et al.* 1999). Since we used one profile each for the four seasons in the KMA analysis, we are seeing in these variations all the transitional stages when going from winter to summer configuration, *i.e.*, the progressive gaining of elevation and accumulation of sand around the berm position.

3.5.2.2 **LB036 EOF results**

The analysis of LB036 clearly shows the yearly oscillations around an equilibrium position (Fig. 3.11, Fig. 3.12). The first transverse EOF component –which explains 85% of the variability of the system-, has a large peak at around $2m$ NAVD88, corresponding approximately with the mean high tide level. The raw profiles presented in Fig. 3.7-c indicate that the beach is prograding and the zone around 2-3m elevation is gaining sand, probably mostly due to gradients in longshore sediment transport (Ruggiero *et al.* 2010; 2016). The variability in the second component indicates the cycle for berm formation and erosion is a repetitive pattern over the foreshore segment, with a peak over the berm position and a pivot point (Aubrey 1979) around $80m$ from the dune crest on the cross shore position. The first temporal component from 1997 to 2015 shows a periodic pattern, going from positive in summer to negative in winter due to the seasonality in wave climate. The entire dry beach gains sand during "low" energetic periods with a peak around $3m$ elevation. This pattern is reproduced every year. On the other hand, the second temporal component presents a peak at the end of each summer period and goes to negative at the end of winter period, responding to the seasonality in berm development and destruction, reproducing in an interannual oscillation the same general behavior that South Beach displayed over one year.

3.6 Conclusions

Utilizing spatially and temporally rich beach morphology datasets from the US Pacific Northwest, inter- and intra-annual variations of the profile that gives shape to the dry part of the

beach system are explored. Using *K-Means* and *EOF* analyses, we observed that around 70% of the year the DBP offers a flat straight-slope profile from the MHW to the dune toe. The mean dry beach slope is around 0.03 in winter and 0.02 in summer, due to the DBP widening. During 30% of the time, the DBP presents a berm-like profile, mostly during summer when wave conditions are less energetic. EOF analysis offers a complement to the KMA analysis and illustrates where and when the changes over the profile take place. We observed the following generalized behavior: from a flat dissipative DBP, during summer, there is a constant gain of elevation on the foreshore segment until the berm height reaches a mean elevation around $3.2m$ (NAVD88). Consequently, the dry beach seasonally widens an averaged value for CRLC around 15-20m each year. The profile forms a steeper foreshore ending in a berm. From the berm crest to landwards, a positive straight slope is formed until the dune toe, where the profile adopts the dune curvature. There are still lots of unknowns regarding the feedbacks and dynamics governing changes in beach morphology. Here we report how the environmental conditions of a high energy dissipative coastline define the DBP morphology and modulate its variations associated with seasonality in wave climate. This work is part of an exhaustive study oriented in pursuit of a complete understanding of the DBP, where the most common morphologies, the equilibrium configurations and the variations and deviations from it are investigated, described and integrated.

4

A parametric model for dry beach equilibrium profiles

Abstract [1]

Predictions of dry beach morphologies are extensively required in coastal research for multiple purposes -*e.g.*, dune erosion forecasting, inundation heights determination and beach fill design optimization. In this paper, we introduce and test a parametric model that describes the equilibrium shape of the dry beach in the cross-shore direction, *i.e.*, an equation for the dry beach equilibrium profile. The model consists of a three-parameter equation formed by two terms: an exponential that defines the foreshore and berm morphology, plus a linear term that defines the slope from the berm to the landward limit as a planar far field behaviour. The three morphological parameters that shape the equation are related to the nearshore wave climate (H_s and T_p) and the sediment characteristics (d_{50}) in a form which is consistent with previous knowledge of dry beach morphodynamics, thus proposing the runup driver $[HL]^{(1/2)}$ and the dimensionless fall velocity Ω as the fundamental variables defining the equation parameters. We tested the predictive capacity of the model against an independent data set from Narrabeen Beach, which, depending on longshore location and the time of year, offers beach modal states ranging from dissipative to reflective. The exponential term of the equation correctly explains the foreshore and berm morphology under mean wave climate, and the linear term predicts the slope of the asymptotic-planar segment, all with good correlation coefficients (0.95) between modelled cross-shore transects and observations. The proposed model helps in defining the main shapes of subaerial beach profiles over the

[1] This chapter is based on Díez et al. (2017b): Díez, J., Cánovas, V., Uriarte, Ad., Medina, R., 2016. *A parametric model for dry beach equilibrium profiles.* Coastal Engineering (in press)

long term and it may also be useful as a coastal management tool for predicting dry beach morphologies.

4.1 Introduction

One of the prime goals of research in the subaerial zone of a sandy beach is to forecast its morphology, which is governed by local hydrodynamics. The response of the cross-shore morphology of this zone, defined here as the segment between the mean high water level (MHW) and the landward edge (dune toe, seawall or cliff), depends essentially on the beach modal state (Hesp 2012), but also on the pre-existing topography. Knowing that a beach is a highly dynamic environment and that changes occur due to the almost instantaneous movements of sand in the swash zone as well as from decadal changes driven by fluctuations in sea level, measuring these changes requires a huge investment in both economic and temporal terms. Consequently, there is a demand for the development of parametric models for dry beach topography, which may lead us to give an account of the main features, widths and heights that define the cross-shore section of the dry beach under mean wave and grain size conditions. One of these parametric models is the widely accepted equilibrium beach profile (EBP), which represents typical forms under natural forcing. It serves as a proxy in cases where it is difficult to acquire bathymetric and topographic data, and also for forecasting long term equilibrium forms in response to long term climatologic events. The EBP, theoretically, is the curve under which the sediment transport is equal to zero in any direction. Nonetheless, EBPs can be estimated as simple parametric forms obtained by comparing their similarity to well-known real equilibrium cases (Dean 1977). Numerous works dealing with EBPs (Dean 1991, Larson & Kraus 1995, Romanczyk *et al.* 2005) have been done since Brunn (1954) made the first approach by proposing a power law approach in the form:

$$h = Ax^{2/3} \tag{4.1}$$

where h is the depth, x is the cross-shore length and A is a sediment-dependent parameter (Dean 1991). This power law is underpinned by the assumption that the energy dissipation is constant along the profile, and despite its simplicity, it predicts most portions of a sandy beach cross-shore section relatively well. Some inconsistencies arise from this law –the absence of features such as bars and forecasts of infinite slopes at the shoreline- that several authors have dealt with (Bernabeu *et al.* (2003), Holman *et al.* (2014), among others), but its application is still essential today for multiple engineering designs. We will see throughout this Chapter that the proper selection of the wave parameters that modulate the shape is crucial to understanding the interplay between dynamics and morphology. When considering

equilibrium and the forces that modulate it, it is important to point out that the onshore-offshore cross-shore sediment transport is entirely asymmetric in both its origin and in its corresponding temporal scale. Offshore sediment transport is associated with storm conditions and normally occurs over a time scale of a few days or even hours, whereas onshore sediment transport is driven by mean wave conditions and its time span is much longer, ranging from weeks to months; *i.e.*, beach morphology does not immediately react to changes in the wave field. Several authors have demonstrated that instantaneous measurements of Ω and observed beach states rarely show good correlations, especially in high-energy beaches with frequent storms and seasonal recovery periods (Anthony 1998, Jiménez *et al.* 2008, Lee *et al.* 1998). In addition, Wright *et al.* (1985) suggested that the recent history of beach morphology and past wave fields also play a role in determining the current beach state. This time lag between stress and response implies that beaches have "memory" regarding past forcing. As a consequence, the shape of the subaerial beach is not modulated by the current-wave height, but by the past wave climate (Jara *et al.* 2015). We must be cognizant of these references when calculating wave statistics throughout this study. In the present Chapter, using a data driven and geometric approach, we propose a static equilibrium model for the DBP, which, unlike other dynamic models, does not require any sediment transport relation. Taking this into consideration, our purpose is two-fold. The first is to propose a parametric equation for a DBEP that fits a wide range of beach modal states, from flat and featureless dissipative DBPs to berm-like reflective DBPs. It must satisfy requirements such as *i*) offering continuity between the submerged and emerged zones, proving that our equation satisfactorily predicts the foreshore slope at Mean High Water level (MHW) and *ii*) convincingly reproducing the slope of the asymptotic-planar zone between the berm crest and the landward edge. Our second goal is to test the new model over an independent data set and assess its predictive skills for the study of DBP morphologies. In the next section, we describe the methodology and the two data sets used for this study: for the development of the model, a large profile data set of Spanish beaches (Tomás *et al.* 2015) with a large spatial coverage that encompasses the entire range of beach modal states, and for the validation of the model, a long-term data set from Narrabeen Beach in Eastern Australia (Turner *et al.* 2016). The equation is then presented, described and tested.

4.2 Data set and methodology

In this chapter we introduce the data sets for both model development and validation, and we then discuss the framework and theoretical basis on which the model is based.

4.2.1 Data set for model development

The profile database used for this study was obtained from a large profile database composed of Digital Terrain Models developed by IGN (the Spanish Geographical National Institute) and collected during the IOLE project (Tomás *et al.* 2015). The DTMs were obtained from LIDAR surveys covering the entire Spanish coast, and the dates of the survey flights are known and comprise dates from 2009 to 2012. The mesh of the DTMs was built using a resolution of $5m$ x $5m$. Profiles were obtained by interpolation of the DTMs along the cross-shore direction, offering vertical and horizontal resolutions of $0.1m$ and $5m$, respectively. The cross-shore section is available from the zero-reference level for the Spanish Coast (Alicante Zero Reference Level, NMMA) to the landward edge. Beach sites for this study were selected to cover the four different wave climate regions described in Díez *et al.* (2016). From Zones I and II (the Northern and West Atlantic coasts of Spain where the presence of fine golden sandy beaches dominates, forming sand spits and coastal dune systems, and also medium-coarse grained, urban-pocket beaches backed by promenades): Hondarribia (Gipuzkoa), Orio (Gipuzkoa), Zarautz (Gipuzkoa), Usgo (Cantabria), Xagó (Asturias) and Peñaredonda (Asturias). From Zone III (the South Atlantic Spanish coast, with a predominance of large coastal dune fields and very large, straight beaches composed of medium-fine sand): El Palmar (Cádiz) and Zahara de los Atunes (Cádiz); From Zone IV (the Mediterranean coast, where small, narrow beaches formed by coarse sand or even gravel dominates, and long, straight beaches with medium-coarse grained sands): Nerja (Málaga), Gandía (Valencia), Mataró (Barcelona) and Blanes (Girona) (see Locations in Fig. 4.1 and Characteristics in Table 4.1). We selected profiles unaffected by lateral boundaries and which best represent an average form of the profiles at each beach site and oriented to similar mean-exposure situations. They display a configuration that correlates accordingly to mean wave conditions at the beachfront around the date of the survey, *i.e.*, the dry beach profile must present some sort of average shoreface profile cross section (Pilkey *et al.* 1993). For further information regarding the profiling, readers may refer to Tomás *et al.* (2015). Wave statistics were obtained from the *DOW* hindcast database (Perez *et al.* 2015, Reguero *et al.* 2012). The database is a new grid with 0.25 grades of nearshore resolution and a temporal resolution of one hour and covers 60 years, from 1948 onwards. The location of hindcast nodes allows us to obtain wave data immediately seawards of each selected transect. Wave data selection corresponding to each profile was done following the recommendations made by Wright *et al.* (1985). As pointed out in the introductory section, they introduced the concept of "beach memory" by evaluating the time-averaged dimensionless fall velocity values Ω_∞ in Narrabeen Beach (AU). They stated that the current value of Ω_∞ made negligible contributions in explaining day-to-day beach state observations, whereas the antecedent conditions show good correlations for predicting current beach states. Through analyses of the diverse parameters used

to calculate Ω_∞, the dimensionless fall velocity associated to the equilibrium, they found that the values that best represent the current state of the beach were those with D approximately equal to 30 days, better than the instant value of Ω_i, where D is the state of the beach 30 days previous. We accordingly associated wave statistics to beach sites following this criterion. Wave data for the study sites are listed in Table 4.1.

Table 4.1: Mean wave parameters corresponding to the mean of D =30 days before the date of survey along with sediment sizes for the study sites.

beachsite	*ID*	*surveying date*	$D_{50}[mm]$	$H_s[m]$	$H_b[m]$	$T_p[s]$	$[HL_0]^{1/2}$	Ω_∞
Hondarribia	$H1, H2$	Sept'10	0.30	0.7	1.16	10	10.61	2.14
Orio	$O1$	Sept'10	0.48	1.2	1.82	10.5	14.36	1.98
Zarautz	Z1,Z2,Z3	Sept'10	0.25	1.8	2.66	12	20.11	6.2
Usgo	$U1, U2$	Sept'12	0.50	1.2	1.78	10	13.68	1.89
Xagó	$X1, X2, X3$	Sept'12	0.20	1.8	2.66	12	20.11	6.1
Peñaredonda	$Pe1$	Sept'12	0.20	1.2	1.78	10	11.27	5.03
ElPalmar	$P1, P2$	Oct'12	0.30	0.95	1.39	8.5	10.34	3
ZaharaAtun	Z_{a1}, Z_{a2}, Z_{a3}	Oct'12	0.32	0.93	1.26	7	8.43	3.4
Nerja	$N1, N2$	Oct'12	0.50	0.6	0.72	4.2	4.06	2.1
Gandía	$G1, G2, G3$	Oct'09	0.23	0.7	0.90	5.4	5.64	4.6
Mataró	$M1, M2$	Oct'10	0.70	0.7	0.89	5.2	5.43	1.4
Blanes	$B1, B2, B3$	Oct'10	1.30	0.7	0.88	5	5.43	0.7

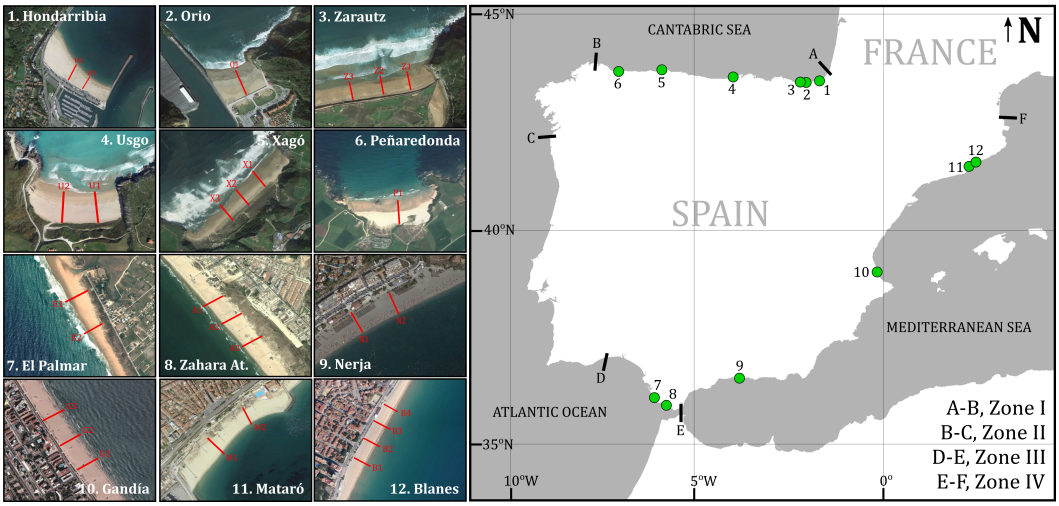

Figure 4.1: *Right panel*: Location of the study sites along the Spanish coast. The coastline is divided into four zones characterized by specific wave and tidal climates (Díez *et al.* 2016). Aerial pictures in the *left panel* show the profile locations for each beach site. The DBPs used at each beach site were the ones that best represent the average of all the profiles available at each beach site under similar exposure conditions.

4.2.2 Data set for model validation

We validated the proposed model using field data from the Narrabeen Beach (one of Sydney's Northern beaches in Southeast Australia) Long-Term Data Set, which encompasses wave data and monthly subaerial beach profiling from 1976 to 2016 (still ongoing). Details concerning the background, profiling methods and more detailed information on the beach system can be found in Turner *et al.* (2016). Wave data was obtained at $10m$ water depth immediately seawards of each transect, derived from recorded deep-water wave data. The wave climate has seasonal behaviour during the year, and depending on the profile site, the beach is either more dissipative (northern side) or more reflective (southern side). This variability in wave climate and beach characteristics allowed us to test our model under two different wave climates and under both more-dissipative and more-reflective conditions. Table 4.2 lists the data employed for model validation.

Table 4.2: Data set for model validation. We used PF1, PF6 and PF8 for model validation (see location and additional information in Turner *et al.* (2016).

site	*surveysundertaken*	*transectsID*	*dates*
Narrabeen	6	$PF1, PF6, PF8$	$14aug'06/18jan'10/13jul'10$ $13jul'11/11jan'12/26jun'13$

4.2.3 Theoretical basis

Our model must use a single expression to reproduce the four main DBP types found by Díez *et al.* (2016), *i.e.*, the two extremes and the transitionary stages between them: from a straight featureless positive slope (winter Type 1) to a steep-convex foreshore segment –bermy shaped- with an almost horizontal planar state in the far field (Type 3). The proposed parametric expression that defines the equilibrium was tackled using a heuristic approach, and is defined here as eq. 4.2.

$$f(x) = A(1 - e^{-bx}) + mx, \forall x \epsilon [0, x_f] \tag{4.2}$$

Where 0 is set at the MHW level with positive curve values in the z direction and x_f indicating the cross-shore position of the landward edge (Fig. 4.2). The expression is the sum of an exponential function, which deals fundamentally with the foreshore segment, defining its curvature, length and height, and an asymptotic planar slope, which mostly defines the shape of the segment between the berm and the landward edge. Variations of the three morphological parameters A, b and m shape the function and are modulated by dynamics and sediment characteristics, which arise as the main determining factors of the DBP shape,

as previously stated. Fig. 4.2 shows all the possible changes induced in the shape by varying the three parameters and the two extreme cases where the same parameters reduce to zero. It verifies that eq. 4.2 satisfactorily reproduces all the DBP Types schematized in Fig. 2.8.

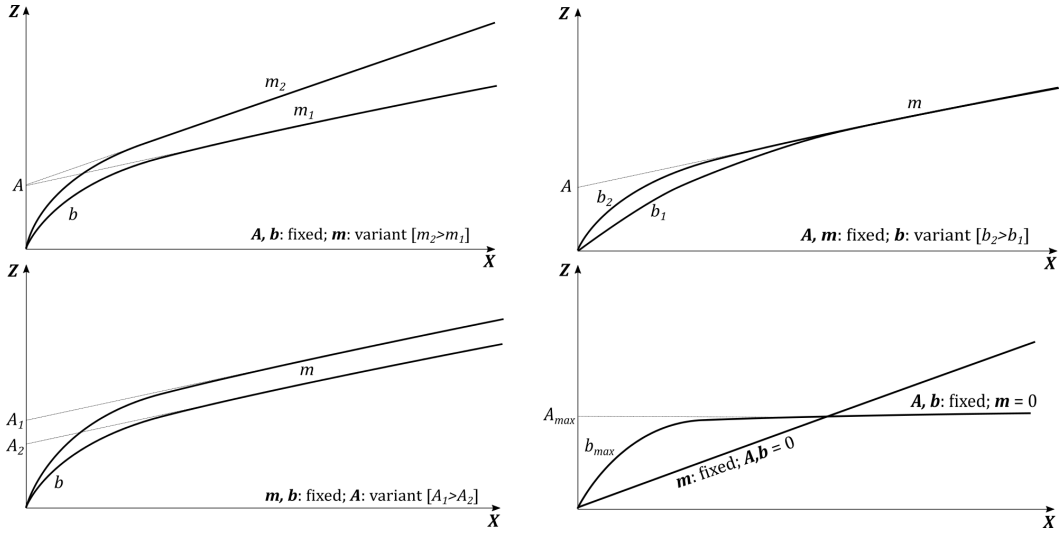

Figure 4.2: The DBEP schematic representation of eq. 4.2. The first three panels represent the changes induced in shape by varying the morphological parameters. The last panel shows the two extreme configurations, achieved when either A, b or m are equal to zero. The origin of the coordinate axes is set at the MHW level.

4.2.4 First considerations about the parameters' behaviour

Parameter **b** $[m^{-1}]$ defines the curvature or convexity of the foreshore segment. The convexity rises with the value of b. Moreover, a curve with a larger value of b needs less length in the cross-shore direction to reach height **A** $[m]$; hence, a profile with large values of b is steeper and narrower, and a profile with a larger value of A is higher in the far field. From the height defined by A, the curve progressively loses its curvature, terminating in a straight line with a slight positive slope which asymptotes to a planar far field behaviour, defined by **m** $[dimensionless]$. Fig. 4.2 lists these statements.

4.2.4.1 Parameter b

Numerous works in the literature demonstrate that foreshore morphology is dominated by both wave conditions and sediment characteristics (Masselink *et al.* 2006, Wright & Short 1984). Based on this, and observing changes in the shape induced by changes in b (Fig. 4.2), we assume that this parameter is mainly modulated by wave steepness –b is inversely proportional to H_s- and grain size -b is proportional to d_{50}-, taking the dimensionless fall velocity Ω as the main driving factor. It is well proven in the literature that the more dissipative

a beach is, the "flatter" the foreshore segment is in order to dissipate the energy from the incident waves (Short 1999). Lower values of b make the segment "flatter" and less steep (Fig. 4.2); hence we assume that if Ω increases –indicating a "more" dissipative beach-, b must tend progressively towards zero. When the profile is flat and featureless without a berm -normally in cases with very high values of Ω, (Díez *et al.* 2017)-, b must be zero. In such cases, eq. 4.2 is defined only by the linear term $\backsim mx$.

4.2.4.2 **Parameter** A

Formulations in the literature concerning berm height are skeptical about the role of sediment size in modulating the equilibrium height of the berm, and the degree of dependence still remains ambiguous. Takeda & Sunamura (1982) concluded that berm height is not dependent on sediment size in the range of $0.22mm$-$1.3mm$, while Okazaki & Sunamura (1994) introduced a sediment-dependent reduction factor in their formula to predict berm heights. Here, we assume that parameter A is mainly associated with the height at which the berm crest leads to a planar segment (see Fig. 4.2) and is fully modulated by waves, ignoring possible changes in berm height due to variations in sediment size. We then consider that A increases with the runup. Formulations like Stockdon *et al.* (2006) propose a direct relation between runup and wave parameters and explain the runup elevations in terms of H and L (eq. 1.5). Based on the current literature regarding berm development (Weir *et al.* 2006) and through the mathematical interpretation of eq. 4.2, we adopted $(HL)^{1/2}$ as the likely parameter driving this process and hence, modulating the A parameter.

4.2.4.3 **Parameter** m

Parameter m defines the slope of the zone between the berm and the landward delimiter (dune toe, wall or cliff). In cases with highly energetic environments or fine-grained beaches that do not allow berm building, this parameter defines the entire dry beach profile, as stated above. Fig. 4.3 describes a DBP moving from a winter-featureless (1) to a summer-bermy (3) configuration. Stage (2) refers to a transitionary mode. In (1), the value of A is its maximum value –induced by large values of $(HL)^{1/2}$-, the value of b is zero in this extreme case –denoting the absence of foreshore curvature and berm- and the entire profile is defined by $\backsim mx$. In (3) the asymptotic-planar segment grows, causing an elongation, and the profile is defined by the three parameters. From the most extreme condition in winter -$A_{max}, b_{min}, m_{max}$-, the berm is being moved progressively seaward and losing height until the most stable summer-bermy configuration is reached -$A_{min}, b_{max}, m_{min}$- (Weir *et al.* 2006). Changes in m coincide with changes in slope and height, and are also linked to the berm's landward migration and the development of the asymptotic-planar form. We also know that

reflective beaches, which are generally less exposed to energetic waves and normally formed with coarse grain sizes, display an almost flat inter-annual segment (Díez *et al.* 2016) and so the difference in height between the landward limit and the berm height is less than that observed in a dissipative beach. We thus selected the dimensionless fall velocity as a proxy describing this process and we associated it with variations in m.

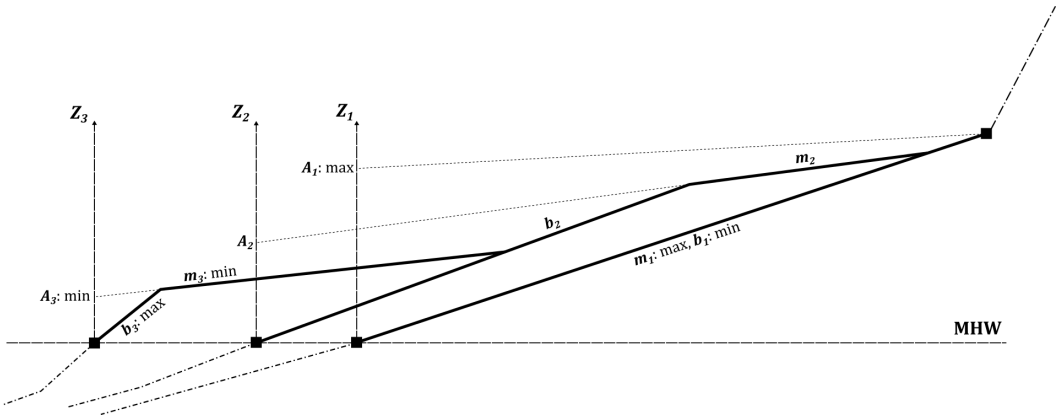

Figure 4.3: Theoretical scheme of two extreme DBEP configurations for a single beach subjected to seasonality - (1) and (3) - and a transitionary state - (2) -. When transitioning from winter to summer conditions, the berm is being moved progressively seawards and the slope of the asymptotic-planar segment becomes smoother. The slope represented by m decreases, and the curvature of the foreshore segment, represented by b, increases. The value of A is progressively being reduced until a stable state is reached.

Table 4.3: Dry beach profile types and shape parameters. *Note*: in the case of A, when a single beach moves from dissipative to reflective, the value of A decreases, as indicated in this table and in Fig. 4.3. In the case of different beaches with the same value of Ω but with different runup values, A is higher in the case of higher runup. *I.e.*, A varies directly with the runup even if Ω does not vary. This is why in Fig. 4.6, Orio and Blanes, for example, which are reflective with values of Ω close to 2, present large differences in A. The runup in Orio is much larger due to its higher exposure to waves.

$Type1 - dissipative-$	$Type2 - intermediate-$	$Type3 - reflective-$
$\Omega > 5$	$2 < \Omega < 5$	$\Omega < 2$
$A \to max$	$A \neq 0$	$A \to min$
$b \to 0$	$b \neq 0$	$b \to max$
$m \to max$	$m \neq 0$	$m \to 0$
$y \sim mx$	$y \sim A[1 - exp(-bx)] + mx$	$y \sim A[1 - exp(-bx)]$

4.3 Model set up

4.3.1 Parameter validation

In Fig. 4.4, we compare the measured profiles with the best fittings to eq. 4.2, demonstrating its ability to describe all types of profile morphologies. The coefficients for the best fitting

were obtained by iteration, minimizing the RMS error (Table 4.4). To compare and validate the predicted morphology using best fit, in Fig. 4.5 we contrast the slope measured at the origin and also the slope of the asymptotic planar segment with the values given by the fitting parameters. The slope at the origin corresponds to the derivative of eq. 4.2 evaluated at $x = 0$, *i.e.*, $y = Ab + m$. The slope of the asymptotic planar segment corresponds to the parameter m obtained from fitting. In light of this comparison we assume that the slope of the dry beach at the origin (MHW level) is comparable to the relation of the morphological parameters $Ab + m$, and the slope of the asymptotic planar may be related to m. The parameters reproduce the main morphological index of the dry beach profile.

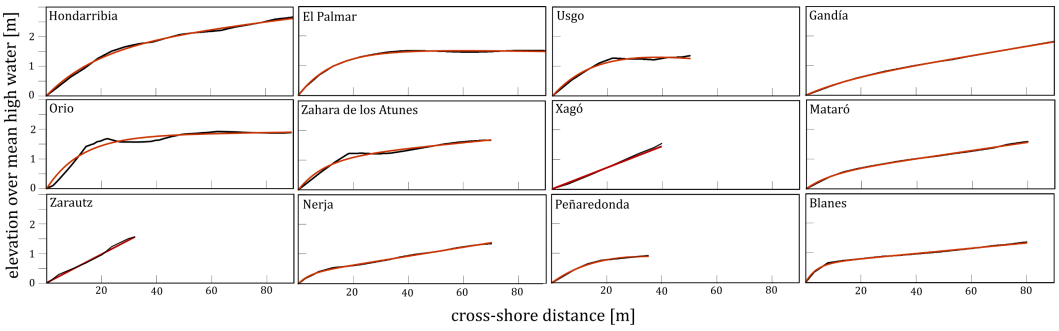

Figure 4.4: Field measurements (black) and best fittings (red) to eq. 4.2.

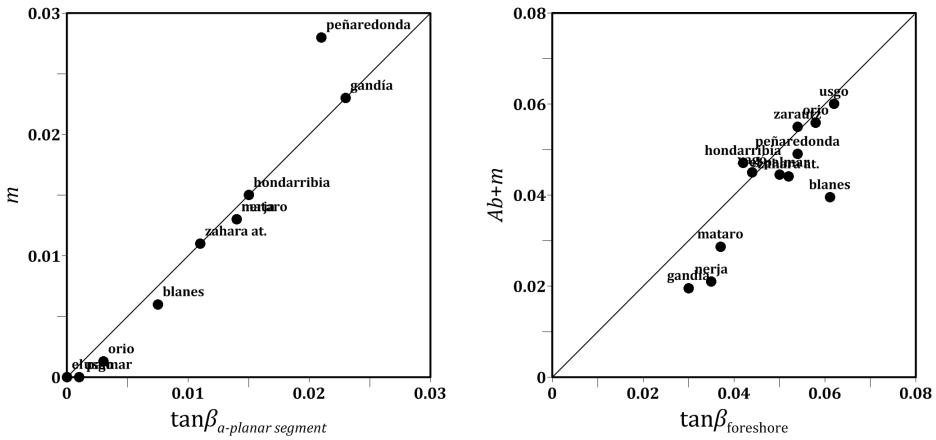

Figure 4.5: *Left panel*: parameter m produced by fitting eq. 4.2 to the measured profiles and the measured slope of the asymptotic planar segment. *Right panel*: first derivative at the origin of eq. 4.2 and the measured foreshore slope at the MHW level.

4.3.2 Relations between the morphological parameters

Using best fit, we determined the empirical relations between the morphological parameters $-A, b, m$- and the runup driver $(HL)^{1/2}$ to be in the range of $4m < (HL)^{1/2} < 15m$, and the dimensionless fall velocity Ω_∞, to be in the range of $0.5 < \Omega < 6.5$:

$$A = 0.15[HL]^{1/2} - 0.27 \tag{4.3}$$

$$b = \begin{cases} -0.02\Omega + 0.16 \quad \forall \quad \Omega_\infty < 6.5 \\ 0 \quad \forall \quad \Omega_\infty > 6.5 \end{cases} \tag{4.4}$$

$$m = 0.003 \exp[0.39\Omega_\infty] \tag{4.5}$$

The parameters are summarized in Table 4.4, and Fig. 4.6 presents the best fittings of the morphological parameters with the driving parameters. The empirical expressions for parameters b and m, eq. 4.4 and eq. 4.5 respectively, suggest that the variations of these morphological parameters agree with the hypothesis set out in Section 4.2.4.1 and Section 4.2.4.3, which predicted a relation between the beach modal state and the slope of the asymptotic-planar segment and the curvature and size of the foreshore. In the case of b, there is a decreasing trend when moving to dissipative states until a certain value -$\Omega_\infty \backsim$ 6.5- from which point the parameter goes to zero. In the case of m, the best fit –that making R-squared a minimum- suggests an exponential fit –better than the linear fit in this particular case-, indicating that the slope of the planar zone gets larger when moving to dissipative states. In the case of eq. 4.3 and Fig. 4.6 -a, a clear positive trend is identified. The parameter A goes to a maximum when moving to higher values of runup, which indicates that the asymptotic-planar state is achieved at a higher height. We can observe this behaviour in real cases and fits in Fig. 4.4. Usgo beach, which has a measured value of $(HL)^{1/2} = 13.6m$, reaches the planar state at a value of $A = 1.95m$, while Gandía, which has a runup estimator of $(HL)^{1/2} = 5.64m$, reaches the planar state at a value of $A = 0.42m$. In our model, both terms of eq. 4.2 vary as functions of runup and beach modal state under the relationships proposed in eq. 4.3, eq. 4.4 and eq. 4.5. The joint effect of these variables shapes the profile, and depending on their range of values, they are capable of representing in real cases, defining different grades of convexity and slope, each of the single DBP Types schematized in Fig. 4.2. Table 4.3 lists the transitioning between types when the morphological parameters vary as a response to changes in the governing variables $(HL)^{1/2}$ and Ω.

4.4 The predictive capacity of the DBEP model: Narrabeen Beach

We evaluated the predictive capabilities of the model against an independent data set from Narrabeen Beach in Australia. The estimation of the parameters using the relations eq. 4.3,

Table 4.4: Morphological parameters from fitting, measured slope of the foreshore at the origin and measured slope of the asymptotic-planar segment (inter-annual segment).

	$A_{bestfit}[m]$	$b_{bestfit}[m^{-1}]$	$m_{bestfit}$	R^2	$\beta_{foreshore(field)}$	$\beta_{a-planar(Field)}$
Hondarribia	0.53	0.126	0.015	0.99	0.049	0.015
Orio	1.76	0.079	0.001	0.95	0.068	0.003
Zarautz	-	0	0.055	0.98	0.054	0
Usgo	1.95	0.059	0	0.98	0.064	0.001
Xagó	-	0	0.045	0.99	0.044	0
Peñaredonda	2.06	0.042	0.05	0.99	0.044	0.021
El Palmar	1.60	0.075	0	0.99	0.070	0
Zahara Atun.	1.1	0.104	0.009	0.97	0.052	0.011
Nerja	0.32	0.200	0.015	0.99	0.052	0.014
Gandía	0.42	0.061	0.020	0.99	0.024	0.023
Mataró	0.46	0.110	0.013	0.99	0.047	0.014
Blanes	2.27	0.110	0.006	0.99	0.139	0.007

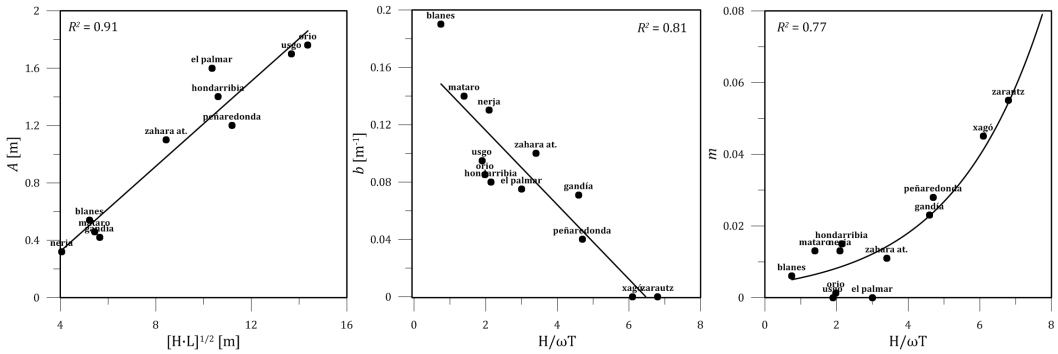

Figure 4.6: Shape coefficients as function of dynamics and sediment characteristics. Fits of the three panels are from eq. 4.3, eq. 4.4 and eq. 4.5.

eq. 4.4 and eq. 4.5 characterizes the DBP equilibrium shape by computing the value of $(HL)^{1/2}$ and Ω in the nearshore. We tested the reliability of the model by formulating different parametric equations according to the different exposure to wave conditions that this beach may present (Fig. 4.7).

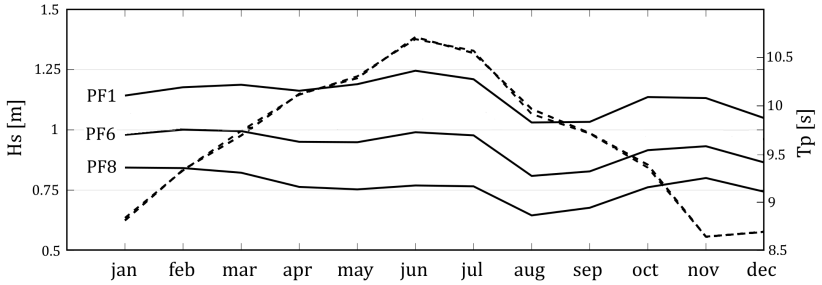

Figure 4.7: Monthly averaged significant wave height H_s (solid line) and peak period T_p (dashed line) at $10m$ water depth immediately seawards of PF1, PF6 and PF8. The peak period is essentially the same for the two sites. The two dashed lines overlap. Readers may refer to Turner *et al.* (2016) for a more detailed site and wave climate description.

We used profiling from the two extremes of the beach, PF1 and PF8, because they offer the two most extreme beach modal states. PF1 tends to be more dissipative and is backed by a dune system, while PF8 tends to be more reflective and is backed by a promenade (Turner *et al.* 2016). PF6 presents intermediate conditions. For the three transects we assumed the mean grain size to be d_{50}=0.3mm, and we used this value to calculate the values of Ω. In order to carry out a suitable model application on the Narrabeen profiling data set, we used average wave climate conditions, as we did during model development. Through the analysis of Fig. 4.7 we observed two distinct wave regimes during a single year. We therefore selected profiling from January and July in order to encompass these two different main conditions. The data in Table 4.2 lists the dates of each profiling used for model validation. We calculated the mean wave statistics associated with each month using the wave data from Turner *et al.* (2016). A summary of the wave data calculated for this study is listed in Table 4.5 and Fig. 4.7. As stated in the introduction, the selection of instantaneous values of the wave parameters in order to associate them with the current form of the profile is not recommended. Instead, we first calculated wave statistics to then compute the morphological parameters following the recommendation given by Wright *et al.* (1985), as noted in the introductory section. The reliability of the model and its predictive capabilities are here addressed by the comparison between real and predicted DBPs. Table 4.5 presents the hydrodynamic values and shape parameters, and also the best fitting parameters obtained from fitting eq. 4.2 to the real profiles. Fig. 4.8 presents both predicted (dashed line) and best fitting (red line) profiles to the measured profile (black solid line) for the six selected cases.

Table 4.5: Data used for model validation in Narrabeen, parameters predicted by the model (A_m, b_m, m_m) -eq. 4.3, eq. 4.4 and eq. 4.5- and best fit parameters (A_{bf}, b_{bf}, m_{bf}) from eq. 4.2. RMS and R^2 from the comparison between model and best fit are also presented.

ID	$H_s[m]$	$T_p[s]$	$[HL]^{1/2}[m]$	Ω_∞	$A_m[m]$	$b_m[m^{-1}]$	m_m	$A_{bf}[m]$	$b_{bf}[m^{-1}]$	m_{bf}	RMS	R^2
PF1Jan12	1.16	9.1	12.3	3.4	1.65	0.092	0.013	1.53	0.120	0.017	0.12	0.99
PF1Jul10	0.94	9.6	11.6	2.6	1.44	0.127	0.009	0.43	0.470	0.044	0.36	0.93
PF6Jul11	0.98	10.5	12.9	2.5	1.70	0.109	0.008	0.44	0	0.116	0.30	0.95
PF6Jan10	0.69	7.9	8.2	2.3	0.97	0.113	0.007	0.71	0.250	0.058	0.32	0.97
PF8Aug06	0.85	11.3	12.6	1.9	1.67	0.121	0.007	1.46	0.131	0.019	0.29	0.97
PF8Jun13	0.89	9.3	10.9	2.5	1.44	0.108	0.009	2.05	0.086	0	0.32	0.98

4.4.1 Error analysis

Fig. 4.10 presents a Taylor diagram (Taylor 2001) which summarizes the relative accuracy with which the dry beach profiles predicted by eq. 4.2 reproduced the state of equilibrium on the selected dates. Statistics for the two months and the two transects were computed. The location of the red points on the diagram quantifies the matching between model and observations, assuming that the mean best fit of eq. 4.2 to real profiles represents the real mean configuration –we observed the ability of eq. 4.2 to accurately reproduce all types of DBPs described in Chapter 2- . To explain Fig. 4.10, we consider, for example, point

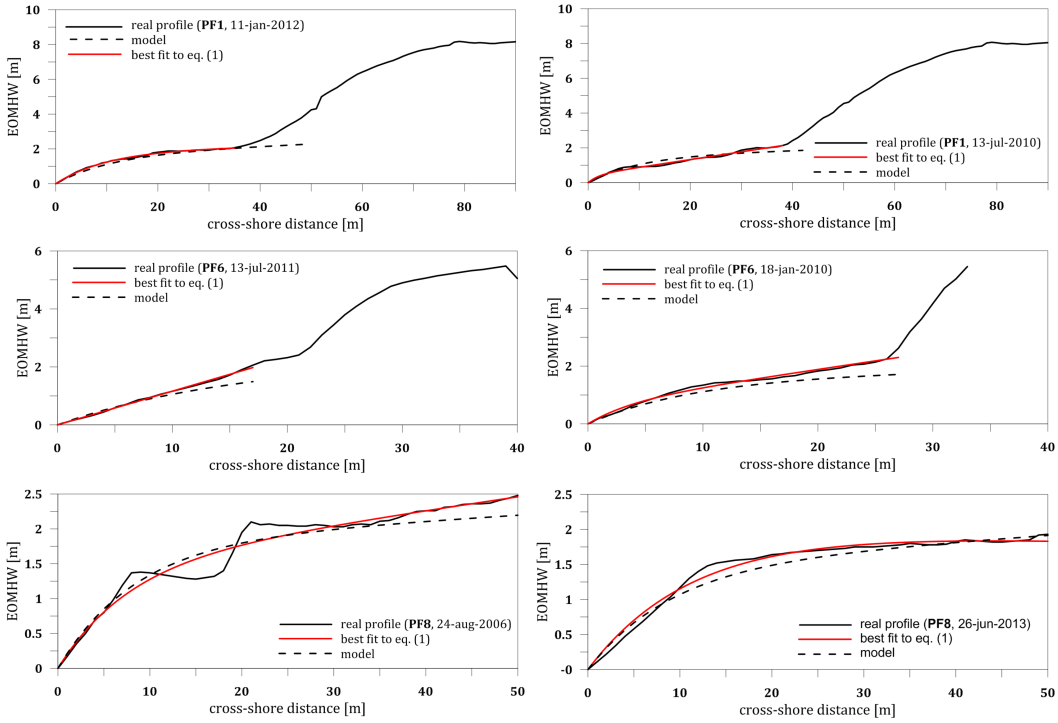

Figure 4.8: Examples of the comparisons between real profiles (black solid line), profiles predicted by the model (black dashed line) and best fit of eq. 4.2 to the real profile (red line). The upper panels correspond to PF1, the middle panels to PF6 and the lower panels to PF8. Two dates per transect were selected for this representation. The vertical axis represents the elevation over the MHW (EOMHW) level. The parameter values are listed in Table 4.5.

PF6Jul'11. Its pattern correlation with the measured profile is around 0.95; we consider that if the value is equal to one, the match is perfect. The RMSD value (dashed green line), which indicates the sample standard deviation of the differences between predicted and observed values, is near $0.2m$. It demonstrates that the accuracy of the modelled value is around this value. The standard deviation quantifies the dispersion of the simulated values around its mean and is proportional to the radial distance from the origin. Here all the values are around $0.4m$ and $0.7m$. Low standard deviation values indicate that the differences in height along the profile are less than for simulations that present higher height differences. The best values will lie near the bottom axis, where the value of the correlation coefficient is equal to one. Fig. 4.9 offers a more visual comparison by plotting model height values against best fit values. The best match in the cross-shore direction occurs on the foreshore, where the correlation is good. At higher heights, especially in the far field of the asymptotic-planar segment simulations, the model underestimates the height of this segment by an average of around $0.3m$.

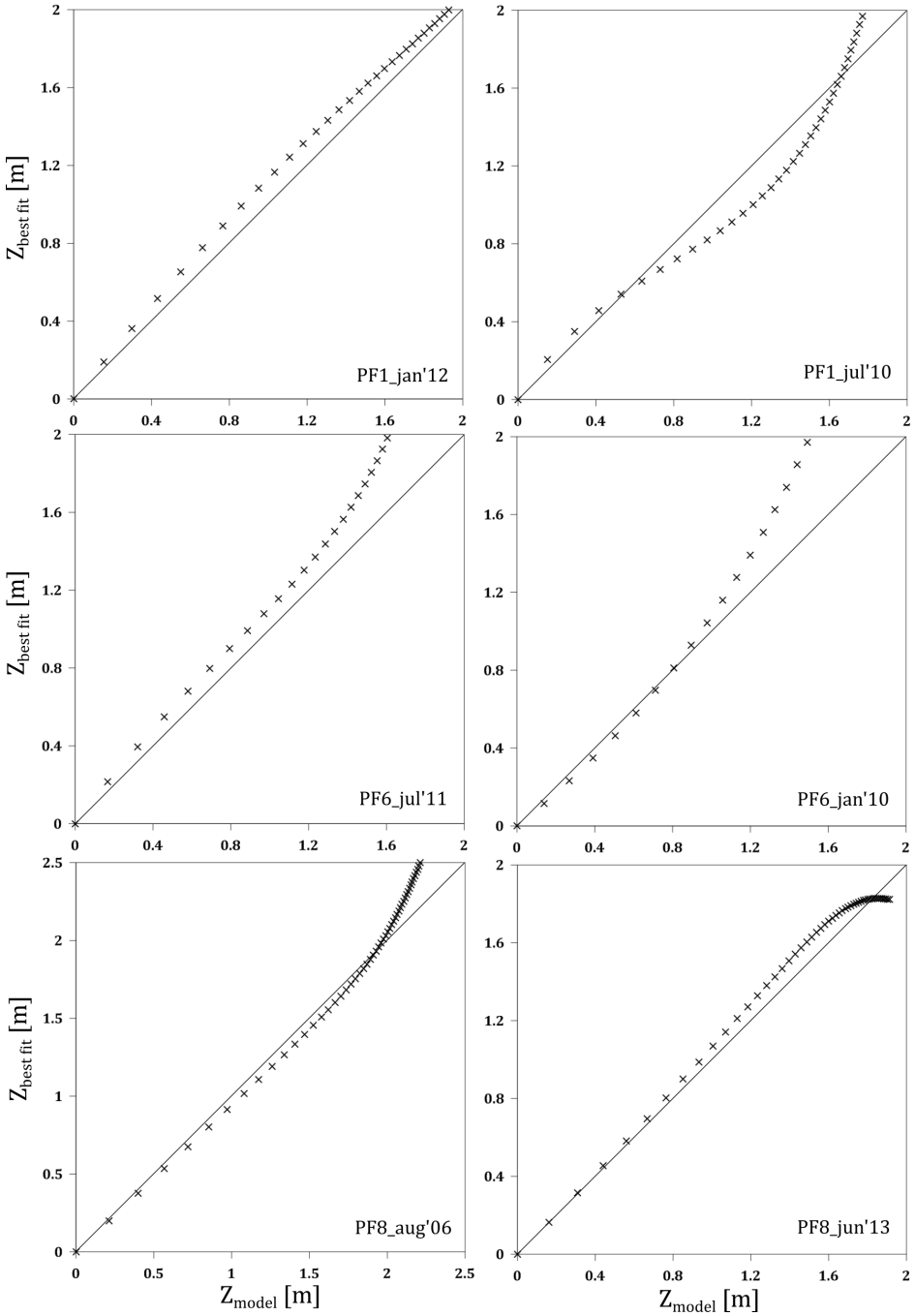

Figure 4.9: Heights predicted in the cross-shore direction using the model vs heights calculated by best fit of eq. 4.2 to the data.

4.5 Discussion

Through the model development and testing we proved our hypotheses to be valid: when the runup gets higher, the parameter A increases accordingly; when the beach moves to a more dissipative state, the parameter b gets smaller until it becomes zero. At this value, beaches do not present berms and the DBEP is defined only by the m parameter; when the

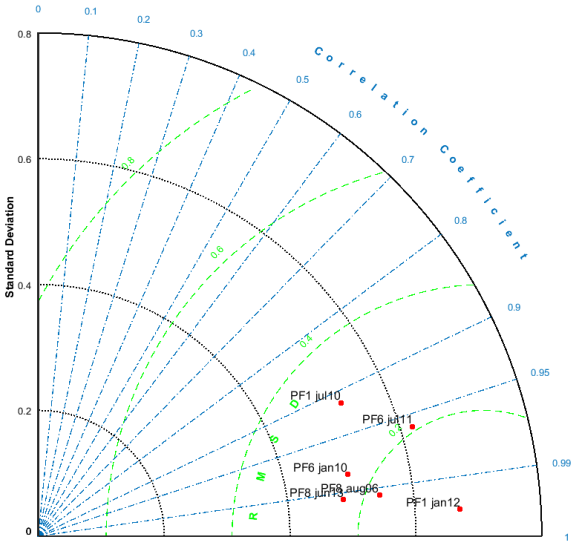

Figure 4.10: Taylor diagram (Taylor 2001) displaying a statistical comparison between the mean best fit of eq. 4.2 and the modelled profiles.

beach is fully dissipative, the morphology is modulated mainly by this parameter. When the beach moves to more reflective states, the process, schematized in Fig. 4.3, is as follows: a berm starts to form at the foreshore, and it is progressively moved seaward while its crest height reduces due to the less energetic wave conditions. As a consequence, the slope of the asymptotic-planar segment gently adopts a more planar/horizontal form due to the width of the dry beach, which makes the relative slope of this segment smoother. In the subsequent two sub-chapters we discuss the efficiency of the model, the role of the shaping parameters and the limits of application of our proposed model.

4.5.1 Accuracy of the model

This study has documented DBEPs for a wide variety of beaches, ranging from fully reflective (Ω=0.7) to almost fully dissipative (Ω=6.2). The characterization of this set of equilibrium profiles allow us to correlate the profile shape to a parametric equation formed by the sum of an exponential and an asymptotic planar slope, and serves as a good proxy to reproduce the average configuration that the DBP displays in relation to mean wave and grain size conditions. This equation is formed by three "shaping parameters", here designated A, b and m. The variations of these parameters are modulated by the runup estimator and the dimensionless fall velocity by eq. 4.3, eq. 4.4 and eq. 4.5. Depending on their values, eq. 4.2 is able to reproduce a form typical of reflective beaches, with a steep foreshore, a large marked berm and a quasi-horizontal asymptotic-planar segment, and can also adopt a form typical of dissipative beaches, *i.e.*, a straight-positive slope with no features along the entire profile. We then proved the fundamental equation, eq. 4.2, to be valid over an independent data set

from Narrabeen Beach. From the comparisons between real profiles and the model arises two main facts: *i)* the DBP configuration is well represented by the model in terms of error analysis and shape (Fig. 4.9, Fig. 4.10). The prediction properly defines (with correlation coefficients and $RMSD$ around ~ 0.99 and $\sim 0.2m$, respectively) the berm and the curvature and slope of the foreshore; the slope of the asymptotic-planar segment is well resolved and also shows good agreement. *ii)* From Fig. 4.8 and Fig. 4.9, parameters m and b adequately represent the slope of the asymptotic-planar segment in the far field and the curvature and slope of the foreshore. On the other hand, parameter A, which estimates the height at which the planar state begins to dominate, slightly underestimates the real values, being off by around $0.4m$ in the worst case (PF6Jan10).

4.5.2 The parameters' behaviour and model limitations

We carried out the development of the equation in mean conditions, which is a major advantage when representing the long term DBP configuration of a beach. We must bear in mind that this morphological model requires the beach to be able to reach equilibrium under mean wave climate conditions at the beachfront, and that it also needs enough time to completely achieve equilibrium. Additionally, beaches presenting values of Ω larger than 7 were not analysed here, so the application of this model to highly dissipative beaches with very large values of Ω should be done taking this into consideration. For our range of application, we proved that parameter A shows good correlations -improvable in any case- in defining the height at which the planar slope begins to dominate. Parameter b also offers good matches, predicting the curvature and length of the foreshore segment when a berm is present. Parameter m accurately predicts the slope of the straight segment of the beach in most cases. According to the model, for values of Ω larger than 6 the profile does not display berms because parameter b goes to zero. Mathematically, this implies that the exponential term of eq. 4.2 reduces to zero and the profile is entirely defined by the second term of the equation $y \backsim mx$. An increase in A implies an increase in the height at which the planar slope dominates. According to Fig. 4.6-a, A may increase indefinitely with the runup, which is absolutely incorrect. The scheme proposed in Fig. 4.3 also shows that as the runup increases, the value of A increases. The berm cannot grow and gain height indefinitely because in real cases the sand supply is always limited and also due to the limited landward boundary. When a berm gains height, it is progressively being displaced landwards. Then one of two things can happen: either the berm is destroyed (*"berm-height" paradox*, Weir *et al.* (2006)), or the berm reaches the dune toe. There, the profile becomes a straight line defined by m and the value of A has no implications in the equation because b is equal to 0, negating the exponential term of eq. 4.2. The other inconsistency that this model may produce is the exponential growth of

the parameter m, according to eq. 4.5 and Fig. 4.6-c. Obviously, slope cannot grow infinitely. Due to these two limitations, we must be cautious when applying this model and its empirical relationships to highly energetic environments. We therefore recommend the use of the model exclusively for beach modal states with dimensionless fall velocity values no larger than 6. Our model is capable of representing the main morphological shapes. However, in some cases, the berm crest forms a rather concave curvature before adopting a straight positive slope (Okazaki & Sunamura 1994) –for example, the real profile of PF8Aug06 in Fig. 4.8-. These secondary morphological variations, similar to those describing submerged bars and troughs for subaqueous equilibrium profile formulations (Holman *et al.* 2014), may be incorporated in the model if describing this berm characteristic is desirable. Despite this limitation, volume calculation for beach-fill designs, for instance, is not affected by this fact. Around the berm crest, the model smooths the crest and overestimates and underestimates in the same proportion just backwards and frontwards of the crest. The boundary condition at the origin also serves to provide continuity with other formulations for subaqueous EBP. Taking the beach profile as a whole, the MWH may be regarded as a joint point which blends both parts of the profile, providing continuity from the closure depth to the dune toe. This should be investigated and developed in future research.

4.6 Conclusions

This study introduces a model that describes equilibrium dry beach profiles under different sediment and wave conditions by means of a parametric equation. The equation has two terms: an exponential defining mostly the curvature and height of the foreshore segment, and a straight line with an asymptotic planar behaviour in the far field defining the slope from the berm crest to the landward edge. Empirical relations were obtained by relating the equation's morphological parameters (A, b and m) -obtained from fitting real profiles to the general eq. 4.2- with the driving parameters that control the morphology: $(HL)^{1/2}$ and Ω. The equation and the associated empirical relationships can explain the range of equilibrium dry beach profile morphology from dissipative beaches, where the profile is constituted by a straight line without features and represented mostly by the linear term $y \backsim mx$, to reflective beaches, where the profile is formed by a steep foreshore, a marked berm and an almost horizontal inter-annual segment, represented mainly by the exponential term $y \backsim A[1 - exp(-bx)]$. Intermediate beach states are a combination of both terms, and the equilibrium dry beach profile is represented as $y \backsim A[1 - exp(-bx)] + mx$. We tested the model over an independent data set from Narrabeen Beach (AU), which offers both dissipative and reflective modal beach states during the year, obtaining good correlations. The proposed model delivers a feasible framework and provides new and useful insight into dry beach

dynamics and morphology. Characterization of DBEPs with this parametric model requires knowledge of the nearshore wave climate and also of beach sediment characteristics. Both types of data are easy to measure and relatively cost effective, so the model offers a great advantage due to its conceptual simplicity and its ease of application to beach design studies.

5

Conclusions and future research

5.1 Summary of contributions

The overall aim of this thesis was to broaden our knowledge of the dry beach, focusing on its equilibrium profile. The work has yielded to three peer reviewed papers, which have been adapted to the three main chapters of this thesis. The goals set out in Chapter 1 were accomplished through these three main Chapters.

5.1.1 Summary and contributions of "*Characterization of the dry beach profile: a morphological approach*"

- The data base offered by IOLE provides a wide range of beach types, extending from fully dissipative to fully reflective. This allows investigating the dry beach from a broad perspective. Thus, the characterization of the dry beach profile is undertaken under different wave climates and sediment characteristics, easing the interpretation of the different parts and segments that the DBP present.

- The zonation of the DBP proposed in this chapter helps to understand dry beach shapes, slopes, heights and widths. The foreshore segment comprises from the Mean High Water to the berm crest, in case of existence; the seasonal segment appears on beaches subjected to seasonality in wave climate and encompasses the cross-shore section between the two seasonal –winter and summer- berms. The inter-annual segment encompasses the zone between the most stable berm and the dry beach landward edge.

- Through a data mining technique (*K-Means* Algorithm), we classified automatically the large profile data base into a desired number of categories. From the output we obtained four different clusters, each of them characterized by a Profile Type (or centroid) and formed with the real profiles that best fit in each of the four categories. We demonstrate this technique to be valid to classify dry beach profile morphologies.

- We related each Profile Type, or morphotype, to one specific range of dimensionless fall velocity values. We obtained, in this way, a conceptual model that describes the main features of each morphotype and relates them with a certain beach modal state. Now we are able to know the main morphological characteristics and shapes that the dry beach profile will present by just knowing the modal state of the beach: dissipative are associated to **Type 1**, intermediate to **Type 2**, reflective to **Type 3** and ultradissipative to **Type 4**.

- This classification offered an adequate framework and set the basis for the subsequent Chapters, which dealt with the temporal variations and the equilibrium configuration of the DBP.

5.1.2 Summary and contributions of "*Spatial and temporal variability of dissipative dry beach profiles in the Pacific Northwest U.S.A.*"

- The extensive monitoring program carried out along the Columbia River Littoral Cell since 1997 (still ongoing) offers a complete dry profile data set (among other bathymetric-topographic-wave data) which allows to characterize the temporal variations over the dry beach profile in both intra and inter-annual scales.

- Generally, the beaches along this stretch of coast are highly dissipative and are subjected to a marked seasonality in wave climate: we then hypothesized that the most common DBP Type along the coast should be Type 1, according to the characterization described in the previous chapter. We linked the modal state of the beaches with their morphology and observed a clear relation between the variations in the modal state and the variations in DBP morphology.

- We applied two well know mathematical methods to give account about the seasonal back and forth sediment exchange between the submerged and emerged parts of the beach system and we identified the main inter and intra annual changes over the DBP. *K-Means* Algorithm offered the main configurations that the dry beach profile experiences over time, and Empirical Orthogonal Functions explained the variability of the collected data in space and time. Now we know that Pacific Northwest dissipative

beaches present two main DBP configurations, both inside Type 1 Profile: winter featureless upward slope and summer berm like profile. We identified and quantified their main morphological indexes and ranges of variations in heights and widths.

5.1.3 Summary and contributions of "*A parametric model for dry beach equilibrium profiles*"

- We proposed a parametric equation that is able to reproduce all the four Types of Profile found out in Chapter 2. *I.e.*, it is capable to adjust to any DBP morphology present in beaches ranging from dissipative to reflective.

- The equation was developed using several beaches presenting a wide variety of wave climate and sediment characteristics, and so presenting different modal states and morphologies. The data base encompasses from dissipative beaches presenting an upward straight line without features, to reflective beaches, where the profile is formed by a steep foreshore, a marked berm and an almost horizontal inter-annual segment.

- The equation, proposed under a heuristic approach, is formed by two terms and three parameters: an exponential defining mostly the curvature and height of the foreshore segment, and a straight line with an asymptotic planar behavior on the far field defining the slope from the berm crest to the landward edge. The morphological or shape parameters, named here A, b and m, are related to the runup driver $(HL)^{1/2}$ and to the dimensionless fall velocity Ω. Thus knowing these beach hydrodynamic values at the nearshore, the equation is defined.

- We tested the model against an independent data set from Narrabeen Beach (AU). This beach offers a broad range of dimensionless fall velocity values, depending on the beach longshore location and the season of the year. The tests offered good correlation between simulations and real averaged equilibrium profiles. The model reproduces satisfactorily the foreshore slope and curvature, and also the berm height and the slope of the segment between the berm crest and the landward edge.

- The proposed model provides a useful tool to beach design studies and to calculate and predict the most stable configuration of the dry beach in the long term by just knowing the mean nearshore wave climate and the sediment grain size.

5.2 Future research

From the overall evaluation of this work and looking at each chapter in detail, there are some topics that open gates to further development or to a more detailed evaluation. Here are resumed the six main issues that should be approached in future related research.

1. Regarding the evaluation of wave drag forces *vs* wind drag forces over the dry beach and their capacity to mobilize sand, no experiments or field measurements were carried out for the present work. There are works in literature dealing with these specific topic, and most of them assert that sand mobilization by waves is several orders of magnitude greater than wind mobilization, but it would be stimulating to monitor certain beaches where the wind is strong and persistent along a year (*e.g.,* Spanish beaches near the Strait of Gibraltar) to investigate if the wind may have a non-negligible contribution to the equilibrium dry beach profile shape.

2. Regarding the feedbacks between dynamics and morphology of the dry beach there are still numerous unknowns. The presence or not of subaqueous bars, conditioned by long-shore sediment transport, sometimes determine the presence or not of seasonal berms, as some authors have pointed out. Due to that, under the same wave conditions at the nearshore, the same beach may present berm or not, depending on the long-shore location. This should be investigated by managing a proper bathymetric and topography data set along a single beach for a certain time span enough to appreciate cross-shore changes such us bar migration and berm development and destruction.

3. The last point is related with this one: there is a fine line between the growing of the berm due to the runup rising and its sudden destruction, brought to the light by several authors. This fact conditions if the beach will present one type of configuration or another. A detailed process-based approach should be carried out to investigate this complex mechanism, so called berm height-paradox.

4. Our parametric equilibrium model has some limits on the range of application. Reflective and intermediate beaches are well tested, but beaches displaying values of dimensionless fall velocity larger than 7 are not tested with our model. Highly dissipative beaches, like in CRLC, should be investigated in terms of equilibrium configuration and under the same approach carried out here in Chapter 4.

5. It would be attractive to join efforts and developing a parametric form for the equilibrium profile from the closure depth to the dune toe, integrating both submerged and emerged parts into one single equation without discontinuity points. It may also add, as parametric models that integrate second order variations such us bars, second

order terms to explain certain features in the DBP, such as berm crest and dune toe curvature.

6. It would be enriching to propose a short-medium term numerical model of evolution integrating dynamics, *i.e.,* sediment transport models in the surf and swash zone and extreme water elevations under the two main conditions that models like these need: total mass conservation and orthogonality of the process. A disequilibrium model would be also in consonance with this. This would allow knowing the time needed to reach the equilibrium state under mean wave conditions when the DBP is eroded or accreted. Several works in literature deal with this by building an energetic curve for the equilibrium, but none related to the dry beach equilibrium profile.

Bibliography

Aagard, T., Davidson-Arnott, R.G.D., Greenwood, B. & Nielsen, J. (2004). Sediment supply from shoreface to dunes: linking sediment transport measurements and long term morphological evolution. *Geomorphology*, **60**, 205–224. 9, 22

Ahrens, J. & Seelig, W. (2001). Water quality mangaement-the planning of economically optimal control systems. In *Coastal Engineering Proceedings 1(25)*. 15

Allan, J.C. & Komar, P.D. (2007). Sediment supply from shoreface to dunes: linking sediment transport measurements and long-term morphological evolution. *Journal of Coastal Research*, **18**, 175–193. 50

Allen, J.R. (1980). Sand waves: A model of origin and internal structure. *Sedimentary Geology*, **26**, 347–352. x, 10

Anthony, E.J. (1998). Sediment–wave parametric characterization of beaches. *Journal of Coastal Research*, **14**, 347–352. 24, 38, 69

Anthony, E.J., Vanhee, S. & Ruz, M.H. (2006). Short-term beach-dune sand budgets on the north sea coast of france: Sand supply from shoreface to dunes, and the role of wind and fetch. *Geomorphology*, **81**, 316–329. 5, 16, 24

Aubrey, D.G. (1979). Seasonal patterns of onshore–offshore sediment movement. *Journal of Geophysical Research*, **84**, 6347–6354. 49, 65

Austin, J.M. & Masselink, G. (2006). Observations of morphological change and sediment transport on a steep gravel beach. *Marine Geology*, **229**, 59–77. 20

Bagnold, R. (1941). *The Physics of Blown Sand and Desert Dunes*. Chapman and Hall, London. 10, 12, 17

Baldock, T.E., Hughes, M.G., Day, K. & Louys, J. (2005). Swash overtopping and sediment overwash on a truncated beach. *Coastal Engineering*, **95**, 633—-645. 5, 16

Barcena, J.F., Camus, P., García, A. & Alvarez, C. (2015). Selecting model scenarios of real hydrodynamic forcings on mesotidal and macrotidal estuaries influenced by river discharges using kmeans clustering. *Environmental Modelling and Software*, **68**, 70–82. 33

Bascom, W.N. (1951). Characteristics of natural beaches. *Coastal Engineering*, 163–180. 5, 16, 18, 19, 29

Batjes, J.A. (1974). Surf similarity. *Proceedings 14th International Conference on Coastal Engineering*, 89–108. 15

Bauer, B.O. & Davidson-Arnott, R.G.D. (2002). A general framework for modeling sediment supply to coastal dunes including wind angle , beach geometry , and fetch effects. *Geomorphology*, **49**, 89–108. 23

Bauer, B.O., Davidson-Arnott, R.G.D., Hesp, P., Namikas, S.L., Ollerhead, J. & Walker, I.J. (2008). Aeolian sediment transport on a beach: Surface moisture, wind fetch, and mean transport. *Geomorphology*, **105**, 106–116. x, 9, 11, 13, 44

Bellomo, D., Pajak, M.J. & Sparks, J. (1999). Coastal flood hazards and the national flood insurance program. *Journal of Coastal Research SI*, **28**, 21–26. 15

Bendixen, M., Clemmensen, L.B. & Kroon, A. (2013). Sandy berm and beach ridge formation in relation to extreme sea levels: A danish example in a micro tidal environment. *Marine Geology*, **344**, 53–64. 29

Bernabeu, A.M., Medina, R. & Vidal, C. (2003). Wave reflection on natural beaches: an equilibrium beach profile model. *Estuarine, Coastal and Shelf Science*, **57**, 577–585. xi, 3, 6, 5, 22, 24, 68

Berry, A.J., Fahey, S. & Meyers, N. (2014). Boulderdash and beachwalls – the erosion of sandy beach ecosystem resilience. *Ocean and Coastal Management*, **96**, 104–111. 1

Bird, E.C. (1985). *Coastline Changes: A Global Review*. John Wiley and Sons, Chichester. 2

Birkemeier, W.A. (1984). Time scales of nearshore profile changes. *Coastal Engineering Proceedings*, **1**. 22

Brunn, P. (1954). Coast erosion and the development of beach profiles. *Beach erosion board technical memorandum. U.S. Army Engineer Waterways Experiment Station*, **1**. 3, 5, 22, 68

Butt, T. & Russell, P. (2000). Hydrodynamics and cross shore sediment transport in the swash zone of natural beaches: A review. *Journal of Coastal Research*, **16**, 255–268. 14

Camus, P., Mendez, F.J., Medina, R. & Cofino, A.S. (2011). Analysis of clustering and selection algorithms for the study of multivariate wave climate. *Coastal Engineering*, **58**, 453–462. 31, 33

Cariolet, M. & Suanez, S. (2013). Runup estimations on a macrotidal sandy beach. *Coastal Engineering*, **74**, 11–18. 3, 5

Chappell, J. & Eliot, I.G. (1979). Surf beach dynamics in time and space. an australian beach study and elements of a predictive model. *Marine Geology*, **32**, 231–250. 3, 6

Clarke, D.J. & Eliot, I.G. (1975). Description of littoral alongshore sediment movement from empirical eigenfunction analysis. *Journal of the Geological Society of Australia*, 1979—-1986. 8, 56

Cohn, N. & Ruggiero, P. (2015). The influence of seasonal to interannual nearshore profile variability on extreme water levels: Modeling wave runup on dissipative beaches. *Coastal Engineering*, **115**, 79–92. 5, 17, 48, 49, 50, 53, 54, 63

Dalrymple, R.A. & Thompson, W.W. (1976). Study of equilibrium profiles. *Coastal Engineering Proceedings*, **15**. 6

Davidson-Arnott, R.G.D. (1988). Temporal and spatial controls on beach dune interaction, long point, lake erie. *Journal of Coastal Research Special Issue*, **3**, 131–136. 9, 23, 42, 44

Davidson-Arnott, R.G.D. & Bauer, B.O. (2009). Aeolian sediment transport on a beach: Thresholds, intermittency, and high frequency variability. *Geomorphology*, **105**, 117–126. 11, 12, 44

Díaz, S., Fargione, J., Chapin, F.S. & Tilman, D. (2006). Biodiversity loss threatens human well being. *PLoS Biology*, **4**, 117–131. 1

Dean, R.G. (1977). Equilibrium beach profiles: Us atlantic and gulf coasts. *Ocean Engineering*, **12**. 6, 9, 22, 68

Dean, R.G. (1991). Equilibrium beach profiles: Characteristics and applications. *Journal of Coastal Research*, **7**, 53–84. 3, 6, 5, 22, 68

Defeo, O., McLachlan, A., Shoeman, D.S., Schalcher, A., Dugan, J., Jones, A., Lastra, M. & Scapini, F. (2009). Threats to sandy beach ecosystems: A review. *Estuarine and Coastal Shelf Science*, **81**, 1–12. 1

Delgado-Fernández, I. & Davidson-Arnott, R.G.D. (2011). Meso scale aeolian sediment input to coastal dunes: The nature of aeolian transport events. *Geomorphology*, **126**, 217–232. 9, 12

Delgado-Fernández, I., Davidson-Arnott, R.G., & Ollerhead, J. (2009). Application of a remote sensing technique to the study of coastal dunes. *Journal of Coastal Research*, **25**, 1160–1167. 4, 23, 44

deVries, S., Southgate, H., Kanning, W. & Ranasinghe, R. (2012). Dune behavior and aeolian transport on decadal timescales. *Coastal Engineering*, **67**, 41–53. 3, 5

Díez, J., Cánovas, V., Uriarte, A. & Medina, R. (2016). Characterization of the dry beach profile: a morphological approach. *Journal of Coastal Reseach (in press)*, **0**, 0–1. xiii, 48, 55, 60, 70, 71, 72, 75

Díez, J., Cohn, N., Kaminsky, G., Medina, R. & Ruggiero, P. (2017). Spatial and temporal variability of dissipative dry beach profiles in the pacific northwest, u.s.a. *Marine Geology (in press)*, **0**, 0–1. 74

Duarte, C.M. (2004). Marine biodiversity and ecosystem services: an elusive link. *Journal of Experimental Marine Biology and Ecology*, **250**, 117–131. 1

Fayyad, U., Piatetsky-Shapiro, G. & Smyth, P. (1996). From data mining to knowledge discovery in databases. *AI Magazine*, **17**, 37–53. 8, 32, 49, 54

Finkl, C.W. (2004). Coastal classification: Systematic approaches to consider in the development of a comprehensive scheme. *Journal of Coastal Research*, **20**, 166–213. 32

Garcia-Medina, G., Ozkan-Haller, H.T. & Ruggiero, P. (2014). Wave resource assessment in oregon and southwest washington, usa. *Renewable Energy*, **64**, 203–214. 49, 59

Gomez-Pujol, L., Orfila, A., Canellas, B., Alvarez-Ellacuria, A., Mendez, F.J., Medina, R. & Tintore, J. (2007). Morphodynamic classification of sandy beaches in low energetic marine environment. *Marine Geology*, **242**, 235–246. 4, 7

Guanche, Y., Minguez, R. & Mendez, F.J. (2014). Autoregressive logistic regression applied to atmospheric circulation patterns. *Climate Dynamics*, **42**, 537–552. 33, 36, 54

Hastie, T., Tibshirani, R. & Friedman, J. (2001). *The Elements of Statistical Learning*. Springer, New York. 33, 54, 55

Hesp, P.A. (1988). Surfzone, beach and foredune interactions on the australian south east coast. *Journal of Coastal Reseach Special Issue*, **3**, 15–25. 4, 8, 42, 43

Hesp, P.A. (1999). *Handbook of Beach and Shoreface Morphodynamics*. John Wiley and Sons, Chichester. 13, 32, 44

Hesp, P.A. (2002). Foredunes and blowouts: initiation, geomorphology and dynamics. *Geomorphology*, **48**, 245–268. x, 5, 14, 29, 32, 40

Hesp, P.A. (2012). Surfzone-beach-dune interactions. *NCK-days 2012: Crossing borders in coastal research : jubilee conference proceedings*. 3, 5, 23, 68

Hinkel, J., Nicholls, R.J., Tol, R.S., Wang, Z., Hamilton, J., Boot, G., Vafeidis, A., McFadden, L., Ganopolski, A. & Klein, R.J. (2013). A global analysis of erosion of sandy beaches and sea-level rise: An application of diva. *Global and Planetary Change*, **111**, 150–158. ix, 3

Holland, K.T., Raubenheimer, B., Guza, R.T. & Holman, R.A. (1995). Runup kinematics on a natural beach. *Journal of Jeophysical Research*, **100**, 4985–4993. 14, 15

Holman, R.A. (1986). Extreme value statistics for wave run-up on a natural beach. *Coastal Engineering*, **9**, 527–544. 5, 9, 15

Holman, R.A., Lalejini, D.M., Edwards, K. & Veeramony, J. (2014). A parametric model for barred equilibrium beach profiles. *Coastal Engineering*, **90**, 85–94. 6, 22, 68, 84

Hotta, S., Kubota, S., Katori, S. & Horikawa, K. (1984). Sand transport by wind on a wet sand surface. *Coastal Engineering Proceedings*, **19**, 1265–1281. 11

Hughes, M.G. & Turner, I.L. (1999). *Chapter 5, The Beach Face, In: A D Short, Handbook of Beach and Shoreface Morphodynamics*. John Wiley and Sons, Inc, New York. 13

Hunt, I.A. (1959). Design of seawalls and breakwaters. *Proceedings of the American Society of Civil Engineers*, **85**, 123–152. 15

Jackson, D.W., Cooper, J.A. & del Rio, L. (2005). Geological control of beach morphodynamic state. *Marine Geology*, **216**, 297–314. 4, 7, 38

Jackson, J.E. (1991). *A Users Guide to Principal Components*. John Wiley and Sons, Inc, New York. 56

Jackson, N.L., Nordstrom, K.F., Eliot, I. & Masselink, G. (2002). Lowenergy sandy beaches in marine and estuarine environments: a review. *Geomorphology*, **48**, 147–162. 65

Jara, M.S., González, M. & Medina, R. (2015). Shoreline evolution model from a dynamic equilibrium beach profile. *Coastal Engineering*, **99**, 1–14. 24, 25, 69

Jiménez, J.A., Guillén, J. & Falqués, A. (2008). Comment on the article "morphodynamic classification of sandy beaches in low energetic marine environment" by gómez-pujol,

l., orfila, a., cañellas, b., alvarez-ellacuria, a., méndez, f.j., medina, r. and tintoré, j., marine geology, 242, pp. 235–246, 2007. *Marine Geology*, **255**, 96–101. 24, 69

Kaminsky, G.M., Ruggiero, P., Buijsman, M.C., McCandless, D. & Gelfenbaum, G. (2010). Historical evolution of the columbia river littoral cell. *Marine Geology*, 96–126. 49

Karambas, T.V. (2003). Modelling of infiltration exfiltration effects of cross shore sediment transport in the swash zone. *Coastal Engineering*, **45**, 63–82. 14

Katoh, K. & Yanagishima, S. (1992). Berm formation and berm erosion. *Coastal Engineering*, 2136–2149. 5, 16, 18, 29

Komar, P.D. (1998). *Beach Processes and Sedimentation*. PrenticeHall, Upper Saddle River, N J. xi, 21

Komar, P.D., Lizarraga-Arciniega, J.R. & Terich, T.A. (1976). Oregon coast shoreline changes due to jetties. *Journal of Waterways, Harbors, and Coastal Engineering*, **102**, 13–30. 50

Larson, M. (1988). Quantification of beach profile change. *Department of Water Resources Engineering, Lund University, Sweden*, **1**. 18, 56

Larson, M. & Kraus, N.C. (1995). Prediction of cross-shore sediment transport at different spatial and temporal scales. *Marine Geology*, **126**, 111–127. 5, 22, 68

Larson, M., Erikson, L. & Hanson, H. (2004). An analytical model to predict dune erosion due to wave impact. *Coastal Engineering*, **51**, 675–696. 15

Lee, G., Nicholls, R.J. & Birkemeier, W.A. (1998). Storm driven variability of the beach—nearshore profile at duck, north carolina, 1986–1991. *Marine Geology*, **148**, 163–177. 24, 69

Lemke, L., Miller, J.K., Gorton, A. & Livermont, E. (2014). Eof analysis of shoreline changes following an alternative beachfill within a groin field. *Coastal Engineering Proceedings*, **1**. 56

Leonardo, D.D. & Ruggiero, P. (2015). Regional scale sandbar variability: Observations from the u.s. pacific northwest. *Continental Shelf Research*, **95**, 74–88. 48, 50

Losada, M.A., Medina, R., Vidal, C. & Roldan, A. (1991). Historical evolution and morphological analysis of el puntal spit, santander (spain). *Journal of Coastal Research*, **9**, 785–800. 56

Losada, M.A., Medina, R., Vidal, C. & Losada, I.J. (1996). *History and Heritage of Coastal Engineering*. ASCE, Ed: N Kraus. 33

Mase, H. (1988). Spectral characteristics of random wave runup. *Coastal Engineering*, **12**, 175–189. 15

Masselink, G. & Puleo, J.A. (2006). Swash-zone morphodynamics. *Continental Shelf Research*, **26**, 661–680. x, 13, 15

Masselink, G. & Short, A.D. (1993). The effect od tide range on beach morphodynamics and morphology: a conceptual model. *Journal of Coastal Research*, **9**, 785–800. ix, 6, 7

Masselink, G., Kroon, A. & Davidson-Arnott, R.G.D. (2006). Morphodynamics of intertidal bars in wave-dominated coastal settings — a review. *Geomorphology*, **73**, 33–49. xv, 4, 5, 16, 42, 73

Medina, R., Vidal, C., Losada, M.A. & Roldan, A.J. (1993). Three-mode principal component analysis of bathymetric data, applied to 'playa de castilla' (huelva, spain). *Proceedings of the Coastal Engineering Conference*, **2**, 2251–2264. 56

Miller, J.K. & Dean, R.G. (2007). Shoreline variability via empirical orthogonal function analysis: Part ii relationship to nearshore conditions. *Coastal Engineering*, **54**, 133–150. 56

Ministerio de Medio Ambiente, D.G.d.C.M. (2007). Manual de restauración de dunas costeras (in spanish). 33, 43

Morton, R.A. & Speed, F.M. (1998). Evaluation of shorelines and legal boundaries controlled by water levels on sandy beaches. *Journal of Coastal Research*, **14**, 1373–1384. 22

Mull, J. & Ruggiero, P. (2014). Estimating storm-induced dune erosion and overtopping along u.s. west coast beaches. *Journal of Coastal Research*, **298**, 1173–1187. 3, 5, 32

Muñoz-Perez, J. & Medina, R. (2010). Comparison of long, medium and short term variations of beach profiles with and without submerged geological control. *Coastal Engineering*, **57**, 241–251. 56

Nicholls, R.J., Wong, P.P., Burkett, V.R., Codignotto, J.O., Hay, J.E., McLean, R.F., Ragoonaden, S. & Woodroffe, C.D. (2007). Coastal systems and low-lying areas. *Global and Planetary Change*, **111**, 150–158. 2

Nielsen, P. & Hanslow, D.J. (1992). Wave runup distributions on natural beaches. *Journal of Coastal Research*, **7**, 1139–1152. 14, 15

Nordstrom, K.F. & Jackson, N.L. (2012). Physical processes and landforms on beaches in short fetch environments in estuaries, small lakes and reservoirs: A review. *Earth Science Reviews*, **111**, 232–247. 23

Nordstrom, K.F., Jackson, N.L., Korotky, A.L.F.K.H., & Puleo, J.A. (1992). Effects of beach raking and sand fences on dune dimensions and morphology. *Geomorphology*, **179**, 106–115. 5, 12

Okazaki, S. & Sunamura, T. (1994). Quantitative predictions for the position and height of berms. *Geographical Review of Japan*, **67**, 101–116. x, 19, 74, 84

Orford, J.D., Forbes, D.L. & Jennings, S.C. (2002). Organisational controls, typologies and time scales of paraglacial gravel-dominated coastal systems. *Geomorphology*, **48**, 51–85. 5, 16

Otvos, E.G. (2000). Beach ridges: Definition and significance. *Geomorphology*, **32**, 83–108. 5

Perez, J., Menéndez, M., Camus, P., Mendez, F.J. & Losada, I. (2015). Statistical multi model climate projections of surface ocean waves in europe. *Ocean Modelling*, **96**, 161–170. xii, 31, 50, 51, 53, 70

Peterson, C.D., Jol, H.M., Vanderburgh, S., Phipps, J.B., D, D.P. & Gelfenbaum, G. (2010). Dating of late holocene beach shoreline positions by regional correlation of coseismic retreat events in the columbia river littoral cell, usa. *Marine Geology*, **273**, 44–61. 49

Pilkey, O.H., Young, R.S., andA S Smith, S.R.R., Wu, H. & Pilkey, W.D. (1993). The concept of shoreface profile of equilibrium: a critical review. *Journal of Coastal Research*, **9**, 255–278. 31, 70

Puleo, J.A., Beach, R.A., Holman, R.A. & Allen, S. (2011). Swash zone sediment suspension and transport and the importance of bore-generated turbulence. *Journal of Geophysical Research*, **105**, 17021–17044. 13

Rector, R.L. (1954). Laboratory study of equilibrium profiles beaches. *Beach Erosion Board Tech*, **41**. 18

Reguero, B.G., Méndez, M.M.F., Mínguez, R. & Losada, I. (2012). A global ocean wave (gow) calibrated reanalysis from 1948 onwards. *Coastal Engineering*, **65**, 38–55. xii, 51, 53, 70

Romanczyk, W., Boczar-Karakiewicz, B. & Bona, J.L. (2005). Extended equilibrium beach profiles. *Coastal Engineering*, **52**, 727–744. 22, 68

Ruggiero, P., Komar, P.D., McDougal, W.G., Marra, J.J. & Bach, R. (2001). Wave runup, extreme water levels and the erosion of properties backing beaches. *Journal of Coastal Research*, **17**, 407–419. 5, 15, 48

Ruggiero, P., Holman, R.A. & Beach, R.A. (2004). Wave run-up on a high-energy dissipative beach. *Journal of Geophysical Research C: Oceans*, **109**, 1–12. 50

Ruggiero, P., Kaminsky, G.M., Gelfenbaum, G. & Voigt, B. (2005). Seasonal to interannual morphodynamics along a high-energy dissipative littoral cell. *Journal of Coastal Research*, **213**, 553–578. xi, xii, 6, 10, 21, 22, 48, 49, 50, 51, 53, 54, 59

Ruggiero, P., Buijsman, M., Kaminsky, G.M. & Gelfenbaum, G. (2010). Modeling the effects of wave climate and sediment supply variability on large-scale shoreline change. *Marine Geology*, **273**, 127–140. 48, 65

Ruggiero, P., Kratzmann, M.G., Himmelstoss, E.A., Reid, D., Allan, J. & Kaminsky, G. (2013). National assessment of shoreline change: Historical shoreline change along the pacific northwest coast. *US Geological Survey Open-File Report 2012-1007*, **1**. 50, 53

Ruggiero, P., Kaminsky, G.M., Gelfenbaum, G. & Cohn, N. (2016). Morphodynamics of prograding beaches: A synthesis of seasonal- to century-scale observations of the columbia river littoral cell. *Marine Geology*, **376**, 51–68. 49, 65

Ruz, M.H. & Meur-Ferec, C. (2004). Influence of high water levels on aeolian sand transport: Upper beach dune evolution on a macrotidal coast, wissant bay, northern france. *Geomorphology*, **60**, 73–87. 9, 23

Scott, T., Masselink, G. & Russell, P. (2011). Morphodynamic characteristics and classification of beaches in england and wales. *Marine Geology*, **286**, 1–20. ix, 4, 7, 8

Senechal, N., Gouriou, T., Castelle, B., Parisot, J., Capo, S., Bujan, S. & Howa, H. (2009). Morphodynamic response of a meso to macro tidal intermediate beach based on a long-term data set. *Geomorphology*, **107**, 263–274. 16

Sherman, D.J. & Bauer, B.O. (1993). Dynamics of beach dune interaction. *Progress in Physical Geography*, **17**, 413–447. 44

Sherman, D.J., Jackson, D.W., Namikas, S.L. & Wang, J. (1998). Wind blown sand on beaches: an evaluation of models. *Geomorphology*, **22**, 113–133. x, 11

Short, A.D. (1999). *Handbook of Beach and Shoreface Morphodynamics*. Chichester: Willey. ix, 3, 5, 7, 33, 39, 45, 74

Short, A.D. (2006). Australian beach systems nature and distribution. *Journal of Coastal Research*, **221**, 11–27. 3, 6, 37, 43

Short, A.D. & Hesp, P.A. (1982). Wave, beach and dune interactions in southeastern australia. *Marine Geology*, **48**, 259–284. 4, 8, 12, 29, 44

Stive, M.J., Cloin, B., Jimenez, J. & Bosboom, J. (1999). Long-term cross-shoreface sediment fluxes. *Proceedings Coastal Sediments*, **1**, 505–518. 65

Stockdon, H.F., Holman, R.A., Howd, P.A. & Sallenger, A.H. (2006). Empirical parameterization of setup, swash, and runup. *Coastal Engineering*, **53**, 573–588. 5, 12, 15, 74

Suanez, S., Cariolet, J.M., Cancouet, R., Ardhuin, F. & Delacourt, C. (2012). Dune recovery after storm erosion on a high energy beach: Vougot beach, brittany (france). *Geomorphology*, **140**, 16–33. 22, 29

Sunamura, T. (1975). A study of beach ridge formation in laboratory. *Geographical Review of Japan*, **48**, 761–767. 18

Suzuki, T., Isozaki, S. & Sasaki, J. (2013). An improved short term swash zone beach profile change model. *Proceedings of the 7th International Conference on Asian and Pacific Coasts*, **1**. 16

Swart, D.H. (1976). Predictive equations regarding coastal transports. *Coastal Engineering Proceedings*, **15**. 5, 32

Takeda, I. & Sunamura, T. (1982). Formation and height of berms. *Japanese Geomorphological Union*, **3**, 145–157. 18, 74

Takeda, I. & Sunamura, T. (1986). Beach changes by storm waves. *Coastal Engineering*, 1612–1622. 5

Taylor, K.E. (2001). Summarizing multiple aspects of model performance in a single diagram. *Journal of Geophysical Research*, **106**, 7183–7192. xiv, 31, 79, 82

Thomas, K.V. & Baba, M. (2001). Berm development on a monsoon-influenced microtidal beach. *Sedimentology*, **33**, 537–546. 16

Tomás, A., Méndez, F.J., Medina, R., Jaime, F.F., Higuera, P., Lara, J.L., Ortiz, M.D. & Álvarez de Eulate, M.D. (2015). A methodology to estimate wave-induced coastal flooding hazard maps in spain. *Journal of Flood Risk Management*, **9**, 289–305. 9, 13, 30, 69, 70

Turner, I.L., Harley, M.D., Short, A.D., Simmons, J.A., Bracs, M.A., Phillips, M.S. & Splinter, K.D. (2016). A multi-decade dataset of monthly beach profile surveys and inshore wave forcing at narrabeen, australia. *Scientific data*, **3**. xiv, xvi, 12, 69, 72, 78, 79

Udo, K. & Yamawaki, S. (2006). Short-term changes of beach morphology and sand grain size under wave and wind action. In *Vietnam -Japan Estuary Workshop 2006*. 4, 9, 23

Valdemoro, H.I. & Jimenez, J.A. (2006). The influence of shoreline dynamics on the use and exploitation of mediterranean tourist beaches. *Coastal Management*, **34**, 405–423. 2

van-der Burgh, L.M.B., Wijnberg, K.M. & Hulscher, S.J. (2011). Decadal scale morphologic variability of managed coastal dunes. *Coastal Engineering*, **58**, 927–936. 5

vanGent, M.R., vanThieldeVries, J.S., Coeveld, E.M., deVroeg, J.H. & vanDeGraaff, J. (2008). Large scale dune erosion test to study the influence of wave periods. *Coastal Engineering*, **55**, 1041–1051. 17

Weir, F.M., Hughes, M.G., & Baldock, T.E. (2006). Beach face and berm morphodynamics fronting a coastal lagoon. *Geomorphology*, 331–346. x, 5, 17, 19, 20, 29, 74, 83

Wiggs, G.F., Baird, A. & Atherton, R.J. (2004). The dynamic effects of moisture on the entrainment and transport of sand by wind. *Geomorphology*, **59**, 13–30. 12

Wijnberg, K.M. & Terwindt, J.H. (1995). Extracting decadal morphological behaviour from high-resolution, long-term bathymetric surveys along the holland coast using eigenfunction analysis. *Marine Geology*, **126**, 301–330. 56

Winant, C.D., Inman, D.L. & Nordstrom, C.E. (1982). Description of seasonal beach changes using empirical eigenfunctions. *Journal of Geophysical Research*, **29**, 327—-341. 56

Woolf, D.K., Challenor, P.G., & Cotton, P.D. (2002). Variability and predictability of the north atlantic wave climate. *Journal of Geophysical Research*, **107**, 9–14. 34

Wright, L.D. & Short, A.D. (1984). Morphodynamic variability of surf zones and beaches : a synthesis. *Marine Geology*, **56**, 93–118. ix, 3, 6, 7, 8, 43, 73

Wright, L.D., Short, A.D. & Green, M.O. (1985). Short term changes in the morphodynamic states of beaches and surf zones: An empirical predictive model. *Marine Geology*, **62**, 339–364. 6, 24, 25, 31, 37, 38, 69, 70, 79

Yepes, V. & Medina, R. (2005). Land use tourism models in spanish coastal areas . a case study of the valencia region. *Journal of Coastal Research*, **49**, 83–88. 2

Declaration

I herewith declare that I have produced this work without the prohibited assistance of third parties and without making use of aids other than those specified; notions taken over directly or indirectly from other sources have been identified as such. This work has not previously been presented in identical or similar form to any examination board.

The dissertation work was conducted from 2012 to 2016 under the supervision of Dr. Raúl Medina and Dr. Adolfo Uriarte at the Universidad de Cantabria.

This dissertation was finished in Santander on December 2016

This page is intentionally left blank